Design and Developmental Studies On A Six-Degree of Freedom Endoscopic Force/Torque Sensor

Shengmei Wang

A Thesis

In

The Department

Of

Mechanical and Industrial Engineering

Presented in Partial Fulfillment of the Requirements

for the Degree of Master of Applied Science at

Concordia University

Montreal, Quebec

Canada

June 2003

Your file Votre référence
ISBN: 0-612-83886-2
Our file Notre référence
ISBN: 0-612-83886-2

ABSTRACT

Design and Developmental Studies on a Six-Degree of freedom Endoscopic Force/ Torque Sensor

Shengmei Wang

Concordia University, 2003

The project focuses on designing a new type of six-degree freedom force/torque sensor and developmental study on it.

The proposed sensor can independently detect six components of force and moment on a test platform. The response characteristics are linear, close to the design values, and high enough to measure the forces and moments expected to act on the sensor in a Cartesian coordinate system. The sensor frame consists of four symmetric beams and a horizontal cross-beam designed to be monolithic. The sensor design is quite simple and has negligible cross sensitivity in the measurements. These properties, combined with its hollow cylindrical shape and small size, make this sensor an ideal choice for endoscopic applications.

This thesis presents the design of a six-degree freedom force/torque sensor with micro-strain gauges. The design is carried out using strength of material type of approach. It is validated using the finite element analysis method. Some problems of calibration are discussed. An experimental set-up is made in order to test the prototype sensor. Experimental data validate the basic design ideas, and the sensor can be very useful tool to monitor and control the force applied by the surgeon in endoscopic operations.

ACKNOWLEDGEMENTS

This project was carried out at the CONCAVE Research Center of Concordia University, Montreal, Canada. It provided an excellent opportunity for me to gain experience in several exciting new areas in my field. It was an extraordinary learning experience to encounter and overcome the numerous difficulties that arise in research. I am grateful to all those who have contributed to this thesis, in particular to:

My sincere thanks are due to my supervisors, Dr. Bhat and Dr. Dargahi who gave me the chance to work on a multidisciplinary project. They guided and assisted me in all aspects of this research and gave me fruitful comments. They discussed with me about this project on a continuous basis and at last they carefully reviewed and corrected this thesis.

Acknowledgements are due to Mr. Dainius Juras who gave me many interesting ideas and prepared the experimental setup. He assisted me to perform aspiration experiments presented in this thesis.

My sincere thanks are due to Mr. Weiming Pu who provided me with efficient computer support. I thank Professor Zhanqi Wang who discussed with me and helped me to solve many problems with his abundant engineering experiences.

Finally, I would like to express special thanks to my husband, Jian Li, my son, Pinxue Li, and my parents for their love, understanding, encouragement and support.

TABLE OF CONTENTS

List of Tables

List of Figures

List of Symbols

A	Cross-sectional area of the structure
C	Compliance matrix
C^+	Pseudo-inverse matrix
D	Diameter of wire
D(x,y,z)	Elastic matrix
E	Young's modulus
F	Tension force applied to the structure
F_x	X direction force
F_y	Y direction force
F_z	Z direction force
H	Distance from strain gauges glued on vertical beam to horizontal beam
H(x,y,z)	Displacement interpolation matrix
I	Moment of Inertia
K	Total stiffness matrix
$K_1,\ldots K_6$	Coefficients of the force/torque sensor
L_0	Length of the structure
L_1	Distance from strain gauges glued on horizontal beam to vertical beam
L_2	Distance from strain gauges glued on horizontal beam to the center of the coordinates

M	Bending moment
M_x	Moment about x axis
M_y	Moment about y axis
M_z	Moment about y axis
R1	Electrical resistance of wire
R	Length of horizontal beam
S	Length of vertical beam
$S_1,\ldots S_{10}$	Strain value of strain gauges
U	Nodal displacement vector
V	Volume
b	Beam width
c_j	Non-nodes coefficients
f	A measured $n \times 1$ force vector
h	Beam thickness
k	Gauge factor
r_i	Residual for the data pair (x_i, y_i)
u_j	Values of u at the element nodes
u_n	A vector containing the nodal displacements
Ψ_j	Interpolation function
Φ_j	Associated approximation functions

Δ V	Voltage change
Δ R	Changes of the electrical resistance
$\mathcal{R}(C^T)$	Range of C^T
$\mathcal{N}(C^T)$	Null space of C^T
σ	Normal stress
σ_i	Singular values
ε	Axial strain
ε	A measured $m \times 1$ strain vector
ν	Poisson ratio

Chapter 1

Introduction

The concept of six axis sensors and minimal invasive surgery will be introduced in this chapter. Then the development of six axis sensors and their application fields will be reviewed. At last the project objectives and the thesis organization will be discussed.

1.1 Six Degree of Freedom Force/Torque Sensors

Sensor is a device that produces a proportional output signal (electrical, mechanical, magnetic, etc.)[1] when exposed to a physical phenomenon (temperature, displacement, force, etc.). The term transducer is often used synonymously with sensors. However, ideally, a sensor is a device that responds to a change in the physical phenomenon. On the other hand, a transducer is a device that converts one form of energy into another form of energy. Sensors are transducers when they sense one form of energy input and provide an output in a different form.

Force/torque sensor is based on measuring a deflection caused by the force or torque. Force/torque sensor that employs strain gauge elements with built-in microelectronics is common. Both impulsive forces or torques and any varying forces or torques can be monitored using these sensors.

A force/torque sensor has the structure as shown in Figure 1.1. Strain gauges transform strains into changes of the electrical resistance ΔR, an electronic unit detects the resistance change and responds with a voltage change ΔV, and then this ΔV is read to find the force/torque applied on the sensor [2].

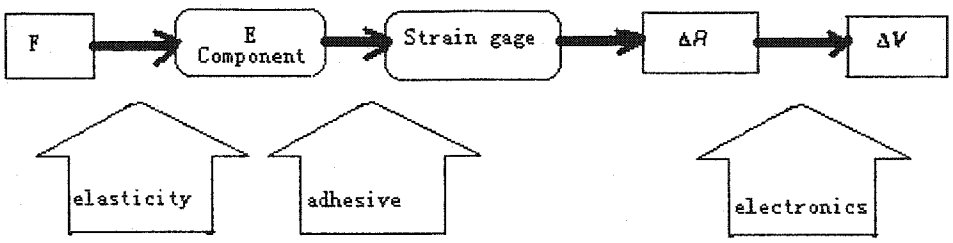

Figure 1.1 Strain Transformation

The six-axis force/torque transducers can measure three force-components and three-moments acting on the transducers. It has been initially developed for applications such as in wind tunnel testing and in thrust stand testing of rocket engines. In the mid seventies, increasing demands for real flexibility and the importance of sensing force and torque with arbitrary directions and magnitudes were becoming crucial, and hence much attention was given to the development of six degrees of freedom sensors [3]. Now, the force/torque sensor is highly effective in applications such as robot manipulation, minimal invasive surgery, tele-operation surgery, aircraft and other vehicle control, and other interactions between the applications involving human and environment.

In this thesis, a new six-axis force/torque sensor is designed, developed and tested, for applications in endoscopes.

1.2 Minimal Invasive Surgery

In the traditional method of surgery, the surgeon opens the patient's body with an incision, finds the sick organ, conducts the surgery and then sutures the incision. The operation is quite complicated and time consuming, the patient might lose a lot of blood

and the recovery time is often long.

Minimal Invasive Surgery (MIS) has recently become a very popular technique to minimize damage to surrounding healthy tissues normally caused by the process of reaching the more inaccessible internal organs during traditional surgical techniques. MIS is also well known as Endoscopic surgery or keyhole surgery. However, Laparoscopic surgery is a type of Endoscopic surgery where the operation is conducted in the abdominal area. In Laparoscopic surgery, the surgical procedures in the internal organs are performed by creating only small incisions on the surface of the human body in order to reduce the damage caused to the tissues [4]. The relatively large incisions in open surgery can be replaced by small perforation holes, which serve as entry points for optical and surgical instruments. Special surgical instruments including laparoscopic tools are introduced through the small holes leading to the internal organs. All manipulations are carried out using instruments from outside the abdomen. The small spatial extent of the tissue injury and the careful selection of the entry points result in fast patient recovery after an operation. The price for this kind of operations is the loss of direct contact for the surgeon with the organ being operated on and the inability to look at the operation site. The advantages of MIS are fast patient recovery, little chance of inflammation and other postoperative problems.

Laparoscopy requires a number of skills that cannot be simply taught by "apprenticeship" due to a shortage of experienced teachers and because of the nature of the skills. A two-dimensional image must be translated into a three-dimensional setting in one's mind, and consequently, one should be able to appreciate depth perception using very subtle visual clues. This requires fine motor skills and hand-eye coordination to

manipulate small tools that move on-screen in a direction opposite to that of the controlling hand. What made one a good technical surgeon in the past may not apply in these cases.

The best method of teaching the novice surgeon to limit excessive loads and improve movement efficiency during surgical procedures can potentially reduce injury to soft tissues and reduce the time during laparoscopic surgery [5]. Direct haptic contact or any direct visual inspection of organs or tissues is not possible, and operating under these restricted conditions requires intensive training of surgeons. The Society of American Gastrointestinal Endoscopic Surgeons (SAGES) describes the use of pre- and post-testing in the evaluation of training courses and the trainers [5]. Training in a simulated environment has several advantages over traditional training. It is less expensive, and results in faster training in complicated procedures [5]. In order to enhance laparoscopic surgical skills, an instrumented laparoscipic grasper is developed measuring the force/torque at the surgeon hand/tool interface. Surgeon usually uses two endoscopes in order to operate and the third endoscope with a camera is inserted through another incision hole to view the entire operation on a video monitor [6]. One of the more difficult tasks in surgical education is to teach the optimal application of instrument forces and torques necessary to conduct an operation. The use of proper force/torque at the human body/tool interface is essential for the success of the operation. All jobs of MIS must be based on the measurement of the force/torque between the operation handle and the organs or tissues [7][8]. The goal of the present study is to create new six degree of freedom micro-force/torque-sensor to measure the forces and torques applied by surgeons on their instruments during minimally invasive surgery.

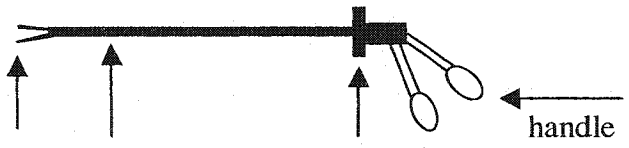

grasper cylindrical tube force/torque sensor

Figure 1.2 Endoscope and force/torque sensor location

1.3 Literature Review

During the past two decades, the force torque sensors have been widely accepted in industrial and engineering applications, such as load cells [9], wind-tunnel balances [10] and robotic engineering [11].

Much research is actively being carried out for applications in robotic manipulators and more sophisticated tasks such as assembly, polishing, etc. A variety of six-component force sensors have been designed for robotic systems mounted on base, table, wrist and finger of robots.

Akihiko Yabuki [12] proposed a wrist force sensor with eight parallel leaf springs and a mechanical stopper for assembly robot. E. Bayo et al [13] devised a new design using elastic members that exhibit truss like behavior as opposed to the commonly used beam behavior.

Lu-Ping Chao et al [14] advocated a systematic shape optimal design methodology for a decoupled six-axis wrist force sensor. Tsuneo Yoshikawa [15]

described a six-axis sensor with three pairs of elastic elements, aligning along three axes to get a rather small cross-coupling between elemnts.

Chul-Goo Kang [16] designed a sensor whose internal structure has a cross shaped form with 8 circular holes, and a circular external structure. They also analyzed the error propagation in measurement.

Optimal geometric structures and evaluation of six-axis sensors were considered in [17][18]. These basic ideas have been extended to more general and mathematical forms by Bicchi [19][20]. He proposed that the condition number of compliance matrix could be the performance index of sensor design.

Most of the 6-axis force sensors have the form of a frame with cross bar. For different applications, other forms of 6-axis force transducers were introduced. D. Stewart described what is known as a Stewart platform-based force transducer first time in 1965[21]. Chul-Goo Kang [22] presented it. M. Sorli et al [23] described the Stewart platform-based force transducer again. The advantages of the Stewart platform based force transducer are that the internal stresses of the transducer material do not appear in the measurement, and the transducer provides passive compliance often needed during a robotic assembly task.

Makoto Kaneko [24][25] proposed an interesting design of twin head multi-axis force sensor based on the principle of pressure pick-up device. The new six-axis force sensor is composed of two three-axis force sensors and a connector. He described the theoretical basis for the operation of this type of sensor and provided the characteristics matrix connecting the load and sensor output vectors.

Koichi Nishiwaki et al [26] described a six-axis force sensor with parallel support

mechanism, which allows large torques and forces to be generated when a robot foot hits the ground.

Dirk Diddens et al [27] developed a ring-shaped multi-axis sensor mounted on the Smartpen™ as a new advanced computer input device.

E. Bayo et al [28] devised a new design that has the elastic members exhibiting truss like behavior as opposed to the commonly used beam behavior.

Recently multi-axis sensors were also used in many new fields. Dzung Viet Dao et al [29] fabricated a six-degree of freedom turbulent flow micro sensor utilizing the piezoresistive effects in silicon. The sensor was used in Geophysics to measure the forces and moments expected to act on the particles in turbulent flow.

In the animal bio-dynamics, Y. H. Chang et al [30] used a 6 components force transducer system to determine the dynamic forces and moments applied by an arm-swinging animal during locomotion.

The appearance of micro robots resulted in several different types of sensors [31]. The integrated micro force sensor system was developed for measuring the gripping forces in robotic arms.

In the surgical operation, the surgeon who is using MIS tools loses almost completely the haptic perception of the manipulated tissue. A. Bicchi [32] presented a first attempt to realize a prototype of surgical tool with sensor that can measure force/torque. Nowadays six degree of freedom force/torque sensor technology has made significant progress and are used widely in laparoscopic tools, surgical simulation and training [33], and tele-operated surgery [34].

A. Bicchi et al [35] provided reliable models of dynamic multi-axis force/torque

sensors, and tried to define optimality criteria for gauge placements in the design of dynamic force/torque sensing devices. The dynamic considerations were also presented in literature [36-39].

1.4 Thesis Objectives and Organization

In this thesis, a new structure for six axis force sensors is proposed that is easy to analyze, is simple in its structure, minimizes cross-sensitivity, is small in size, has light weight, and could be integrated with cylindrical tube of endoscopic tool. The motivation for the study came because of the need for such sensors in endoscopic applications. The specific objectives are:

1. To design a six axis force/torque sensor
2. To make a prototype in order to carry out experiments
3. To analyze the structure using finite element analysis
4. To compare the analytical and experimental results from the point of linearity, and cross sensitivity of the outputs
5. To draw specific conclusions on the design and the performance of the sensor

In order to examine the validity of the new sensor structure, traditional beam model will be used to analyze the distribution of force/ torque in Chapter II, and finite element method model will be employed to obtain more accurate analysis result in Chapter III. Chapter IV provides details of the experimental setup and performance of experiments. Chapter V describes the conclusions and suggestions for future work. The appendix provides mechanical drawing, experimental data and Matlab codes.

The details about design of the six-degree of freedom sensor will be described in the following chapter. The beam theory model will be used to analyse the sensor and get the sensor prototype.

Chapter 2

Sensor Design

In Chapter 1, the six-degree freedom sensor and the concept of minimal invasive surgery were introduced, along with a review of the relevant literature in the area. In this chapter, a model of the six-degree of freedom force/torque sensor will be discussed. A design of the new six-degree of freedom force/torque sensor will be proposed. The design will employ the traditional beam theory model in order to get the dimensions of the sensor in this chapter.

2.1 Force/Torque Sensor Mathematical Model

When an external force acts on a sensor body, the multi-axis force sensor detects elastic deformation of the internal sensor frame and transforms the deformation to an analog or digital form of voltage and calculates the six components of the acting force. The elastic deformation is usually detected by means of either strain gauges, opto-electronics sensors [40], CCD elements [41], or inductive displacement transducers [42].

In the present study, strain gauges and Wheatston bridges [43] are used to detect the force and torque by measuring the surface strain on the elastic structure.

If the elastic deformation of the internal structure in the sensor is within elastic limit, the linear behavior can be hypothesized for the sensor, arriving at the following relation,

$$Cf = \varepsilon \tag{2.1}$$

where f is a measured $n \times 1$ force vector where the elements consist of all or part of the 6×1 forces and moments. The strain ε is a measured $m \times 1$ vector whose elements are

m strain measurements at m points on the internal structure (m = 10 for the present investigation), and C is a $m \times n$ compliance matrix or calibration matrix. It is assumed that $m \geq n$ and $rank(C) = n$, without losing generality. The condition $m \geq n$ implies that the number of strain measurement points is equal to or greater than the number of force components that are sought. Generally n is less than 6.

The vector f includes force and moment components together, and hence the property of the matrix C depends on the units of force and moment.

The solution of the linear algebraic Equation (2.1) can be considered in two different cases, where both the cases are supposed to satisfy the condition $rank[C] < rank[\varepsilon]$. In one case, there are no errors at C and ε, hence there exists a unique solution f. In the other case a unique solution for f does not necessarily exist, and hence Equation (2.1) should be written as

$$Cf \approx \varepsilon \tag{2.2}$$

With this approximation it is possible to obtain an approximate solution instead of the exact solution. The approximate solution f minimizes $||\varepsilon - Cf||^2$ by considering this problem as a least square problem of full rank. In the following, there is always a vector, in fact a unique vector f of minimum norm, which minimizes $||\varepsilon - Cf||^2$ [43].

$$\varepsilon = \varepsilon' + \varepsilon'' \tag{2.3}$$

where:

ε'' is the projection of ε on $\mathcal{R}(C)$

ε' is vector that is orthogonal to the linear manifold $\mathcal{R}(C)$

In other words, $\varepsilon' \in \mathcal{N}(C^T)$, since $Cf \in \mathcal{R}(C)$ for every f, $\mathcal{R}(C^T)$ is the range

of C^T, which means that the set of vectors which are afterimages of vector in the Euclidean space serves as domain of C: $\mathscr{R}(C) = \{z : z = C x\}$

$\mathscr{N}(C^T)$ is null space of C^T, means the null space of C^T: $\mathscr{N}(C^T) = \{x : C^T x = 0\}$

It follows that:

$$\varepsilon'' - Cf \in \mathscr{R}(C)$$

and since

$$\varepsilon' \in \mathscr{R}^{\perp}(C)$$

$$\varepsilon' \perp \varepsilon'' - Cf$$

Therefore

$$\| \varepsilon - Cf \|^2 = \| \varepsilon' + \varepsilon'' - Cf \|^2 = \| \varepsilon'' - Cf \|^2 + \| \varepsilon' \|^2 \geq \| \varepsilon' \|^2 \qquad (2.4)$$

This lower bound is attainable since ε'' being in the range of C, is the afterimage of some f_0:

$$Cf_0 = \varepsilon'' \qquad (2.5)$$

Thus, for this f_0, the bound is attained:

$$\| \varepsilon - Cf_o \|^2 = \| \varepsilon'' - Cf_0 \|^2 + \| \varepsilon' \|^2 \qquad (2.6)$$

Hence the lower bound is attained at f^* only if f^* is such that

$$Cf^* = \varepsilon'' \qquad (2.7)$$

For any such f^*, it can be decomposed into two orthogonal vectors:

$$f^* = f^{*'} + f^{*''} \qquad (2.8)$$

where

$$f^{*'} \in \mathscr{R}(C^T) \quad \text{and} \quad f^{*''} \in \mathscr{N}(C)$$

Thus

$$Cf^* = Cf^{*'} \tag{2.9}$$

so that

$$\| \varepsilon - Cf^* \|^2 = \| \varepsilon - Cf^{*'} \|^2 \tag{2.10}$$

and

$$\|f^*\|^2 = \|f^{*'}\|^2 + \|f^{*''}\|^2 \geq \|f^{*'}\|^2 \tag{2.11}$$

Hence the f_0 minimizes $\| Cf - \varepsilon \|^2$ always exists if and only if $Cf_0 = \varepsilon''$

In the following, it can be proved for any m-vector f,

$$C^+ f = \varepsilon'' \tag{2.12}$$

where C^+ is called Moore-Penrose inverse [44],

Equation (2.12) is vector of minimum norm among those which minimize $\| \varepsilon - Cf \|^2$.

For any m × n matrix C,

$$C^+ = \lim_{\delta \to 0} (C^T C + \delta^2 I)^{-1} C^T$$

$$= \lim_{\delta \to 0} C^T (C^T C + \delta^2 I)^{-1} \tag{2.13}$$

where:

"I" represents the identity matrix whose dimensionality is to be understood from the context.

δ^2 is eigenvalue of $C^T C$.

C^+ always exists, since

$$(C^T C C^T + \delta^2 I C^T) = C^T (C C^T + \delta^2 I) = (C C^T + \delta^2 I) C^T \tag{2.14}$$

$(CC^T + \delta^2 I)$ and $(C^T C + \delta^2 I)$ have inverses when $\delta^2 > 0$

Let ε be a given n-dimensional vector, and decompose ε into its projections on

$\mathcal{R}(C)$ and $\mathcal{N}(C^T)$:

$$\varepsilon = \varepsilon' + \varepsilon'' \tag{2.15}$$

Since

$$C^T\varepsilon = C^T\varepsilon'' \tag{2.16}$$

and since $\varepsilon'' \in \mathcal{R}(C)$ must be the afterimage of some vector ε_0 under C, it can be seen that:

$$(CC^T+\delta^2 I)^{-1}\, C^T\varepsilon = (CC^T+\delta^2 I)^{-1}C^T\varepsilon$$

$$= (CC^T+\delta^2 I)^{-1}C^TCf_0 \tag{2.17}$$

The limit of the last expression always exists and coincides with f_0' , the projection of f_0 on $\mathcal{R}(C^TC)$, and since

$$\varepsilon'' = Cf_0$$

$$= Cf_0'$$

the following equation can be concluded:

$$f_0' \equiv \lim_{\delta\to 0}(C^TC + \delta^2 I)^{-1}C^T\varepsilon \tag{2.18}$$

where f_0' always exists, is an element of $\mathcal{R}(C^T)$, and satisfies the relation

$$Cf_0' = \varepsilon'' \tag{2.19}$$

For any vector ε, $CC^+\varepsilon$ is the projection of ε on $\mathcal{R}(C)$ and $(I-CC^+)\varepsilon$ is the projection of ε on $\mathcal{N}(C^T)$. For any vector f, CC^+f is the projection of f on $\mathcal{N}(C^T)$, and $(I-CC^+)f$ is the projection of f on $\mathcal{R}(C)$.

So the normal equation can be obtained:

$$C^TCf = C^T\varepsilon \tag{2.20}$$

From the equation (2.20), the following solution or approximate solution is obtained.

$$f = C^+\varepsilon \tag{2.21}$$

where $C^+ = (C^TC)^{-1}C^T$, and C^+ is called left pseudo-inverse. The left pseudo-inverse is a special case of Moore-Penrose inverse that can be defined in a matrix with non-full rank. Moore-Penrose pseudo-inverse matrix C^+ can be computed via the singular value decomposition of C, which is a generalization of the diagonal of a symmetric matrix by a similarity transformation with orthogonal matrices [45]. For any matrix C $\in R_{m\times n}$ can be factorized into

$$C = U \Lambda V^T \tag{2.22}$$

with $U \in \mathrm{R}_{m\times m}$ and $V \in \mathrm{R}_{n\times n}$ being orthogonal matrices and $\Lambda \in \mathrm{R}_{m\times n}$ with

$$\Lambda = \mathrm{diag}\ (\sigma_1, \ldots, \sigma_{\min(m,n)})$$

and $\sigma_i \geq 0$.

This factorization is called *singular value decomposition* and the σ_i are called *singular values*.

Some properties of the singular values is noted, which can easily be checked are noted below:

· If $C = C^T$, then the singular values are the eigenvalues of C.

· In general, the σ_i^2 are just the eigenvalues of C^TC.

· If Rank(C) = k < min(m, n) then $\sigma_i = 0$ for $i > k$.

· If Λ = diag ($\sigma_1, \ldots, \sigma_k, 0, \ldots, 0$) then Λ^+ = diag ($\sigma_1, \ldots, \sigma_k, 0, \ldots, 0$)

where U is $m \times m$ orthogonal matrix composed of orthonormal eigenvectors of CC^T, V is $n \times n$ orthogonal matrix composed of orthonormal eigenvectors of C^TC, and Λ is $m \times n$ diagonal matrix in which i,j elements($i \neq j$) equal 0 and i,i elements (i = $1,\ldots,n$) equal the singular value δ_i of C corresponding to the eigenvectors of C^TC. Then

Moore-Penrose inverse C^+ is given as:

$$C^+ = ((U \Lambda V^T)^T U \Lambda V^T)^{-1}(U \Lambda V^T)^T$$

$$= (V \Lambda^T U^T U \Lambda V^T)^{-1}(V \Lambda U^T)$$

$$= (V \Lambda^T \Lambda V^T)^{-1}(V \Lambda U^T)$$

$$= (V^T)^{-1}(\Lambda^T \Lambda)^{-1} V^{-1} V \Lambda U^T$$

$$= V(\Lambda^T \Lambda)^{-1} \Lambda U^T$$

$$= V \Lambda^+ U^T \qquad (2.23)$$

where Λ^+ is $n \times m$ matrix in which i,j elements(i $\neq j$) equal 0 and i,i elements($i = 1,\ldots,n$) equal $1/\delta_i$. The Moore-Penrose inverse C^+ gets equal to the inverse C^{-1} if $m = n$ and C has full rank. Hence the actual force f acting on the sensor can be obtained with the above formulation. It is possible to get the input of force/torque with the measured strains on the structure, when the measured strain information is more then the number of force/torque information.

2.2 Sensor Design

2.2.1 Sensor structure

In general, there are several types of sensors. Most of them are with cross bars. Some of these sensors are shown in Figure2.1

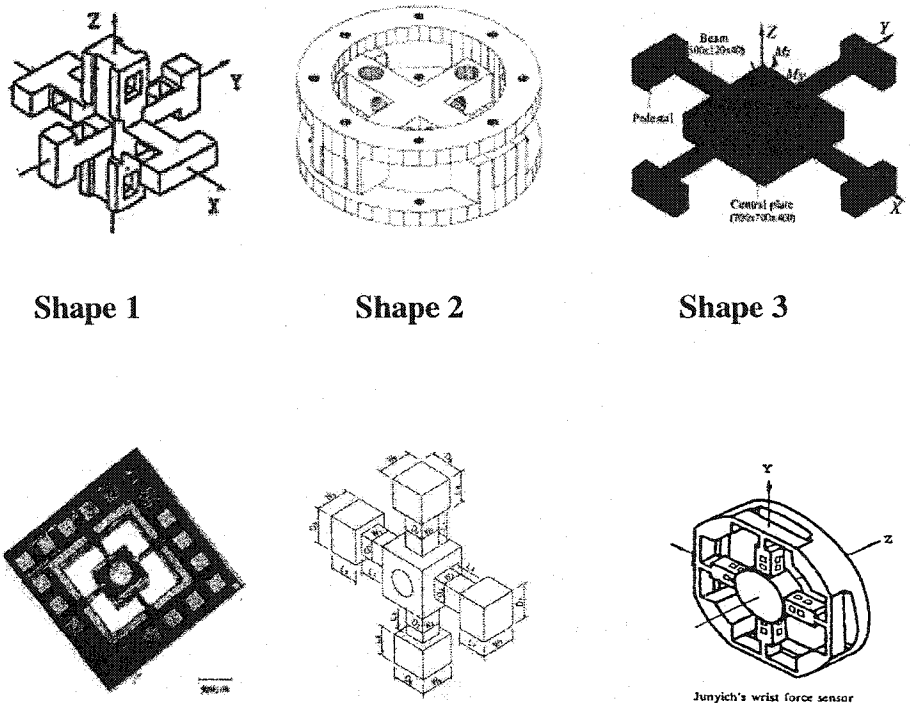

Shape 1 **Shape 2** **Shape 3**

Shape 4 **Shape 5** **Shape 6**

Figure 2.1 Different Force/Torque Sensor Shapes

In Figure 2.1

Shape 1: Tsuneo Yoshikawa et al introduced in 1989 [15]

Shape 2: Chul-Goo kang described in 2001 [16]

Shape 3: Dzung Viet Dao used in 2002 [28]

Shape 4: Dzung Viet Dao discussed and compared in 2002 [28]

Shape 5: Lu-Ping Chao presented in 1997 [14]

Shape 6: Juyich firstly developed [45]

Forces and moments applied to the sensor are evaluated through the measurement of strains at given points on the sensor body. The sensor body is a structural system with

specially designed shape. The sensor will be integrated with the cylindrical tube of the endoscopic tool near the handle (see Figure 1.2). The sensor used in this report is the enhanced sensor that is designed by Weiyi Huang et al [46]. The elastic body structure of the sensor is shown in Figure 2.2.

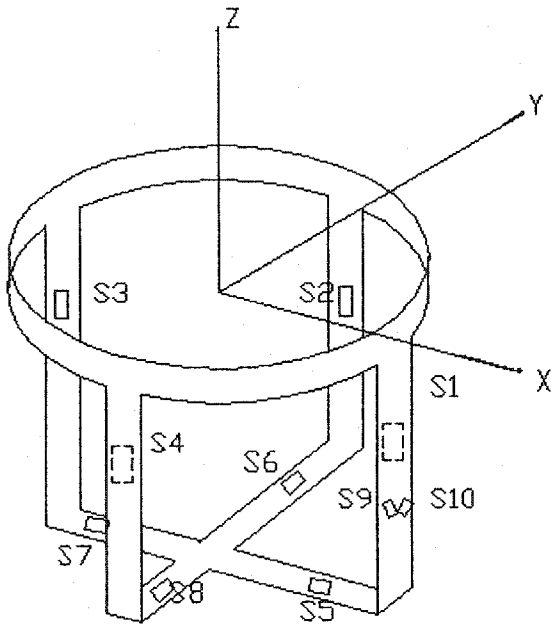

Figure 2.2 The Force/Torque Sensor Frame

All of the 10 micro-strain gauges used on the structure are indicated in Figure 2.2. The ninth and tenth strain gauges are stuck on the vertical beams at 45 degree with the shaft axis. Let the strain gauges outputs obtained from the strain gauge bridges be S_1, S_2, S_3, S_4, S_5, S_6, S_7, S_8, S_9, and S_{10}. Then the force vector F in the coordinate system OXYZ can be obtained as

$$F = \begin{bmatrix} F_x \\ F_y \\ F_z \\ M_x \\ M_y \\ M_z \end{bmatrix} = \begin{bmatrix} K_1(S_1 - S_3 + S_5 + S_7) \\ K_2(S_2 - S_4 + S_6 + S_8) \\ K_3(S_5 + S_6 + S_7 + S_8 + S_1 + S_2 + S_3 + S_4) \\ K_4(S_6 - S_8 + S_2 + S_4) \\ K_5(S_5 - S_7 + S_1 + S_3) \\ K_6(S_9 - S_{10}) \end{bmatrix} \quad (2.24)$$

where K_1, K_2, ... K_6 are the coefficients of the force/torque sensor that are determined when it is designed.

There are some assumptions made in modeling the sensor structure elastic model:

(1) The stiffness of the elastic body designed is high enough for forces and moments to be applied. The deformation of the elastic beam is in the elastic regime.

(2) The strain gauges are glued to the structure in such way that the glue layer is thin and the error caused by glue materials is negligible.

(3) The maximum cross-sensitivity is limited to10%.

(4) Every line of the component force passes through the center of the coordinate as shown in Figure 2.2.

2.2.2 The material of sensor frame

The stiffness and sensitivity characteristics of the force/torque sensor frame are determined by its material properties. The maximum allowable strain for micro-strain gauges is typically 1-1000 μ strain, which is at least one order of magnitude higher than that of industrial metals. Furthermore, the stiffness depends linearly on Young's modulus E of the material. By virtue of Hooke's law:

$$\sigma = E\varepsilon \tag{2.25}$$

It can be concluded that high sensitivity and stiffness are achievable simultaneously only by use of a high-strength material. Because a linear response is desired from the sensor, the chosen sensor frame material must have a linear strain-stress relationship. Steel is the best available industrial material that has good linearity properties within a large stress range.

Standard steel was chosen for the material of sensor frame.

Material characteristics are given in Table 1(http://www.metlab.com)

Table 1 Material Characteristic

Model	AISI 1018 Steel, cold drawn
Elongation at Break	15%(in 50mm)
Reduction of Area	40%
Bulk Modulus	140 Gpa
Shear Modulus	80 Gpa
Young's Modulus	2.067×10^5 N/mm^2
Possion's Ratio	0.3
Tensile Strength Ultimate	440 Mpa
Tensile Yield Strength	370 Mpa
Notes	Medium low-carbon steel, good weldability

2.2.3 The specifications of strain gauges

The specifications of the micro-strain gauges used are given in Table 2.

Table 2 Micro-Strain Gauge Specifications

Model	ESB-020-350
Shape	Bar
Resistance (R)	350 Ω
Gauge Factor	+155
Thermal Coefficient of Resistance	+22% (20°C to 70 °C)
Thermal Coefficient of Gauge Factor	-18% (20°C to 70 °C)

2.3 Force/Torque Analyse

Geometrical structure of the sensor showing the typical vertical and horizontal components of the sensor as well as the position of the strain gauges are given in Figure 2.3.

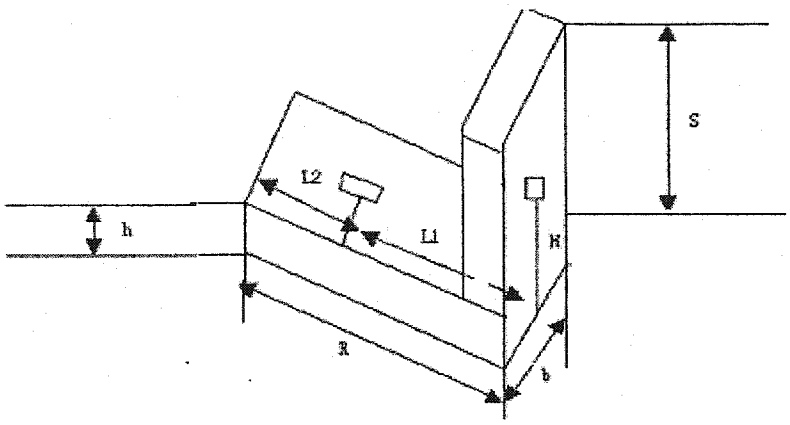

Figure 2.3 The Geometrical Structure of the sensor

The arrangement of strain gauges and force/torque direction are shown in Figure 2.4.

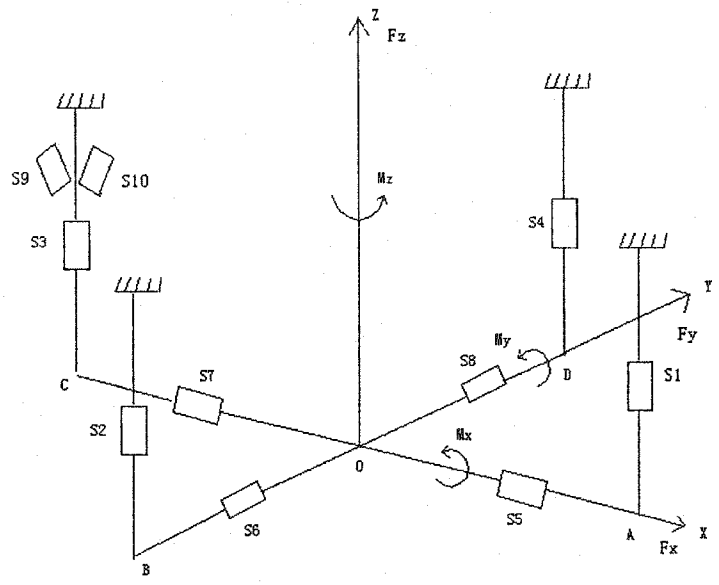

Figure 2.4 The Skeleton drawing of the sensor

2.3.1 The condition when applying a single force F_x

Suppose that a single force F_x is applied to the force/torque sensor. Then,

If beam OA produces compressive deformation, the output of the strain gauges is denoted by S_5;

If beam OC produces tensile deformation, the output of the strain gauges is denoted by S_7;

If beam AE produces bending deformation, the output of the strain gauges is denoted by S_1;

If beam CG produces bending deformation, the output of the strain gauges is denoted by S_3;

Beams OB, BF, OD and DH are under bending moment in the flank of the beam. If the strain gauges are glued at the neutral axis of the beam, the output of the strain gauges is zero [45]. Therefore, the outputs of the strain gauges glued on the beam OB, BF, OD, and DH are zero:

$$S_2 = S_4 = S_6 = S_8 = 0 \tag{2.26}$$

Next, the relation between S_1, S_3, S_5, and S_7 are analyzed. Because the elastic body of the sensor is symmetric, the sizes of the tensile (or compressive) stress of beam OC and that of beam OA are equal, but the direction of the stress of beam OC and that of beam OA are opposite. The sizes of the bending stress at the strain gauges of beam AE and beam CG are equal, but their directions are opposite. Hence the following equations can be deduced:

$$S_1 = -S_3 \tag{2.27}$$

$$S_5 = -S_7 \tag{2.28}$$

The stresses at the center position of the beam OA and OC are:

$$\sigma_{5,7} = \frac{Force}{Cross \quad Sectional \quad Area} = \frac{\frac{F_{x1}}{2}}{bh} = \frac{F_{x1}}{2bh} \tag{2.29}$$

The stresses at the center position of the beam AE and CG are:

$$\sigma_{1,3} = \frac{My}{I} = \frac{\frac{F_{x1}}{2} \times H \times \frac{h}{2}}{\frac{bh^3}{12}} = \frac{3F_{x1}H}{bh^2} \tag{2.30}$$

Here F_{x1} is the component force along the x-axis of the single force F_x in the horizontal crossbeam (Figure 2.4).

$$\frac{\sigma_{5,7}}{\sigma_{1,3}} = \frac{\frac{F_{x1}}{2bh}}{\frac{3F_{x1}H}{bh^2}} = \frac{h}{6H} \tag{2.31}$$

The stress and strain relationship is:

$$S = \frac{\sigma}{E} \tag{2.32}$$

where E is Young's Modulus.

Thus

$$\frac{S_5}{S_1} = \frac{S_7}{S_3} = \frac{h}{6H} \tag{2.33}$$

Combining equation (2.24), (2.26) to (2.33), the force vector F is determined by:

$$F = \begin{bmatrix} F_x \\ F_y \\ F_z \\ M_x \\ M_y \\ M_z \end{bmatrix} = \begin{bmatrix} K_1(S_1 - S_3 + S_5 + S_7) \\ 0 \\ 0 \\ 0 \\ K_5(S_5 - S_7) \\ 0 \end{bmatrix} = 2\begin{bmatrix} K_1S_1 \\ 0 \\ 0 \\ 0 \\ K_5S_5 \\ 0 \end{bmatrix} \tag{2.34}$$

Equation (2.34) shows that when a single force F_x is applied to the force/torque sensor, there is an interference output at the M_y component. The cross-sensitivity can be expressed as:

$$\frac{M_y}{F_x} = \frac{K_5 S_5}{K_1 S_1} = \frac{K_5 h}{6 K_1 H} \tag{2.35}$$

The size of the cross-sensitivity depends on the parameter of the elastic body. For the general case, the structure parameters K_1 and K_5 selected in this design are almost equal and h /H < 1/10. Thus $M_y/F_x < 1/60$, and hence the cross-sensitivity of the force sensor can be ignored.

Equation (2.34) becomes:

$$F = \begin{bmatrix} F_x \\ F_y \\ F_z \\ M_x \\ M_y \\ M_z \end{bmatrix} = \begin{bmatrix} 2K_1 S_1 \\ 0 \\ 0 \\ 0 \\ 0 \\ 0 \end{bmatrix} = -\begin{bmatrix} 2K_1 S_3 \\ 0 \\ 0 \\ 0 \\ 0 \\ 0 \end{bmatrix} \tag{2.36}$$

2.3.2 The condition when applying a single force F_y

Suppose that a single force F_y is applied to the force/torque sensor (see Figure 2.4).

If beam OB produces tensile deformation, the output of the strain gauges is denoted S_6;

If beam OD produces compressive deformation, the output of the strain gauges is denoted by S_8;

If beam BF produces bending deformation, the output of the strain gauges is denoted S_2;

If beam DH produces bending deformation, the output of the strain gauges is denoted by S_4;

Beams OA, AE, OC and CG are under bending moment in the flank of the beam. The strain gauges are glued at the neutral axis of the beam, and hence the output of the strain gauges is zero. Therefore, the outputs of the strain gauges glued on the beam OA, AE, OC and CG are zero:

$$S_1 = S_3 = S_5 = S_7 = 0 \tag{2.37}$$

Next, the relation between S_2, S_4, S_6, and S_8 are analyzed. Because the elastic body of the sensor is symmetric, the sizes of the tensile (or compressive) stress of beam OB and that of beam OD are equal, but the direction of the stress of beam OB and that of beam OD are opposite. The sizes of the bending stress at the strain gauges of beam BF and beam DH are equal, but their directions are opposite. Hence the following equations can be deduced:

$$S_2 = -S_4 \tag{2.38}$$

$$S_6 = -S_8 \tag{2.39}$$

The stresses at the center of the beams OB and OD are:

$$\sigma_{6,8} = \frac{Force}{Area} = \frac{\frac{F_{y1}}{2}}{bh} = \frac{F_{y1}}{2bh} \tag{2.40}$$

The stresses at the center of the beam BF and DH:

$$\sigma_{2,4} = \frac{My}{I} = \frac{\frac{F_{y1}}{2} \times H \times \frac{h}{2}}{\frac{bh^3}{12}} = \frac{3F_{y1}H}{bh^2} \tag{2.41}$$

where F_{y1} is the component force of the y-axis of the single force F_y in the horizontal crossbeam.

$$\frac{\sigma_{6,8}}{\sigma_{2,4}} = \frac{\frac{F_{y1}}{2bh}}{\frac{3F_{y1}H}{bh^2}} = \frac{h}{6H} \tag{2.42}$$

Similarly, according to equation (2.38), (2.39), (2.42), the following equation is obtained:

$$\frac{S_6}{S_2} = \frac{S_8}{S_4} = \frac{h}{6H} \tag{2.43}$$

Combining equation (2.24), (2.37) to (2.43), the force vector F is determined by

$$F = \begin{bmatrix} F_x \\ F_y \\ F_z \\ M_x \\ M_y \\ M_z \end{bmatrix} = \begin{bmatrix} 0 \\ K_2(S_4 - S_2 + S_8 + S_6) \\ 0 \\ K_4(S_8 - S_6) \\ 0 \\ 0 \end{bmatrix} = 2\begin{bmatrix} 0 \\ K_2 S_4 \\ 0 \\ K_4 S_8 \\ 0 \\ 0 \end{bmatrix} \tag{2.44}$$

Equation (2.44) shows that when a single force F_y is applied to the force/torque sensor, there is an interference output at the M_x component. The cross-sensitivity can be expressed as:

$$\frac{M_x}{F_y} = \frac{K_4 S_8}{K_2 S_4} = \frac{K_4 h}{6K_2 H} \tag{2.45}$$

The size of the cross-sensitivity depends on the parameter of the elastic body. For the general case, the structural parameters K_2 and K_4 selected in this design are almost

equal and h /H < 1/10. Thus $M_x/F_x < 1/60$, and hence the cross-sensitivity of the force sensor can be ignored. Equation (2.44) becomes:

$$F = \begin{bmatrix} F_x \\ F_y \\ F_z \\ M_x \\ M_y \\ M_z \end{bmatrix} = \begin{bmatrix} 0 \\ 2K_2S_4 \\ 0 \\ 0 \\ 0 \\ 0 \end{bmatrix} = -\begin{bmatrix} 0 \\ 2K_2S_2 \\ 0 \\ 0 \\ 0 \\ 0 \end{bmatrix} \tag{2.46}$$

2.3.3 The condition when applying a single force F_z:

Suppose that a single force F_z is applied to the force/torque sensor (see Figure 2.4). Beam OA, OB, OC and OD produce bending deformation. Considering the elastic body of the force sensor frame to be symmetric, the bending stresses at the strain gauges of the four horizontal beams are equal.

Hence

$$S_5 = S_6 = S_7 = S_8 \tag{2.47}$$

The stresses at the center position of the beams OA, OB, OC and OD are:

$$\sigma_{5678} = \frac{My}{I} = \frac{\frac{F_z}{4} \times L_2 \times \frac{h}{2}}{\frac{bh^3}{12}} = \frac{6F_z L_2}{4bh^2} \tag{2.48}$$

Beam AE, BF, CG and DH produce compressive deformation and the compressive stresses at the strain gauges of the four vertical beams are equal.

Therefore

$$S_1 = S_2 = S_3 = S_4 \tag{2.49}$$

The stresses at the center of the beams AE, BF, CG and DH are:

$$\sigma_{1234} = \frac{Force}{Area} = \frac{\frac{F_z}{4}}{bh} = \frac{F_z}{4bh} \tag{2.50}$$

Thus

$$\frac{\sigma_{1234}}{\sigma_{5678}} = \frac{\frac{F_z}{4bh}}{\frac{6F_zL_2}{4bh^2}} = \frac{h}{6L_2} \tag{2.51}$$

Similarly, according to equation (2.47), (2.49), (2.51), the following equation is obtained:

$$\frac{S_1}{S_5} = \frac{S_2}{S_6} = \frac{S_3}{S_7} = \frac{S_4}{S_8} = \frac{h}{6L_2} \tag{2.52}$$

Combining the equations (2.24), equation (2.47) to (2.52)

The formula of force vector F is determined by:

$$F = \begin{bmatrix} F_x \\ F_y \\ F_z \\ M_x \\ M_y \\ M_z \end{bmatrix} = \begin{bmatrix} 0 \\ 0 \\ 4K_3(S_5 + S_1) \\ 0 \\ 0 \\ 0 \end{bmatrix} \tag{2.53}$$

Equation (2.53) shows that when a single force F_z is applied to the force/torque sensor frame.

If the structure is designed to satisfy the condition $h/L_2 < 1/10$, $S_1/S_5 < 1/60$, then the force vector F in equation (2.53) can be expressed as:

$$F = \begin{bmatrix} F_x \\ F_y \\ F_z \\ M_x \\ M_y \\ M_z \end{bmatrix} = \begin{bmatrix} 0 \\ 0 \\ 4K_3S_5 \\ 0 \\ 0 \\ 0 \end{bmatrix} \quad (2.54)$$

2.3.4 The condition when applying a single moment M_x:

Let a single moment M_x be applied to the force/torque sensor (see Figure 2.4). Beam OA and beam OC produce twisting deformation. Because the sensor frame is symmetric, the output of the strain gauges glued on these two beams is so small that it can be neglected.

$$S_5 = S_7 = 0 \quad (2.55)$$

Beam AE and beam CG are under bending moment in the flank of the beam. The condition of stress is:

$$S_1 = S_3 = 0 \quad (2.56)$$

Beam OB and beam OD produce bending deformation. The magnitude of the bending stress at the strain gauges of these two beams are equal and their directions are opposite. Hence,

$$S_6 = -S_8 \quad (2.57)$$

The stresses at the strain gauges of beam OB and beam OD are:

$$\sigma_{68} = \frac{My}{I} = \frac{\frac{M_{x1}L_1}{2R} \times \frac{h}{2}}{\frac{bh^3}{12}} = \frac{6M_{x1}L_1}{2Rbh^2} \quad (2.58)$$

Beam BF and beam DH produce tensile (or compressive) deformation, and the magnitude of the tensile (or compressive) stress at the strain gauges of these two beams are equal and opposite in direction:

$$S_2 = -S_4 \tag{2.59}$$

The stresses at the center of the beam BF and beam DH are:

$$\sigma_{24} = \frac{Force}{Area} = \frac{\frac{M_{x1}}{2R}}{bh} = \frac{M_{x1}}{2Rbh} \tag{2.60}$$

where M_{x1} is the single moment M_x applied on beam OB, OD, BF and DH.

From Equation (2.58) and (2.60)

$$\frac{\sigma_{24}}{\sigma_{68}} = \frac{h}{6L_1} \tag{2.61}$$

Hence

$$\frac{S_2}{S_6} = \frac{S_4}{S_8} = \frac{h}{6L_1} \tag{2.62}$$

Combining the equation (2.24), equation (2.55) to (2.62), the force vector formula of force vector F can be obtained when a single moment M_x applied, is

$$F = \begin{bmatrix} F_x \\ F_y \\ F_z \\ M_x \\ M_y \\ M_z \end{bmatrix} = \begin{bmatrix} 0 \\ 2K_2S_2 \\ 0 \\ 2K_4S_6 \\ 0 \\ 0 \end{bmatrix} \tag{2.63}$$

Equation (2.63) shows that when a single moment M_x is applied to the force/torque sensor, there is an interference output in the F_y component. The cross-sensitivity can be expressed as:

$$\frac{F_y}{M_x} = \frac{2K_2S_2}{2K_4S_6} = \frac{K_2h}{6K_4L_1} \tag{2.64}$$

The size of the cross-sensitivity depends on the parameters of the elastic body. In general, the structure parameters K_2 and K_4 selected are almost equal and $h/L_1 < 1/10$. Thus $F_y/M_x < 1/60$, and hence the cross-sensitivity of the force sensor can be neglected. The force vector F becomes:

$$F = \begin{bmatrix} F_x \\ F_y \\ F_z \\ M_x \\ M_y \\ M_z \end{bmatrix} = \begin{bmatrix} 0 \\ 0 \\ 0 \\ 2K_4S_6 \\ 0 \\ 0 \end{bmatrix} \tag{2.65}$$

2.3.5 The condition when applying a single moment M_y:

If a single moment M_y is applied to the force/torque sensor (see Figure 2.4), then beam OB and beam OD produce twisting deformation. Because the sensor is symmetric, the output of the strain gauges glued on these two beams is so small that it can be neglected.

$$S_6 = S_8 = 0 \tag{2.66}$$

Beam BF and beam DH are under bending moment in the flank of the beam. The condition of stress is:

$$S_2 = S_4 = 0 \tag{2.67}$$

Beam OA and beam OC produce bending deformation. The sizes of the bending stress at the strain gauges of these two beams are equal and their directions are opposite. Accordingly,

$$S_5 = -S_7 \tag{2.68}$$

The stresses at the strain gauges of beam OA and beam OC are:

$$\sigma_{57} = \frac{My}{I} = \frac{\frac{M_{y1}L_1}{2R} \times \frac{h}{2}}{\frac{bh^3}{12}} = \frac{6M_{y1}L_1}{2Rbh^2} \tag{2.69}$$

Beam AE and beam CG produce tensile (or compressive) deformation, and the size of the tensile (or compressive) stress at the strain gauges of these two beams are equal and opposite in direction:

$$S_1 = -S_3 \tag{2.70}$$

The stresses at the strain gauges of beam AE and beam CG are:

$$\sigma_{13} = \frac{Force}{Area} = \frac{\frac{M_{y1}}{2R}}{bh} = \frac{M_{y1}}{2Rbh} \tag{2.71}$$

here M_{y1} is the single moment M_y in beam OA, OC, AE and CG.

From Equation (2.69) and (2.71)

$$\frac{\sigma_{13}}{\sigma_{57}} = \frac{h}{6L_1} \tag{2.72}$$

Hence

$$\frac{S_1}{S_5} = \frac{S_3}{S_7} = \frac{h}{6L_1} \tag{2.73}$$

Combining the equation (2.24), equation (2.66) to (2.73), the force vector formula of force vector F when applying a single moment M_y is obtained:

$$F = \begin{bmatrix} F_x \\ F_y \\ F_z \\ M_x \\ M_y \\ M_z \end{bmatrix} = \begin{bmatrix} 2K_1S_1 \\ 0 \\ 0 \\ 0 \\ 2K_5S_5 \\ 0 \end{bmatrix} \tag{2.74}$$

Equation (2.74) shows that when a single moment M_y is applied to the force/torque sensor, there is an interference output at the F_x component. The cross-sensitivity can be expressed as:

$$\frac{F_x}{M_y} = \frac{2K_1S_1}{2K_5S_5} = \frac{K_1h}{6K_5L_1} \tag{2.75}$$

The size of the cross-sensitivity depends on the parameters of the elastic body. In general, the structure parameters K_1 and K_5 selected in this design are almost equal and $h/L_1 < 1/10$. Thus $F_x/M_y < 1/60$, and hence the cross-sensitivity of the force sensor can be neglected.

The force vector F becomes:

$$F = \begin{bmatrix} F_x \\ F_y \\ F_z \\ M_x \\ M_y \\ M_z \end{bmatrix} = \begin{bmatrix} 0 \\ 0 \\ 0 \\ 0 \\ 2K_5S_5 \\ 0 \end{bmatrix} \tag{2.76}$$

2.3.6 The condition when applying a single moment M_z

When a single moment M_z is applied to the force/torque sensor, see Figure 2.4, beam OA, OB, OC and OD are under bending moment in the flank of the beam. Hence the output of strain gauges glued on beams OA, OB, OC and OD are zero:

$$S_5 = S_6 = S_7 = S_8 = 0 \tag{2.77}$$

The stress conditions of beams AE, BF, CG and DH are much more complicated. These beams are subjected to a twisting moment as well as to a bending moment in the flank of the beam. According to Weiyi Huang et al [46], applying a bending moment in the flank of the beam produces no output of the strain gauges, the flank bending moment can be neglected.

$$S_1 = S_2 = S_3 = S_4 = 0 \tag{2.78}$$

Only the output of the strain gauges due to the twisting deformation can be considerable.

In this force/torque sensor, two strain gauges are used to form a torque gauge applied in a half bridge. One is positioned so as to be sensitive to the principal compressive strain, and the other observes the principal tensile strain. Note that in the absence of bending moments and axial forces, the principal stress planes lie perpendicular to one another at 45°to the plane about which the tensional moment is applied.

Torque is measured by either sensing the actual shaft deflection caused by a twisting force, or by detecting the effects of this deflection. The surface of a shaft under torque will experience compression and tension, as shown in Figure 2.5. To measure

torque, strain gauge elements usually are mounted in pairs on the shaft, one gauge measuring the increase in length (in the direction in which the surface is under tension), the other measuring the decrease in length in the other direction.

A strain gauge can be installed directly on a shaft because the shaft is rotating. The strain gauges S_9 and S_{10} are fixed on one of vertical beams. They can measure the vertical beam tensile (or compressive) deformation, and the size of the tensile (or compressive) stress at the strain gauges of vertical beams is equal and opposite in direction.

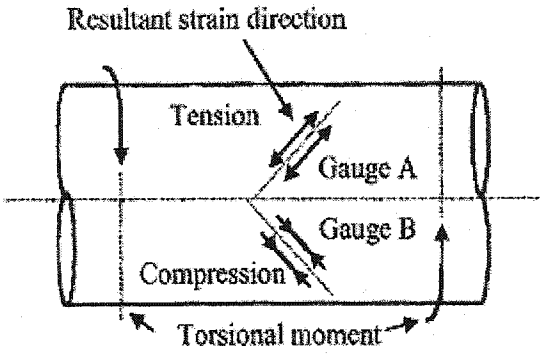

Figure2.5 The Location of Torsion Gauge

$$S_9 = -S_{10} \tag{2.79}$$

According to Alexander Blake [47], the shear stresses at the strain gauges of vertical beam are:

$$\sigma_{9,10} = \frac{Force}{Area} = \frac{3\times\frac{M_{z1}}{4R}}{2bh} = \frac{3M_{z1}}{8Rbh} \tag{2.80}$$

here M_{z1} is the single moment M_z in beams AE, BF, CG and DH.

The force vector formula when applying a single moment M_z is given by:

$$F = \begin{bmatrix} F_x \\ F_y \\ F_z \\ M_x \\ M_y \\ M_z \end{bmatrix} = \begin{bmatrix} 0 \\ 0 \\ 0 \\ 0 \\ 0 \\ 2K_6S_9 \end{bmatrix} \tag{2.81}$$

Therefore, from above analysis, equation (2.24) becomes:

$$F = \begin{bmatrix} F_x \\ F_y \\ F_z \\ M_x \\ M_y \\ M_z \end{bmatrix} = \begin{bmatrix} K_1(S_1 - S_3) \\ K_2(S_2 - S_4) \\ K_3(S_5 + S_6 + S_7 + S_8) \\ K_4(S_6 - S_8) \\ K_5(S_5 - S_7) \\ K_6(S_9 - S_{10}) \end{bmatrix} \tag{2.82}$$

Equation (2.82) enforces the basic input/output relation for the force/torque sensor.

2.4 The Dimension of the Sensor

The dimensions of the sensor frame are chosen with the following constraints that were used in the design,

1. $\frac{h}{H} \leq \frac{1}{10}$

2. $\frac{h}{L_2} \leq \frac{1}{10}$

3. $\frac{h}{L_1} \leq \frac{1}{10}$

After many trails, taking into consideration the above constraints, material availability and machining limitation, the following dimensions are chosen,

b = 6 mm

h = 1 mm

H = 20 mm

S = 35 mm

L1 = 10 mm

L2 = 11 mm

2.5 The coefficients of the sensor

From Equation (2.82)

$$F = \begin{bmatrix} F_x \\ F_y \\ F_z \\ M_x \\ M_y \\ M_z \end{bmatrix} = \begin{bmatrix} K_1(S_1 - S_3) \\ K_2(S_2 - S_4) \\ K_3(S_5 + S_6 + S_7 + S_8) \\ K_4(S_6 - S_8) \\ K_5(S_5 - S_7) \\ K_6(S_9 - S_{10}) \end{bmatrix} \quad (2.82)$$

The following equation can be obtained:

$$F = \begin{bmatrix} K_1 & 0 & -K_1 & 0 & 0 & 0 & 0 & 0 & 0 & 0 \\ 0 & K_2 & 0 & -K_2 & 0 & 0 & 0 & 0 & 0 & 0 \\ K_3 & K_3 & K_3 & K_3 & 0 & 0 & 0 & 0 & 0 & 0 \\ 0 & 0 & 0 & 0_4 & 0 & K_4 & 0 & -K_4 & 0 & 0 \\ 0 & 0 & 0 & 0 & K_5 & 0 & -K_5 & 0 & 0 & 0 \\ 0 & 0 & 0 & 0 & 0 & 0 & 0 & 0 & K_6 & -K_6 \end{bmatrix} \begin{bmatrix} S_1 \\ S_2 \\ S_3 \\ S_4 \\ S_5 \\ S_6 \\ S_7 \\ S_8 \\ S_9 \\ S_{10} \end{bmatrix} \quad (2.83)$$

The above equation is rewritten in the following form

$$\begin{bmatrix} S_1 \\ S_2 \\ S_3 \\ S_4 \\ S_5 \\ S_6 \\ S_7 \\ S_8 \\ S_9 \\ S_{10} \end{bmatrix} = \begin{bmatrix} K_1 & 0 & -K_1 & 0 & 0 & 0 & 0 & 0 & 0 & 0 \\ 0 & K_2 & 0 & -K_2 & 0 & 0 & 0 & 0 & 0 & 0 \\ K_3 & K_3 & K_3 & K_3 & 0 & 0 & 0 & 0 & 0 & 0 \\ 0 & 0 & 0 & 0 & 0 & K_4 & 0 & -K_4 & 0 & 0 \\ 0 & 0 & 0 & 0 & K_5 & 0 & -K_5 & 0 & 0 & 0 \\ 0 & 0 & 0 & 0 & 0 & 0 & 0 & 0 & K_6 & -K_6 \end{bmatrix}^{-1} \begin{bmatrix} F_x \\ F_y \\ F_z \\ M_x \\ M_y \\ M_z \end{bmatrix}$$

(2.84)

The following relations can be deduced:

$$F_x = K_1(S_1 - S_3) \qquad S_1 = -S_3$$

$$F_x = 2K_1S_1$$

$$S_1 = -S_3 = \frac{F_x}{2K_1} \tag{2.85}$$

$$F_y = K_2(S_2 - S_4) \qquad S_2 = -S_4$$

$$F_y = 2K_2S_2$$

$$S_2 = -S_4 = \frac{F_y}{2K_2} \tag{2.86}$$

$$F_z = K_3(S_5^1 + S_6^1 + S_7^1 + S_8^1) \qquad S_5^1 = S_6^1 = S_7^1 = S_8^1$$

where superscript "1" indicates that readouts of the fifth, sixth, seventh, eighth micro strain gauges when force is applied in Z direction.

$$F_z = 4k_3S_5^1$$

$$S_5^1 = S_6^1 = S_7^1 = S_8^1 = \frac{F_z}{4K_3} \tag{2.87}$$

$$M_x = K_4(S_6^2 - S_8^2) \qquad S_6^2 = -S_8^2$$

where superscript "2" indicates that readouts of the sixth, eighth micro strain gauges when torque is applied in along X direction.

$$M_x = 2K_4S_6^2$$

$$S_6^2 = -S_8^2 = \frac{M_x}{2K_4} \tag{2.88}$$

$$M_y = K_5(S_5^2 - S_7^2) \qquad S_5^2 = -S_7^2$$

where superscript "2" indicates that readouts of the fifth, seventh, micro strain gauges when torque is applied along Y direction.

$$M_y = 2K_5 S_5^2$$

$$S_5^2 = -S_7^2 = \frac{M_y}{2K_5} \tag{2.89}$$

$$M_z = K_6(S_9 - S_{10}) \qquad S_9 = -S_{10}$$

$$M_z = 2K_6 S_9$$

$$S_9 = -S_{10} = \frac{M_z}{2K_6} \tag{2.90}$$

From Equations (2.85) to (2.90), the following equations can be obtained

$$S_1 = -S_3 = \frac{F_x}{2K_1} \tag{2.91}$$

$$S_2 = -S_4 = \frac{F_y}{2K_2} \tag{2.92}$$

$$S_5 = S_5^1 + S_5^2 = \frac{F_z}{4K_3} + \frac{M_y}{2K_5} \tag{2.93}$$

$$S_6 = S_6^1 + S_6^2 = \frac{F_z}{4K_3} + \frac{M_x}{2K_4} \tag{2.94}$$

$$S_7 = S_7^1 + S_7^2 = \frac{F_z}{4K_3} - \frac{M_y}{2K_5} \tag{2.95}$$

$$S_8 = S_8^1 + S_8^2 = \frac{F_z}{4K_3} - \frac{M_x}{2K_4} \tag{2.96}$$

$$S_9 = -S_{10} = \frac{M_z}{2K_6} \tag{2.97}$$

Solving for the coefficient from equations (2.91) to (2.97), the parameter of the sensor is obtained:

$$K_1 = \frac{F_x}{2S_1} \tag{2.98}$$

$$K_2 = \frac{F_y}{2S_2} \tag{2.99}$$

$$K_3 = \frac{F_z}{4K_5^1} \tag{2.100}$$

$$K_4 = \frac{M_x}{2S_6^2} \tag{2.101}$$

$$K_5 = \frac{M_y}{2S_5^2} \tag{2.102}$$

$$K_6 = \frac{M_z}{2S_9} \tag{2.103}$$

The coefficient of the sensor are obtained as:

$K_1 = 5.1675*10^5$

$K_2 = 5.1675*10^5$

$K_3 = 9.3955*10^5$

$K_4 = 2.17035*10^7$

$K_5 = 2.17035*10^7$

$K_6 = 4.134*10^7$

2.6 Calibration Matrix

According to equation (2.85)-(2.97), the following equation is obtained:

$$\varepsilon = Cf \tag{2.104}$$

$$\begin{bmatrix} S_1 \\ S_2 \\ S_3 \\ S_4 \\ S_5 \\ S_6 \\ S_7 \\ S_8 \\ S_9 \\ S_{10} \end{bmatrix} = \begin{bmatrix} \frac{1}{2K_1} & 0 & 0 & 0 & 0 & 0 \\ 0 & \frac{1}{2K_2} & 0 & 0 & 0 & 0 \\ -\frac{1}{2K_1} & 0 & 0 & 0 & 0 & 0 \\ 0 & -\frac{1}{2K_2} & 0 & 0 & 0 & 0 \\ 0 & 0 & \frac{1}{4K_3} & 0 & \frac{1}{2K_5} & 0 \\ 0 & 0 & \frac{1}{4K_3} & \frac{1}{2K_4} & 0 & 0 \\ 0 & 0 & \frac{1}{4K_3} & 0 & -\frac{1}{2K_5} & 0 \\ 0 & 0 & \frac{1}{4K_3} & -\frac{1}{2K_4} & 0 & 0 \\ 0 & 0 & 0 & 0 & 0 & \frac{1}{2K_6} \\ 0 & 0 & 0 & 0 & 0 & -\frac{1}{2K_6} \end{bmatrix} \begin{bmatrix} F_x \\ F_y \\ F_z \\ M_x \\ M_y \\ M_z \end{bmatrix} \tag{2.105}$$

The C matrix is:

$$\begin{bmatrix}
\frac{1}{2K_1} & 0 & 0 & 0 & 0 & 0 \\
0 & \frac{1}{2K_2} & 0 & 0 & 0 & 0 \\
-\frac{1}{2K_1} & 0 & 0 & 0 & 0 & 0 \\
0 & -\frac{1}{2K_2} & 0 & 0 & 0 & 0 \\
0 & 0 & \frac{1}{4K_3} & 0 & \frac{1}{2K_5} & 0 \\
0 & 0 & \frac{1}{4K_3} & \frac{1}{2K_4} & 0 & 0 \\
0 & 0 & \frac{1}{4K_3} & 0 & -\frac{1}{2K_5} & 0 \\
0 & 0 & \frac{1}{4K_3} & -\frac{1}{2K_4} & 0 & 0 \\
0 & 0 & 0 & 0 & 0 & \frac{1}{2K_6} \\
0 & 0 & 0 & 0 & 0 & -\frac{1}{2K_6}
\end{bmatrix} \tag{2.106}$$

Substituting the values into the equation (2.106), the C matrix is:

$$\begin{bmatrix} 48.3793 & 0 & 0 & 0 & 0 & 0 \\ 0 & 48.3793 & 0 & 0 & 0 & 0 \\ -48.3793 & 0 & 0 & 0 & 0 & 0 \\ 0 & -48.3793 & 0 & 0 & 0 & 0 \\ 0 & 0 & 13.3042 & 0 & 115.189 & 0 \\ 0 & 0 & 13.3042 & 115.189 & 0 & 0 \\ 0 & 0 & 13.3042 & 0 & -115.189 & 0 \\ 0 & 0 & 13.3042 & -115.189 & 0 & 0 \\ 0 & 0 & 0 & 0 & 0 & 30.237 \\ 0 & 0 & 0 & 0 & 0 & -30.237 \end{bmatrix} \times 10^{-8} \quad (2.107)$$

Then the Moore-Penrose pseudo-inverse matrix is calculated to be:

$$C^{+} = (C^{T}C)^{-1}C \quad (2.108)$$

$$C^{+} = \begin{bmatrix} 1.04 & -1.04 & 0 & 0 & 0 & 0 & 0 & 0 & 0 & 0 \\ 0 & 1.04 & 0 & -1.04 & 0 & 0 & 0 & 0 & 0 & 0 \\ 0 & 0 & 0 & 0 & 1.88 & 1.88 & 1.88 & 1.88 & 0 & 0 \\ 0 & 0 & 0 & 0 & 0 & 0.44 & 0 & -0.44 & 0 & 0 \\ 0 & 0 & 0 & 0 & 0.44 & 0 & -0.44 & 0 & 0 & 0 \\ 0 & 0 & 0 & 0 & 0 & 0 & 0 & 0 & 1.65 & -1.65 \end{bmatrix} \times 10^{6} \quad (2.109)$$

C^{+} is calibration matrix.

From the above analysis, the six-degree of freedom force/torque sensor is designed so as to satisfy the measurement requirements.

In the following chapter, Finite Element Method will be used to analyze the sensor frame, and the result will be compared with those presented in this chapter.

Chapter 3

Finite Element Method Model

In Chapter 2, the mathematical model of the six-degree of freedom sensor was described and the beam theory was employed to analyze the stress of the sensor frame. Then the calibration matrix was obtained. In the following, the stresses in the sensor frame will be analyzed with Finite Element Method. The results will be compared with those obtained in Chapter 2.

3.1 Finite Element Method Model

Applying the beam theory to the sensor structure is acceptable for design purposes. However, in order to get more accurate results for such a complex structure, the finite element method will be used. [48,49]

The finite element method provides an excellent tool to analyze a given force sensor design and to introduce the necessary modifications for a better design. By creating a detailed and accurate finite element model the analyst can estimate the response of given design, calculate the strains at the desired points, and get the corresponding calibration matrix. The process may be repeated for several different designs, under the given loading conditions, until the desired singular values are

obtained.

The steps followed in finite element method are presented below:

(1) Finite element mesh generation: Divide the domain into sub-domains. Each sub-domain is called an element. The elements are interconnected to each other at points called nodes.

(2) Element equations: A typical element is isolated and it requires proper equations to describe its properties. Seek an approximation to the solution as a linear combination of nodal values and approximation functions. The equation is called element equation.

In general, an approximate solution u will be sought to be a differential equation in the form [50]:

$$u = \sum_{j=1}^{n} u_j \psi_j + \sum_{j=1}^{m} c_j \phi_j \qquad (3.1)$$

where u_j are the values of u at the element nodes, Ψ_j are the interpolation functions, c_j are the nodeless coefficients, and Φ_j are the associated approximation functions. A weighted-integral form of the governing differential equation provides one such procedure.

(3) Assembly of element equations and solution: The approximate value of the domain is obtained by putting together the element properties in a meaningful way. This process is called the assembly of the element equations.

(4) Convergence and error estimate

Using the finite element analysis the force/torque sensor is modeled as an

assemblage of discrete elements interconnected at the nodal points on the element boundaries. The displacement field within each element is assumed to be a connection of the displacements at the nodes. Therefore the displacement element field is defined as:

$$u(x, y, z) = H(x, y, z)u_n \tag{3.2}$$

where H(x,y,z) is the displacement interpolation matrix and u_n is a vector containing the nodal displacements.

The right choice of the interpolation functions depends on the elastic model selected for each particular case. The application of the compatibility relationships between strains and displacements yields:

$$\varepsilon(x, y, z) = B(x, y, z)u_n \tag{3.3}$$

where the matrix B(x,y,z) is obtained by proper differentiation of the terms of the matrix H(x,y,z). The constitutive relations of the material render:

$$\sigma(x, y, z) = D(x, y, z)\varepsilon(x, y, z) \tag{3.4}$$

where σ is the stress field, and D(x,y,z) is the elastic matrix whose terms depend on the material properties.

The principle of virtual work can then be applied to set up the equations of equilibrium in an integral form.

$$\sum_i \int_V \varepsilon^{(i)T} \sigma^{(i)} dV^{(i)} = \sum_j u^{(j)T} F^{(j)} \tag{3.5}$$

where summation on i is carried over the number of elements and the summation on j is carried over the number of nodal forces. The integration on V (Volume) is carried over each element. Proper integration and final assemblage of these equations will yield the

structural stiffness matrix and force vector. The assembled system of equations becomes:

$$KU = F \tag{3.6}$$

where K is the total stiffness matrix. U is the nodal displacement vector and F is the force vector. The solution of the system of equation (3.6) for the specified design loads will render the nodal displacements. Direct application of equation (3.3) gives the desired strains and allows the building of the calibration matrix.

A detailed description of the finite element method and the derivation of the above- mentioned matrices are given by J.N. Reddy [51].

3.2 Element Type

In the present application, Model solid 45 in ANSYS (Finite Element Commercial Software) is chosen. SOLID 45-3-D Structural Solid is used for the three-dimensional modeling of solid structures. The element is defined by eight nodes having three degrees of freedom at each node and the orthotropic material properties [52]. Orthotropic material directions correspond to the element coordinate directions: translations in the nodal x, y, and z directions.

The element has plasticity, creep, swelling, stress stiffening, large deflection, and large strain capabilities. A reduced integration option with hourglass control is available. The element is defined by eight nodes.

The geometry, node locations, and the coordinate system for this element are shown in Figure 3.1.

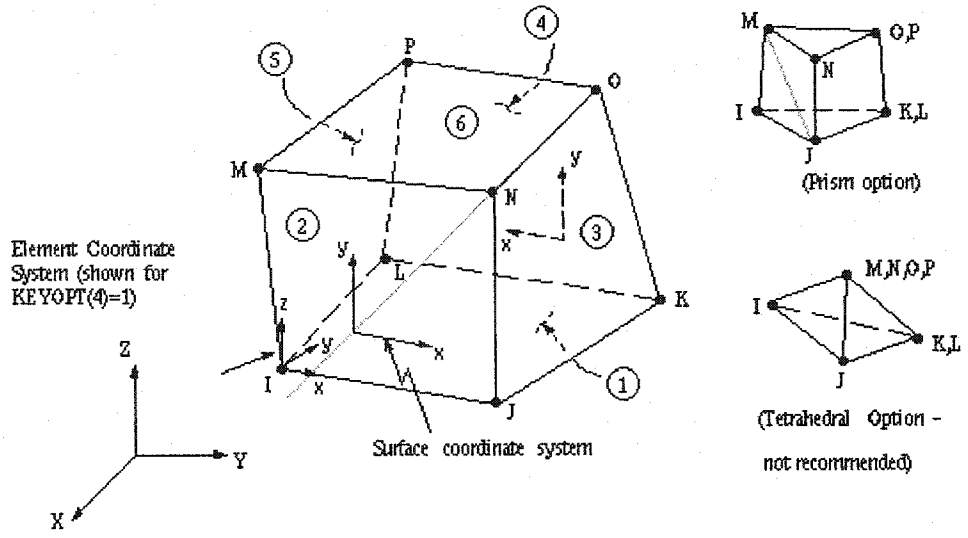

Figure 3.1 SOLID45 3-D Structural

3.3 The Adaptive Mesh

The ANSYS program provides approximate techniques for automatically estimating mesh discretization error for certain types of analyses. Using this measure of mesh discretization error, the program can then determine if a particular mesh is fine enough. If it is not, the program will automatically refine the mesh so that the measured error will decrease. This process of automatically evaluating mesh discretization error and refining the mesh, called *adaptive meshing*, continues through a series of solutions until the measured error drops below some user-defined value (or until a user-defined limit on the number of solutions is reached).

The ANSYS program includes a prewritten macro, ADAPT.MAC, to perform adaptive meshing. The model must satisfy certain preconditions before it can successfully activate the ADAPT. macro. These requirements include the following:

- The standard ADAPT procedure is valid only for single-solution linear static structural and linear steady-state thermal analyses.
- The model should preferably use only *one* material type, as the error calculations are based in part on *average* nodal stresses, and would thus often be invalid at the material interfaces. Also, an element's error energy is affected by its elastic modulus. Therefore, even if the stress discontinuity is the same in two adjoining elements, their error energy will be different if they have different material properties. Abrupt changes in shell thickness should be avoided since such discontinuities will cause similar stress-averaging problems.
- The model must use element types that support error calculations.
- The model must be built using *meshable* solid model entities characteristics that will cause meshing failure must not be built into our model.

In the FEM model of the sensor frame, free volume method is applied to mesh.

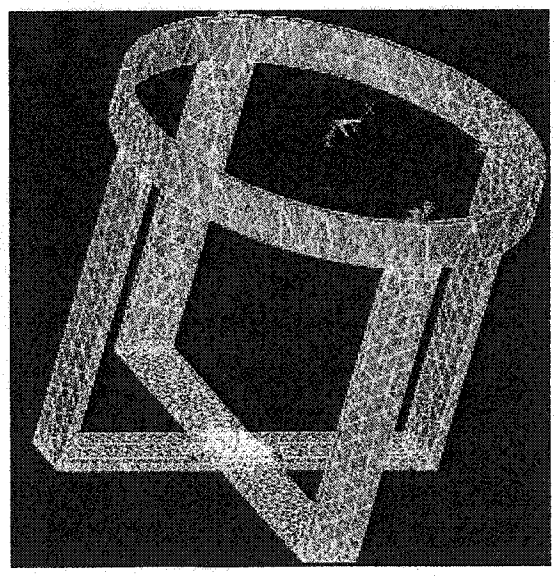

Figure 3.2 The mesh of sensor structure

3.4 Loads and Solution

Loadings are defined to be of two types: nodal and element. *Nodal loads* are defined at the nodes and are not directly related to the elements. These nodal loads are associated with the degrees of freedom at the node. *Element loads* are surface loads, body loads, and inertia loads. Element loads are always associated with a particular element (even if the input is at the nodes).

The solution output associated with the element is in two forms:

- Nodal displacements included in the overall nodal solution
- Additional element output

Several items are illustrated in Figure 3.3. The element stress directions are parallel to the element coordinate system. The surface stress outputs are in the surface coordinate systems and are available for any face. The coordinate systems for faces IJNM and KLPO are shown in Figure 3.1. The other surface coordinate systems follow similar orientations as indicated by the pressure face node description.

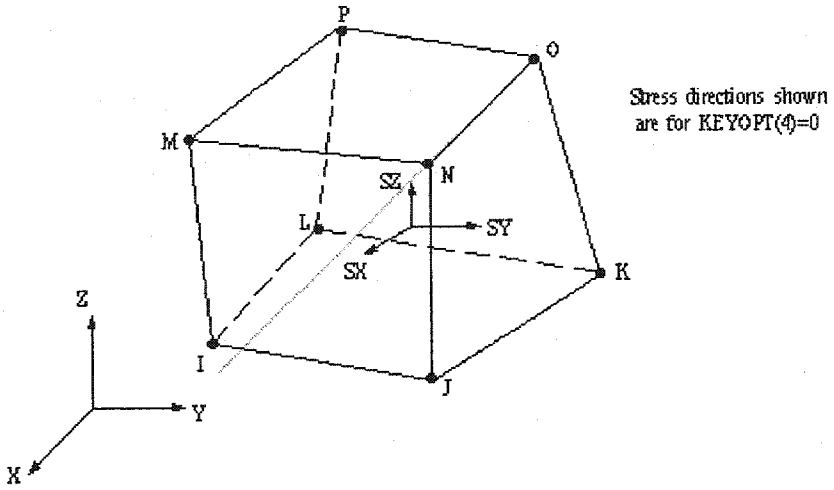

Figure 3.3 SOLID45 Stress Output

The output from the solution consists of the nodal solution (or the primary degree of freedom solution) and the element solution (or the derived solution). Each of these solutions is described below. Solution output is written to the output file, the database, and the results file. The output file can be viewed through the GUI (Graphic User Interface), while the database and results file data (sometimes called the "post-data") can be post-processed.

The output file contains the nodal DOF (Degree of Freedom) solution, nodal and reaction loads, and the element solutions, depending on the settings. The element solutions are primarily the centroidal solution values for each element. Most elements have KEYOPTs to output more information (e.g. integration points)

Boundary condition can be applied with the load in the structure. The tiny portion of the sensor frame is clamped all around.

A hard point of this structure is made. It is special nodal. All loads are applied in the hard point that is located in the center of the two cross horizontal beam.

3.5 Analysis Result

3.5.1 The solution of FEM Model

The following force/moments are applied:

F_x = 0-30N

F_y = 0-30N

F_z = 0-30N

M_x = 0-100Nmm

M_y = 0-100Nmm

M_z = 0-100Nmm

The linear and decoupled results (Calculation result is in Appendix B) can be obtained. The FEM analysis results can be seen in Figure 3.4 (the result that applied F_y or M_y on the sensor are not listed because of symmetric reason):

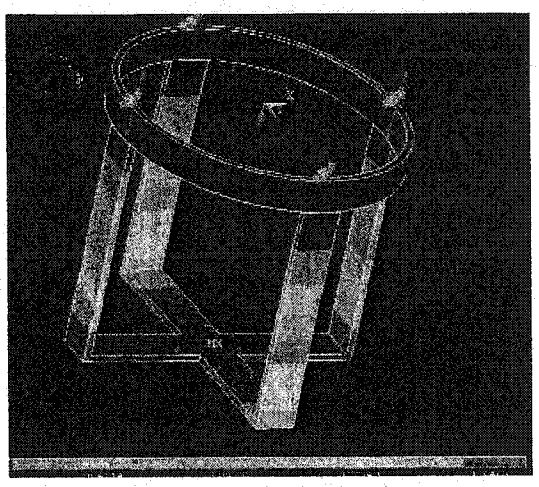

A. Sensor Strain (Load F_x=15N)

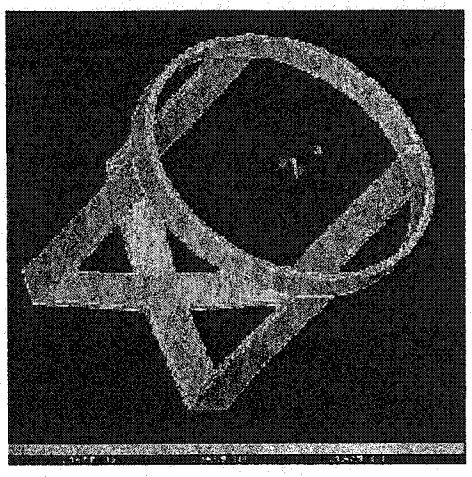

B. Sensor Strain (F_z=15N)

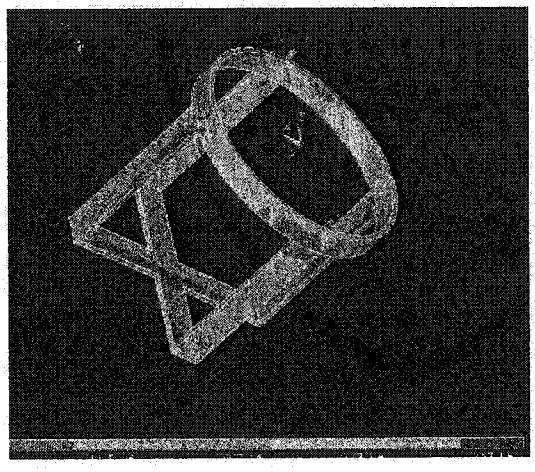

C. Sensor Strain (Load M_x=0.05Nm)

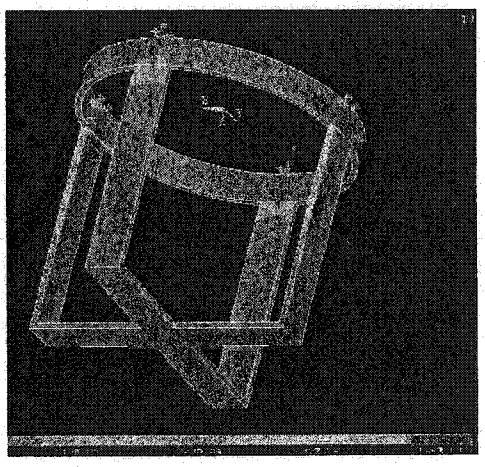

D. Sensor Strain (Load M_z=0.05Nm)

Figure 3.4 The FEM Analysis Result

3.5.2 The Calibration Matrix

From the above analysis the strain/stress at each point in the sensor is obtained. According to the equation:

$$\varepsilon = Cf \tag{3.7}$$

where

$$S = \begin{bmatrix} S_1 \\ S_2 \\ S_3 \\ S_4 \\ S_5 \\ S_6 \\ S_7 \\ S_8 \\ S_9 \\ S_{10} \end{bmatrix} \tag{3.8}$$

$$F = \begin{bmatrix} F_x \\ F_y \\ F_z \\ M_x \\ M_y \\ M_z \end{bmatrix} \tag{3.9}$$

Then the C matrix will be calculated and Moore-Penrose pseudo-inverse matrix C^+ will be obtained.

Using Matlab the calibration matrix of FEM model is calculated to be:

$$C = \begin{bmatrix} 36.2 & 2.9 & -2.2 & 1.9 & -3.7 & 2.8 \\ 5.8 & 36.3 & 3.1 & 3.6 & -1.9 & 2.7 \\ -35.9 & 1.2 & 2.0 & -1.9 & -3.7 & -2.8 \\ -2.6 & -36.2 & 3.0 & 3.7 & -1.9 & 2.7 \\ 0.6 & -1.1 & 17.8 & 10.0 & 118.0 & -11.2 \\ -2.1 & 6.1 & 18.0 & 106.0 & 2.3 & 4.6 \\ -1.0 & 1.3 & 18.3 & 7.7 & -115.0 & 12.3 \\ 1.1 & 6.0 & 18.2 & -102.0 & -2.3 & -4.1 \\ 0.4 & 0.6 & 0.8 & 1.6 & 1.5 & 47.9 \\ -0.4 & -0.6 & -0.8 & -1.6 & -1.5 & -47.9 \end{bmatrix} \times 10^{-8} \quad (3.8)$$

Then the Moore-Penrose pseudo-inverse matrix C^+ calculated as following:

$$C^+ = (C^T C)^{-1} C^T \quad (3.9)$$

$$C^+ = \begin{bmatrix} 1.395 & -0.006 & -1.393 & 0.173 & 0.101 & 0.021 & 0.099 & 0.077 & -0.008 & 0.008 \\ -1.28 & 1.338 & 0.189 & -1.403 & -0.121 & 0.107 & -0.125 & 0.105 & 0.001 & -0.001 \\ 0.032 & 0.010 & -0.053 & 0.476 & 1.372 & 1.324 & 1.399 & 1.366 & -0.004 & 0.004 \\ 0.020 & 0.014 & -0.022 & 0.020 & -0.015 & 0.487 & 0.004 & -0.471 & -0.005 & 0.005 \\ -0.023 & 0.008 & -0.004 & -0.021 & 0.432 & 0.039 & -0.424 & -0.035 & 0.010 & 0.010 \\ -0.001 & -0.001 & 0.001 & 0.001 & -0.003 & -0.004 & -0.001 & -0.001 & 1.044 & -1.044 \end{bmatrix} \times 10^{6} \quad (3.10)$$

C^+ is calibration matrix.

From the FEM analysis, it is noted that:

1. When applying the force F_x, S1 and S3 have the similar value with opposite sign, the values of S1 and S3 are not exactly equal because the nodal

location of S1 and S3 are not exactly same. This is similar to other 5 force/torque components

2. There is a small the cross sensitivity. When applying the force Fx, the other strain gauge values are less than 10% of S1 or S3. The result is similar to the beam model analysis result. When applying F_y, F_z, M_x, M_y, M_z , similar results can be obtained.
3. The FEM results demonstrate that the beam theory is a simple way to analyze the sensor structure, and can be used in preliminary analysis of the sensor frame. The FEM can get more accurate analysis results and closes to reality.
4. The sensor structure and dimension design satisfy the requirement of force/torque measurement, and the measurement accuracy is acceptable
5. In view of the need for more time and effort Element Method can be applied in the final stage of most costly and laborious calibration procedure for improving the analysis.

In the next chapter, the sensor fabrication and experimental analysis will be described. In this section, the sensor will be characterized by studying both the linearity and sensitivity. This will be performed by investigating the static force/torque that are applied on the sensor. Finally, by using the obtained data, the final calibration matrix will be calculated.

Chapter 4

Sensor Fabrication and Experiment

In the previous chapter, the finite element method was applied to analyze the sensor. The FEM results agreed closely with those obtained using the simple beam model. In this chapter, the analytical result will be validated through experimental investigations on a sensor frame that was designed using the beam theory.

4.1 Sensor Fabrication

The sensor frame was fabricated using the design optimization that was reported in section2.2. The sensor frame is fabricated in workshop of the Mechanical Engineering Department of Concordia University. The detail dimension of sensor structure is reported in Chapter II and Chapter III. . The detail fabrication drawing of sensor frame is presented in Figure 4.1. In Figure 4.1, the detail drawing of the sensor shows it's top, front and side view. Special fixtures (in Figure 4.2) were designed in order to apply forces and moments along all the axes.

The strain gauges were positioned in the middle of the vertical and horizontal beams of the frame of the sensor. The micro-strain gauges were glued on the sensor in Concave Center laboratory. The processing of glue was discussed in section 4.4. The sensor was calibrated as described in section 4.2.

Sensor Frame

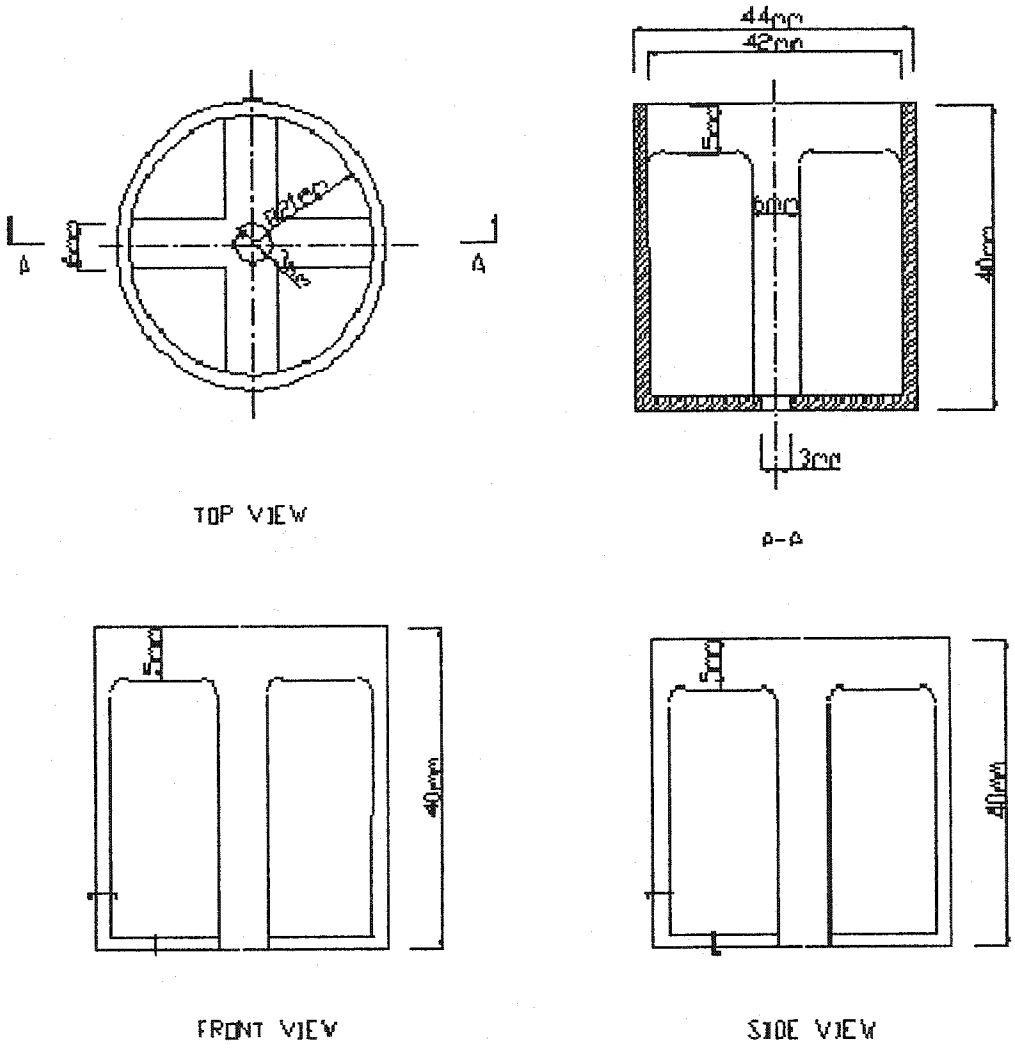

Figure 4.1 The detail drawing of the elastic body of the sensor

4.2 The Experiment Setup

For testing and calibration of the sensor, a series of special equipment are built in order to fix the sensor and apply the force/moment in different directions on it. A base with a cylindrical projection that can be used to mount the sensor frame snugly into it as shown in Figure 4.1 was prepared.

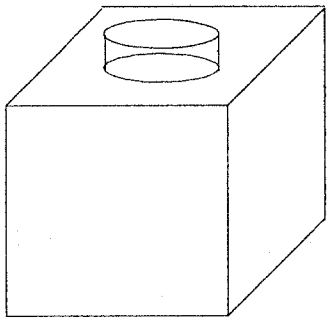

Figure 4.2 Base for Fixing Sensor

Weights are suspended on the cross beam structure to apply loads (forces and moments) to the sensor. Figure 4.3 shows six different configurations for hanging weights. These six configurations yield six linear independent force vectors.

(a) Fz is applied on the sensor

(b) Fx is applied on the sensor

(c) Fy is applied on the sensor

(d) Mx is applied on the sensor

(e) My is applied on the sensor

(f) Mz is applied on the sensor

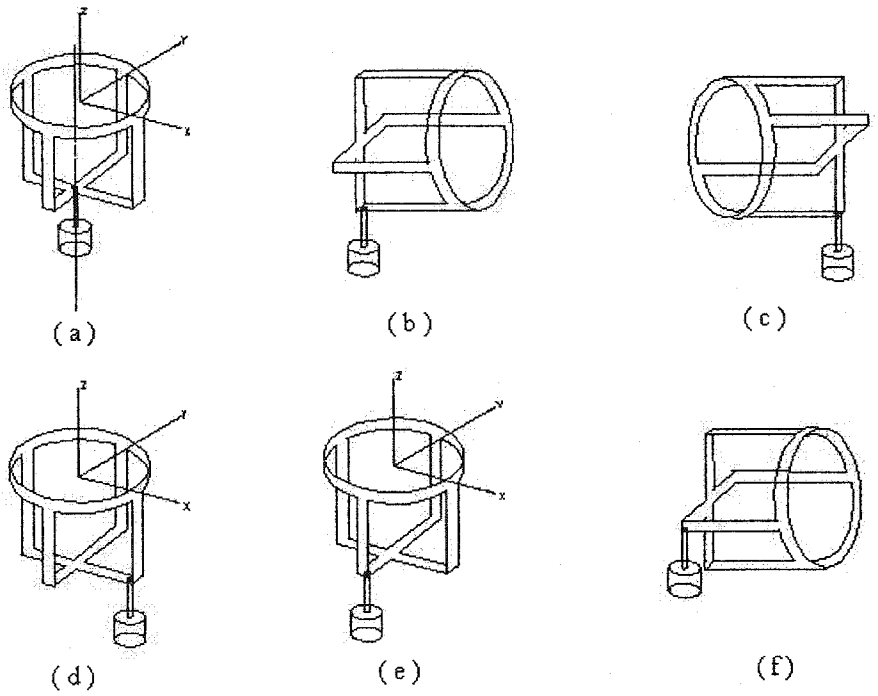

Figure. 4.3 The Way of Force/Torque Applied

4.3 The Specifications of Gauge

The Micro-strain gauges that are commonly used in industrial applications was used for the experiments.

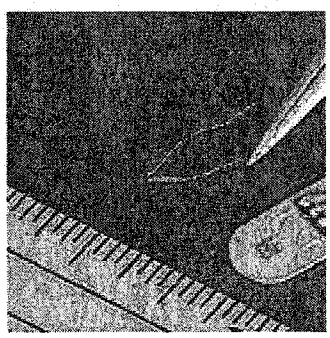

Figure 4.4 The Image of Micro-Strain Gauge [53]

The strain gauge ESB-020-350 of Entran Ltd with the following specifications were chosen for the experiments:

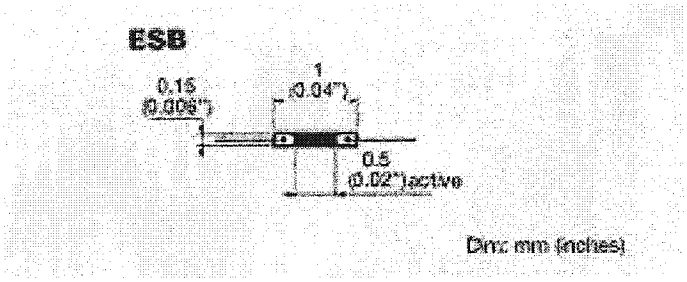

Figure 4.5 The Dimension of ESB [53]

The Characteristics of strain gauge are given in Table 3:

Table 3 The Characteristics of Strain Gauge

Gauge Factor(GF)	$\frac{\Delta R / R}{\Delta L / L} \pm 5\%$
Thermal Coefficient of Resistance(TCR)	$\frac{\Delta GF\ \% \pm 3\%}{100^{\circ} F}$
Gauge Type	P-Type Silicon
Strain Level	1-1000μstrain recommended, 50milliwatt maximum
Wattage Rating (Per gauge)	0-25milliwatt recommended, 50 milliwatt maximum. Watts=(Voltage on Gauge)^2/(Gauge Resistance)
Temperature Range	-100°F to 100°F(-73°C to 315°C)
Lead Wires	Gold, 0.0015'' diameter×0.25'' length min (0.038mm dia ×6.35mm)
Young's Modulus	E=27×10^{8}psi(1.9×10^{8}kg/cm^2)

4.4 The Adhesives and Installation of Strain Gauge

Selection of the correct application techniques and associated materials are quite important to ensure the success of any strain gauge test program. The basic process of applying a gauge to the test surface can be conveniently divided into the following major steps:

(1) Preparation of Test Surface

The sensor surface must be prepared before mounting the gauges on the sensor body. The following preparations are made:

1. Lightly sand with 400 grit sandpaper perpendicular to strain dimension, to a 16 RMS finish, sandblast to at surface.
2. Apply 1,1,1-trichorethane to clean the surface.
3. Blow dry with canned air or another clean source.
4. Acetone clean
5. Blow dry with canned air or another clean source again.

(2) Selection of installation material

In the test, epoxy adhesives that stick the strain gauges on the structure are chosen. Epoxy adhesives have been extensively used for the installation of strain gauges for many years.

In this project, a fine brush (000) is used to pre-coat with thin layer of epoxy, such as Micro Measurement's M-bond 610.

In this processing, five basic operations are usually noted:

(1) General solvent degreasing of the gauging area;

(2) Surface abrading, a minimum requirement is to obtain a bright metal surface;

(3) Application of gauge location layout lines;

(4) Surface conditioning with a mild acid;

(5) Surface neutralizing.

A bright metal surface for protective coating as well as adhesive is prepared. Circular grinder and lapping to reduce direct tracking paths was employed. The application of adhesive and coating were done with a fine brush.

(3) Gauge preparation

Holding the free end of one lead wire of the strain gauge with a fine tweezer, the wire from the tape was removed by gently lifting the wire straight up. The gauge was placed on the wet epoxy and aligned. The process needs to be done carefully. In general, a microscope is needed.

(4) Application of adhesive

The adhesive was checked visually for inclusions, contaminations or discoloration. Ensure containers are slightly above room temperature before opening. Adhesive was applied with adequate pressure at right angles to the glue-line.

(5) Clamping

In order to ensure correct glue-line thickness and assist in the set-up of the adhesive, adequate pressure was applied with thumb pressure and the force acting on clamps for two minutes.

(6) Curing and post curing

After a cure involving heat and pressure the glue-line may have locked in residual stresses. To achieve maximum long-term stability these stresses must be relieved by the process of post curing. To ensure that the adhesive reaches the right viscoelastic state to release the stress the post cure temperature should exceed the cure temperature by 20-30° C. Post curing was done at 150° C for 3 hours minimum.

(7) Lead wire attachment and soldering

Finally a lead wire was attached to the strain gauges under microscope. The set up is shown in Figure 4.5.

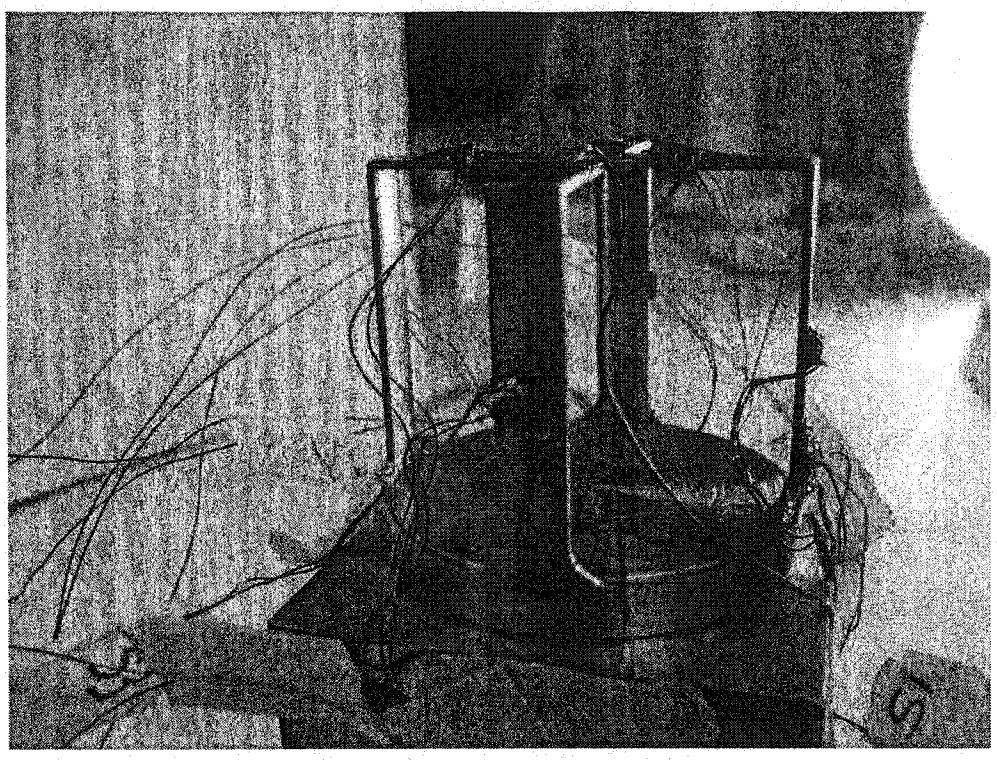

Figure 4.6 The Six DOF Force/Torque Sensor

4.5 Measurement Instrument

The model P-3500 Strain Indicator is applied to read strain gauge's readout. It is a portable, battery-powered precision instrument for use with resistive strain gauges and transducers. The P-3500 will accept full, half and quarter bridge inputs, and all required bridge completion components for 120 ohm and 350 ohm bridges are provided. Strain gauges are normally connected via the front panel binding connector. The P-3500 will accept gauge factors of 0.500 to 9.900, and gauge factor is adjustable to an accuracy of 0.001 by a front panel 10-turn potentiometer. Gauge factor is displayed on the LCD display. But the gauge factor for most semiconductor strain gauges is between 50 and 200, and is beyond the immediate range of the P-3500 gauge factor controls. However,

when the MULT push button is set to the X10 position, the gauge factor range is effectively multiplied by 10.

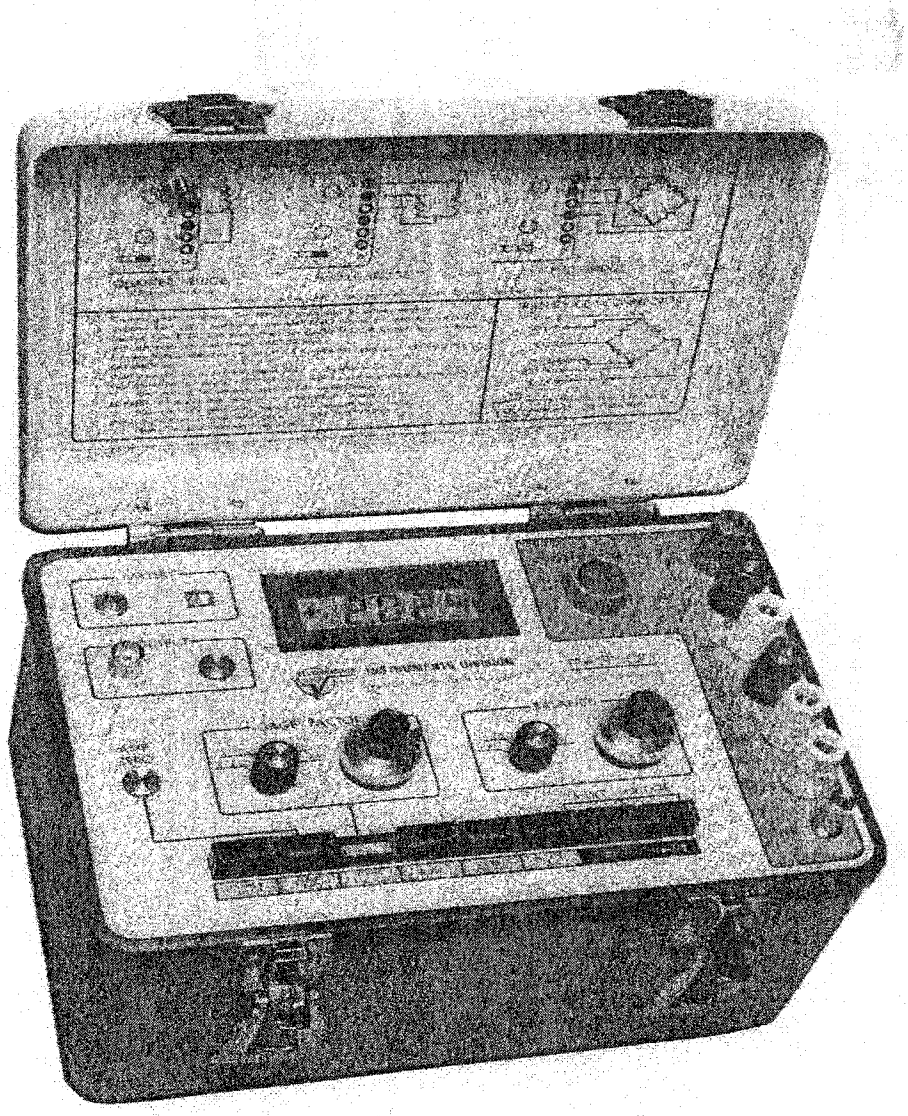

Model P-3500 Strain Indicator

Figure 4.7 P-3500 Strain Indicator

4.6 The Principle of Strain Gauge Force/Torque Sensor

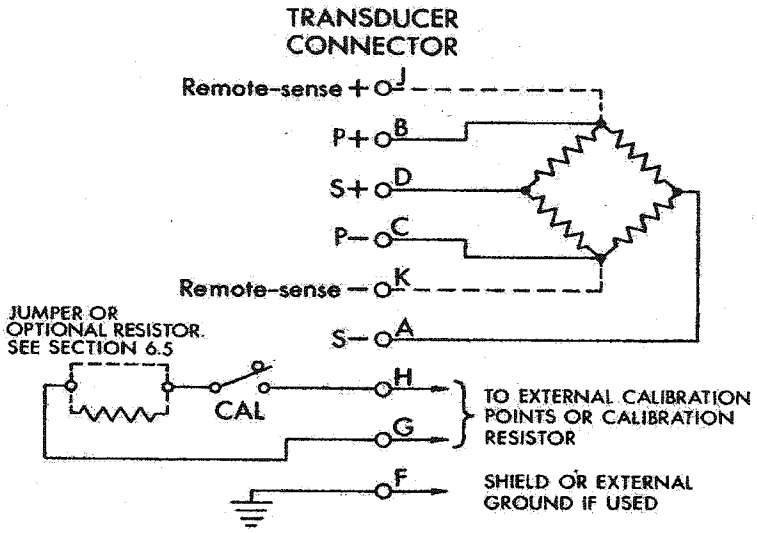

Figure 4.8 Wheatstone Bridge

The quarter bridge strain gauge is connected at the P+ and S+ port. For the half bridge connection, the strain gauges are connected at (P+, S+) and (P-, S-). For the full bridge, the gauges are connected according (P+, S+), (S+, P-), (P+, S-), and (P-, S-). H and G port is used to choose the resistor of strain gauge, H is used for 120 Ohm gauge, and G is used for 350 Ohm gauge. The instrument also can be used for remote output or external measurement instruments, the output port is J and K. F is external ground port.

4.7 Measures to overcome the possible problems in the experiment

In order to overcome possible problems in the experiment, the following precautions were taken.

(1) Using soldering tin to solder the lead and wire to make the conductive characteristic stable because the glue characteristics are unstable sometimes.

(2) Using dummy gauge to compensate the temperature because the strain gauge is sensitive to the temperature change, especially in a quarter bridge. The dummy gauge is connected as showing in Figure4.9.

(3) Using external resistor to compensate the gauge resistive value to 350 ohms to solve zero drift problem because the installation. There are differences between the resistors. The balance of Wheatstone bridge is hard to be obtained. After use extra resistors, eventually the satisfying result is obtained

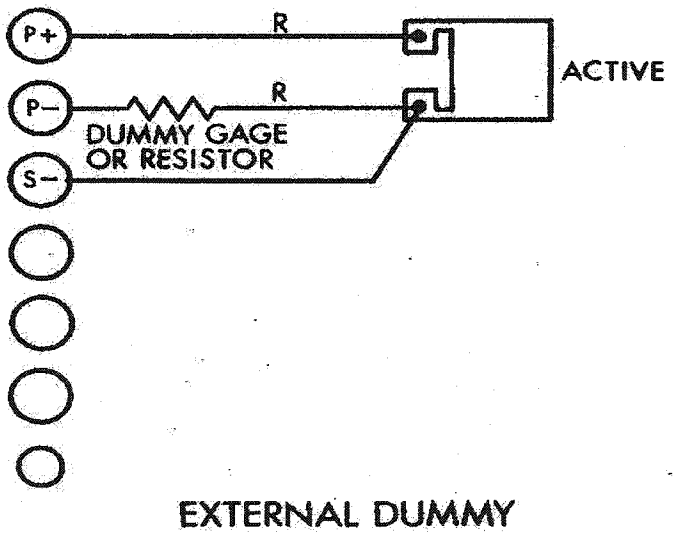

Figure 4.9 External Dummy gauge

In the next chapter, the experiments will be carried out and the results will be obtained. Results from beam model, FEM model and Experiments will be compared. And the calibration matrix will be calculated.

Chapter 5

Data Processing and Comparison of the Results

In the preceding chapter, fabrication of the sensor frame, and the experimental issues were discussed. In this chapter, the experimental results will be presented and discussed. The data analysis will be made and compared with analytical results.

5.1 Data Processing

Experimentally observed discrete set of data of the form $\{x_t, f_t \mid i=1,...n\}$ should be represented as a function of the form $f(x)$ over the domain of the independent variable x[54][55]. From the beam model and FEM model analyzed, the relationship of strain and the applied force is linear, given m pairs of data:

$$(x_i, y_i),\ i = 1, \ldots, m \tag{5.1}$$

The coefficients α and β can be found such that

$$F(x) = \alpha x + \beta \tag{5.2}$$

In order to obtain a least squared error fit to the data, the difference between the y data and the fit function is obtained at each point,

$$r_i = y_i - F(x_i) = y_i - (\alpha x_i + \beta) \tag{5.3}$$

where r_i is called the residual for the data pair (x_i, y_i), and it is the vertical distance between the known data and fit function.

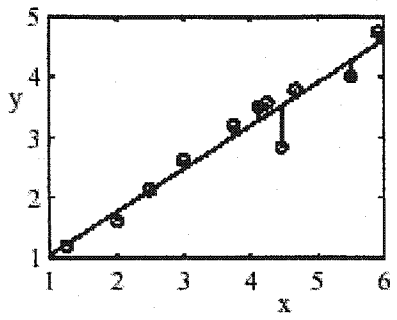

Figure 5.1 Data and Fit Function

The best fit is obtained in such a way as to:

$minimize \Sigma r_i^2$

It means, $\rho=\Sigma r_i^2$

$$\rho = \sum r_i^2 = \sum_{i=1}^{m} [y_i - (\alpha x_i + \beta)]^2 \tag{5.4}$$

The least squares fit is obtained by choosing the α and β in Equation (5.2)

Denoting:

$$\rho = \sum_{i=1}^{m} r_i^2 \tag{5.5}$$

and

$$\rho = \rho(\alpha, \beta) \tag{5.6}$$

the coefficients α and β are obtained by minimizing ρ with respectto them as follows:

$$\left.\frac{\partial \rho}{\partial \alpha}\right|_{\beta=cons\,tant} = 0 \tag{5.7}$$

and

$$\left.\frac{\partial \rho}{\partial \beta}\right|_{\alpha=cons\,tant} = 0 \tag{5.8}$$

Let

$$\alpha x + \beta = y \tag{5.9}$$

Writing out the Equation (5.9) for all of the known points (x_i , y_i). $i = 1, \ldots, m$ gives the over-determined system.

Let

$$Ac = y \tag{5.10}$$

where

$$A = \begin{bmatrix} x_1 & 1 \\ x_2 & 1 \\ \vdots & \vdots \\ x_m & 1 \end{bmatrix} \tag{5.11}$$

$$c = \begin{bmatrix} \alpha \\ \beta \end{bmatrix} \tag{5.12}$$

$$y = \begin{bmatrix} y_1 \\ y_2 \\ \vdots \\ y_m \end{bmatrix} \tag{5.13}$$

The equation $Ac = y$ can not be solved with Gaussian elimination unless the system is consistent. It is impossible to find the $c = (\alpha, \beta)^T$ that exactly satisfies all m equations. The system is consistent only if all the data points lie along a single line.

Compute

$$\rho = \| r \|_2^2 \tag{5.14}$$

where

$$r = y - Ac \tag{5.15}$$

$$\rho = \| r \|_2^2 = r^T r = (y - Ac)^T (y - Ac)$$

$$= y^T y - (Ac)^T y - y^T (Ac) + c^T A^T Ac$$

$$= y^T y - 2y^T (Ac) + c^T A^T Ac \tag{5.16}$$

Minimizing ρ requires

$$\frac{\partial \rho}{\partial c} = -2A^T y + 2A^T Ac = 0 \tag{5.17}$$

or

$$(A^T A)c = A^T b \tag{5.18}$$

Suppose $\hat{y}$ is the value of the fit function at the known data points

$$\hat{y} = c_1 x_i + c_2 \tag{5.19}$$

for a line fit, and $\bar{y}$ is the average of the y values

$$\bar{y} = \frac{1}{m}\sum y_i \tag{5.20}$$

In order to measure how well the fit function follows the trend in the data, parameter R^2 can be defined as:

$$R^2 = \frac{\sum(\hat{y}_i - \bar{y})^2}{\sum(y_i - \bar{y})^2} = 1 - \frac{\|r\|_2^2}{\sum(y_i - \bar{y})^2} \tag{5.21}$$

where

$$0 \leq R \leq 1 \tag{5.22}$$

When $R^2 \approx 1$ the fit function follows the trend of the data.

When $R^2 \approx 0$ the fit function is not significantly better than approximating the data by its mean.

5.2 The Experimental Data

5.2.1. Applying Fx on the sensor

The measured strains when F_x is applied on the sensor frame are shown in Figure 5.2. The coefficient R^2 is calculated in Table 4.

Table 4 The coefficient when applying Fx

	R^2	α	β
S1	0.9980	1.0e-006 *0.3361	1.0e-006 *0.1195
S2	0.9928	1.0e-007 *0.3293	1.0e-007 *0.4097
S3	0.9946	1.0e-006*(-0.3333)	1.0e-006 *0.1460
S4	0.9901	1.0e-007 *0.3091	1.0e-007 *0.0755
S5	0.9953	1.0e-007 *0.3121	1.0e-007 *0.3352
S6	0.9908	1.0e-007 *0.3025	1.0e-007 *0.3500
S7	0.9819	1.0e-007 *0.3170	1.0e-007 *0.5822
S8	0.9849	1.0e-007 *0.2751	1.0e-007 *0.4739
S9	0.9007	1.0e-008 *0.4721	1.0e-008 *0.8350
S10	0.9007	1.0e-008 *0.4721	1.0e-008 *0.8350

Least Square Line Fit to Measurement Data

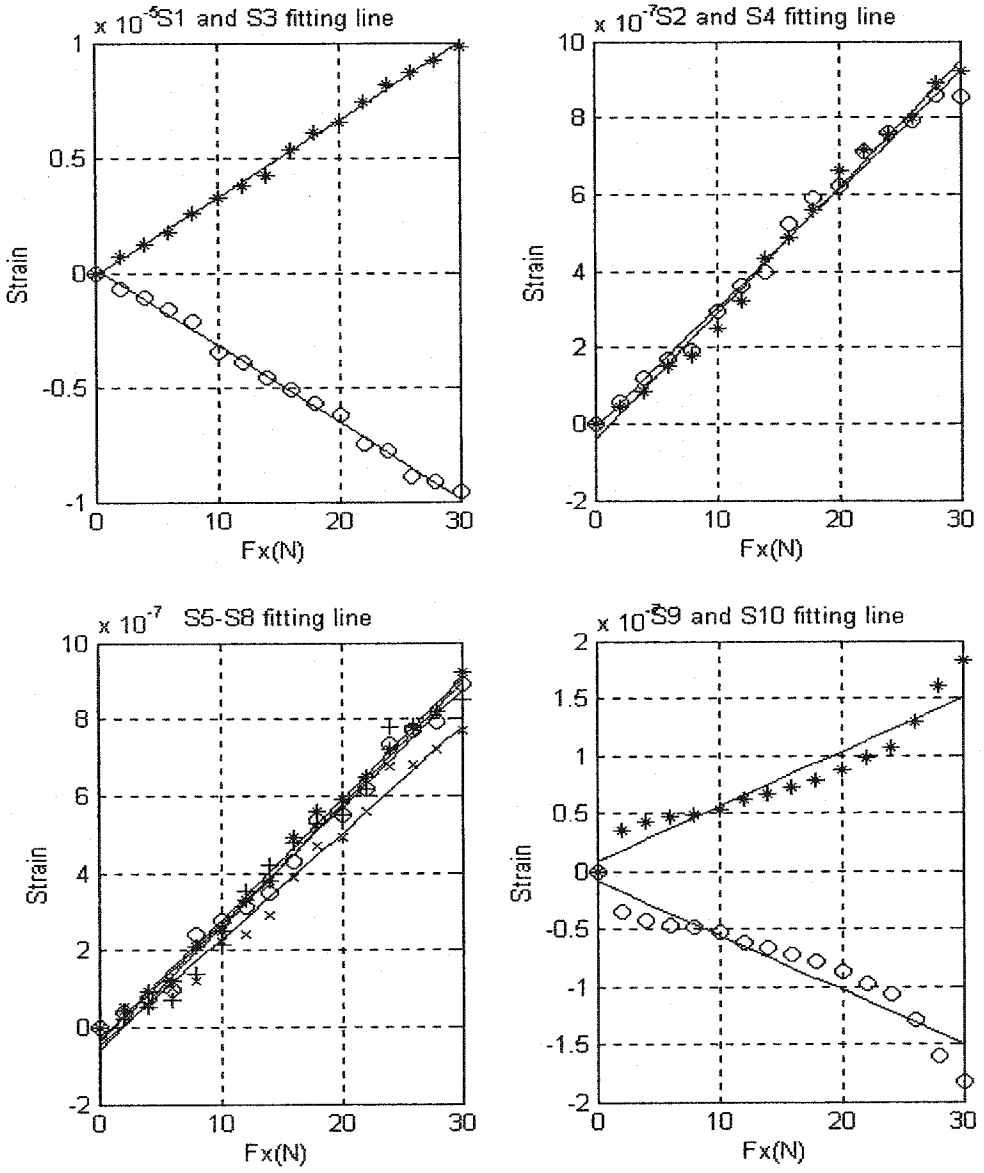

Figure 5.2 Strain Gauge Line Fit when Applying Fx

From above data analysis, it is found that when Fx is applied on the sensor, the α of S1 and S3 are 1.0e-006 *0.3361 and 1.0e-006 *0.3333. The α of other gauges' (S2, S4, S5, S6, S7, S8, S9, S10) are 1.0e-008 *0.4721 to 1.0e-007 *0.3293, less than 10% value

of S1 and S3. It shows that the only readouts when Fx is applied are S1 and S3. The R^2 of the gauges values are the 0.9007 to 0.9988, which means that the lines fit the experimental data well.

5.2.2 Applying Fy on the sensor

The measured strains when F_y is applied on the sensor frame are shown in Figure 5.3. The coefficient R^2 is calculated in Table 5.

Table 5 The coefficient when applying Fy

	R^2	α	β
S1	0.9896	1.0e-007 *0.3144	1.0e-007 *0.5475
S2	0.9923	1.0e-006 *0.3326	1.0e-006 *0.0679
S3	0.9983	1.0e-007 *0.3285	1.0e-007 *0.4234
S4	0.9971	1.0e-006 *(-0.3436)	1.0e-006 *0.1968
S5	0.9951	1.0e-007 *0.3215	1.0e-007 *0.3272
S6	0.9930	1.0e-007 *0.3160	1.0e-007 *0.4184
S7	0.9941	1.0e-007 *0.3081	1.0e-007 *0.2631
S8	0.9930	1.0e-007 *0.3160	1.0e-007 *0.4184
S9	0.9564	1.0e-008 *0.8502	1.0e-007 *0.6328
S10	0.9564	1.0e-008 *0.8502	1.0e-007 *0.6328

Least Square Line Fit to Measurement Data

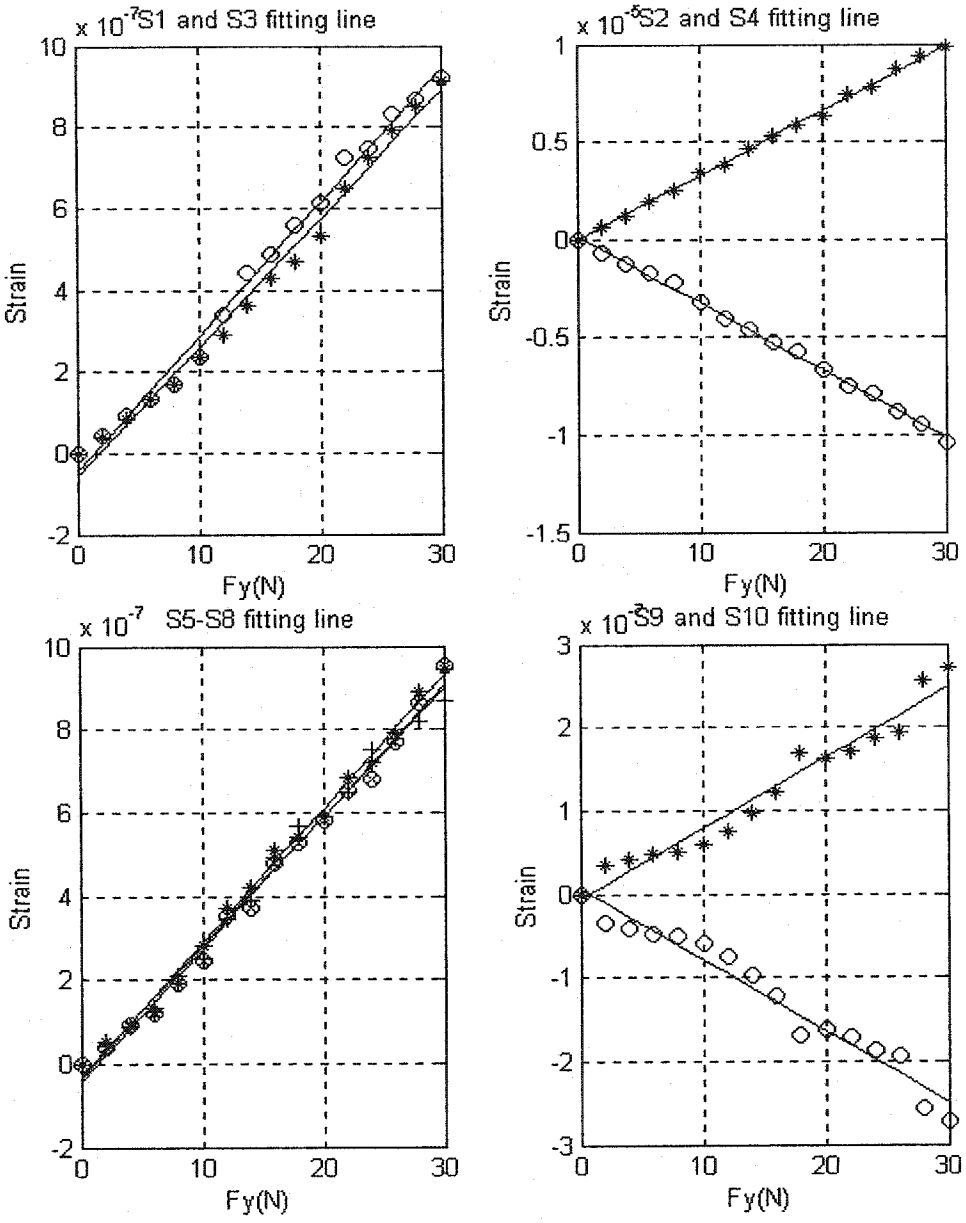

Figure 5.3 Strain Gauge Fit Line when Applying Fy

From above data analysis, it is found that when Fy is applied on the sensor, the α of S2 and S4 are 1.0e-006 *0.3326 and 1.0e-006 *0.3436. The α of other gauges' (S1, S3, S5, S6, S7, S8, S9, S10) are 1.0e-008 *0.8501 to 1.0e-007 *0.3285, less than 10% values of S2 and S4. It shows that there are only readouts of S2 and S4 when Fy is applied. The R^2 of the gauges values are the 0.9564 to 0.9983, which means that the lines fit the experimental data well.

5.2.3. Applying Fz on the sensor

The measured strain when F_z is applied on the sensor frame are shown in Figure 5.4. The coefficient R^2 is calculated in Table 6.

Table 6 The Coefficient when Applying Fz

	R^2	α	β
S1	0.9833	1.0e-008 *0.2541	1.0e-008 *0.8467
S2	0.9295	1.0e-007 *0.0218	1.0e-007 *0.1693
S3	0.9044	1.0e-007 *0.0223	1.0e-007 *0.1462
S4	0.9774	1.0e-008*0.2318	1.0e-008 *0.9155
S5	0.9961	1.0e-006 *0.1843	1.0e-006 *0.1865
S6	0.9913	1.0e-006*0.1938	1.0e-006 *0.2025
S7	0.9958	1.0e-006*0.2031	1.0e-006 *0.1402
S8	0.9909	1.0e-006 *0.1890	1.0e-006 *0.2377
S9	0.9568	1.0e-008 *0.2489	1.0e-008 *0.6718
S10	0.9568	1.0e-008 *(-0.2489)	1.0e-007 *(-0.6718)

Least Square Line Fit to Measurement Data

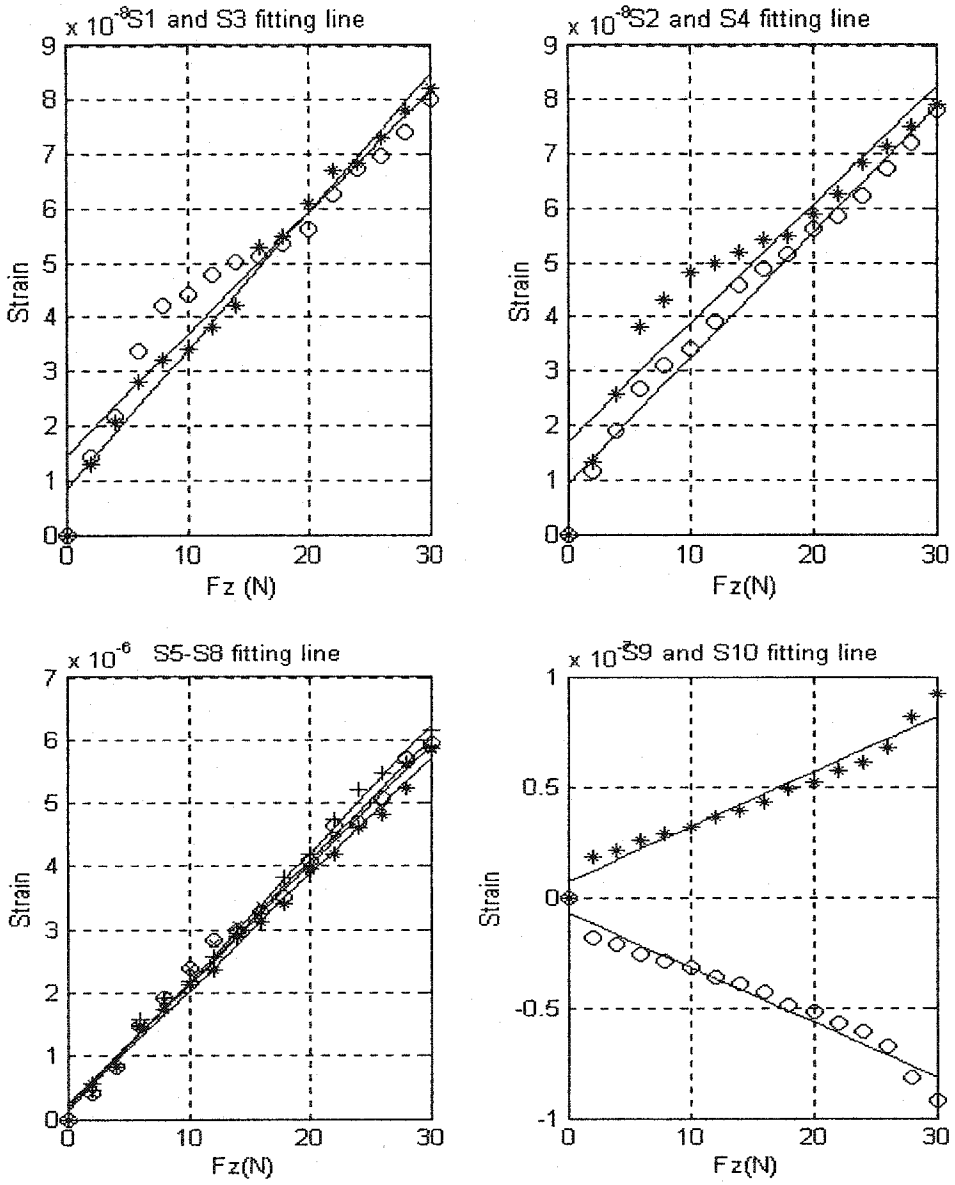

Figure 5.4 Strain Gauges Line Fit when Applying Fz

From above data, it is seen that when Fz is applied on the sensor, the α of S5, S6, S7 and S8 are 1.0e-006*0.1843, 1.0e-006*0.1938, 1.0e-006*0.1938 and 1.0e-006*0. 2031. The α of other gauges' (S1, S2, S3 S4, S9, S10) are 1.0e-008*0.2180 to 1.0e-008*0.2489, about 10% values of S5–S8. It shows that there are only readouts of S5 – S8

when Fz is applied. The R^2 of the gauges values are the 0.9041 to 0.9961, which means that the lines fit the experimental data well.

5.2.4 Applying Mx on the sensor

The measured strains when M_x is applied on the sensor frame are shown in Figure 5.5. The coefficient R^2 is calculated in Table 7.

Table 7 The coefficient when applying Mx

	R^2	α	β
S1	0.9558	1.0e-007*(-0.0067)	1.0e-007*(-0.1021)
S2	0.9897	1.0e-008*(-0.0623)	1.0e-008*(-0.4427)
S3	0.9680	1.0e-008*(-0.0576)	1.0e-008*(-0.7718)
S4	0.9744	1.0e-008*(-0.0479)	1.0e-008*(-0.6309)
S5	0.9750	1.0e-008*(0.0463)	1.0e-008*(-0.5895)
S6	0.9374	1.0e-008*0.9635	1.0e-008*0.2182
S7	0.9989	1.0e-008*(-0.0375)	1.0e-008*(-0.8209)
S8	0.9928	1.0e-007*(-0.0909)	1.0e-007*(-0.1914)
S9	0.9649	1.0e-008*0.0433	1.0e-008*0.6750
S10	0.9649	1.0e-008*(-0.0433)	1.0e-008*(-0.6750)

Least Square Line Fit to Measurement Data

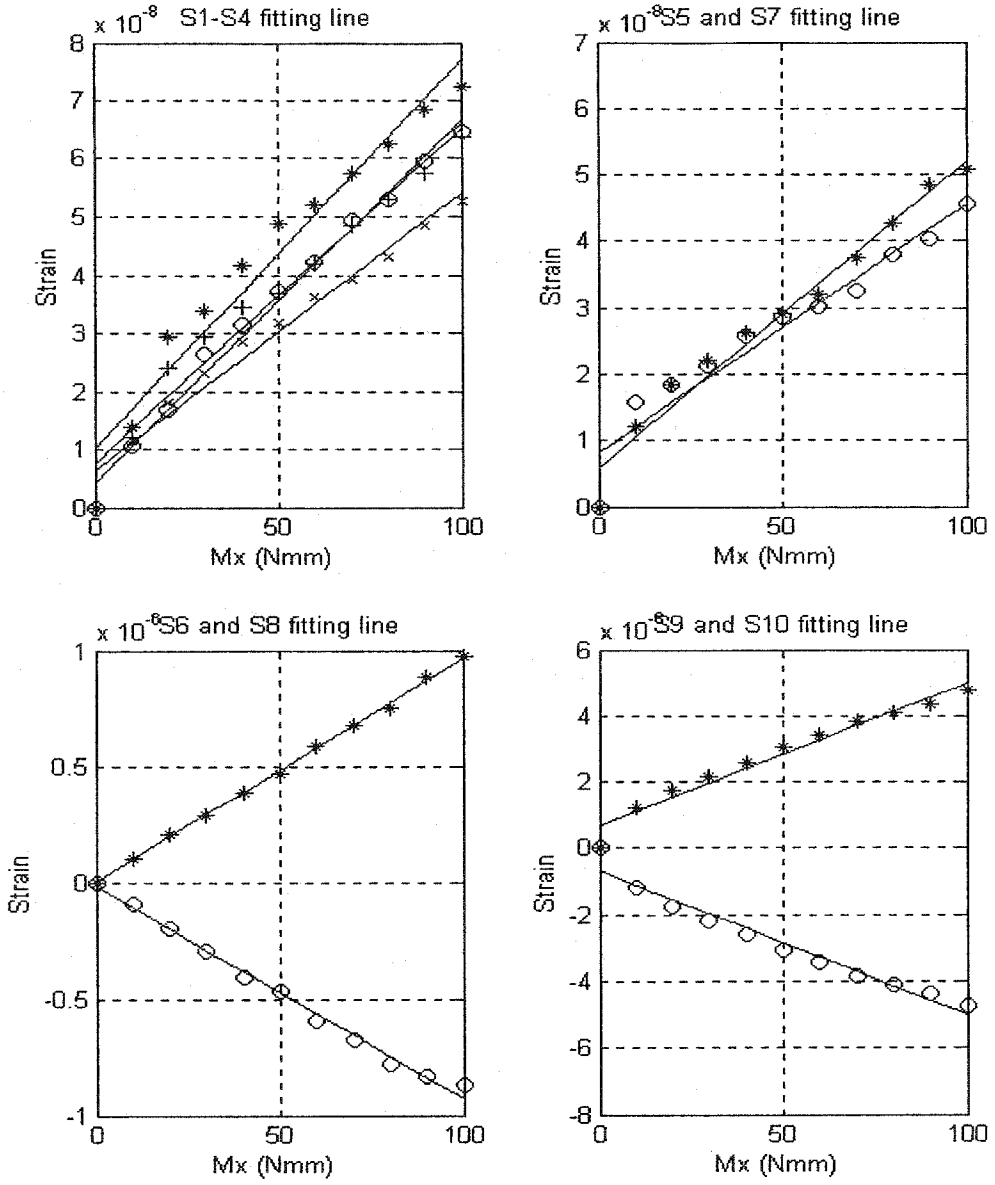

Figure 5.5 Strain Gauge Line Fit when Applying Mx

From above data analysis, it is found that when Mx is applied on the sensor, the α of S6 and S8 are 1.0e-008*(0.9635) and 1.0e-008*(-0. 909). The α of other gauges' (S1, S2, S3 S4, S5, S7, S9, S10) are 1.0e-009*0.433 to 1.0e-009*0.670, less than 10% values of S6 and S8. It shows that there are only readouts of S6 and S8 when Mx is applied. The

R^2 of the gauges values are the 0.9371 to 0.9989, which means that the lines fit the experimental data well.

5.2.5 Applying My on the sensor

The measured strains when M_y is applied on the sensor frame are shown in Figure 5.6. The coefficient R^2 is calculated in Table 8.

Table 8 The Coefficient when applying My

	R^2	α	β
S1	0.9354	1.0e-008 *0.0389	1.0e-008*0.6445
S2	0.9082	1.0^e-008 *0.0445	1.0e-008*0.8750
S3	0.9923	1.0e-008 *0.0355	1.0e-008*0.8073
S4	0.9395	1.0e-008 *0.0325	1.0e-008*0.6786
S5	0.9983	1.0e-007 *0.0955	1.0e-007*0.1850
S6	0.9988	1.0e-007 *0.0430	1.0e-007*0.5486
S7	0.9753	1.0e-007 *(-0.1029)	1.0e-007*(-0.2009)
S8	0.9270	1.0e-008 *0.0338	1.0e-008*0.8323
S9	0.9838	1.0e-008 *0.0503	1.0e-008*0.5136
S10	0.9838	1.0e-008 *(-0.0503)	1.0e-008*(-0.5136)

Least Square Line Fit to Measurement Data

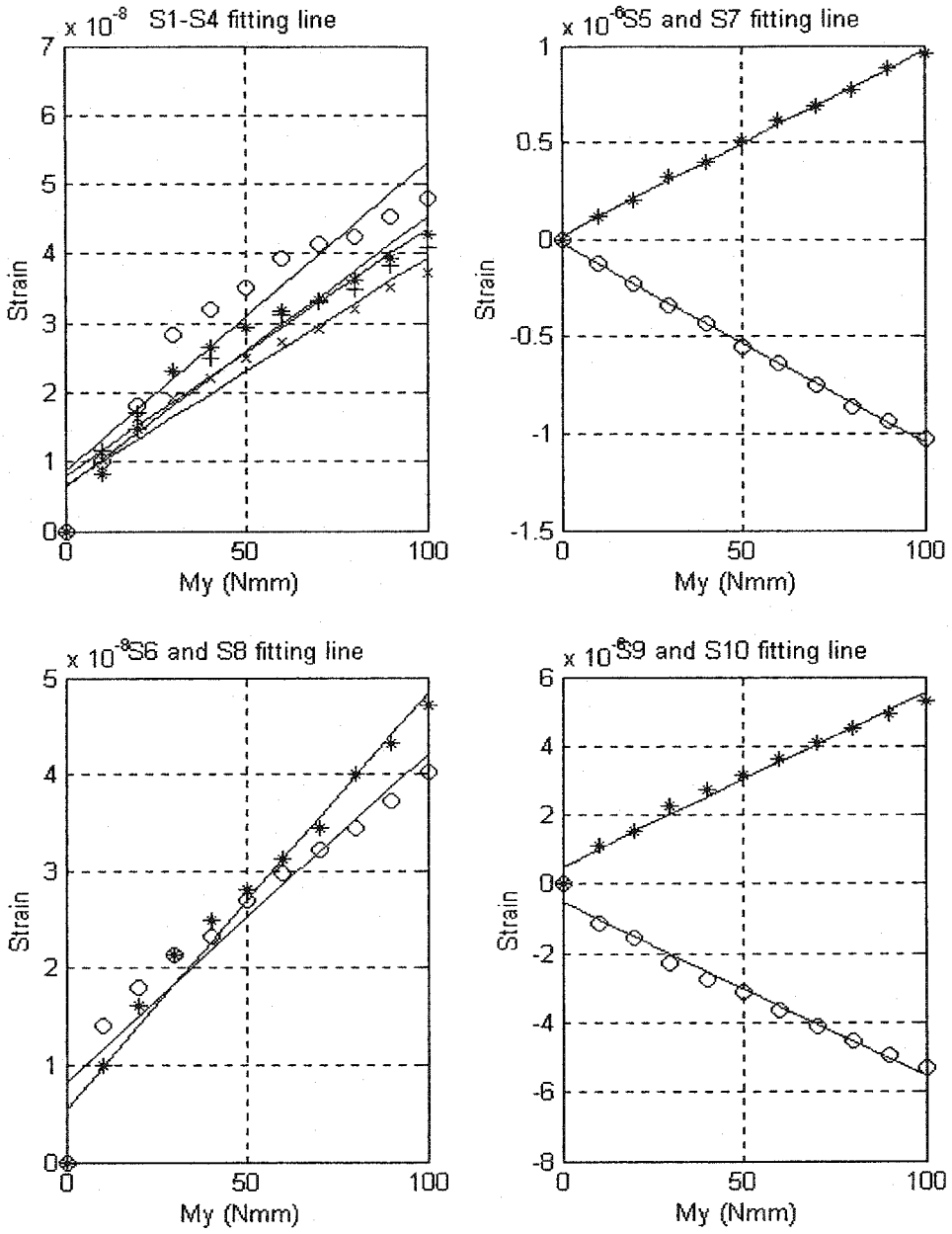

Figure 5.6 Strain Gauge Line Fit when Applying My

From above data analysis, It is seen that when My is applied on the sensor, the α of S5 and S7 are 1.0e-008*0.9550 and 1.0e-007*(-1.2029). The α of other gauges' (S1, S2, S3 S4, S6, S8, S9, S10) are 1.0e-009*0.3250 to 1.0e-009*0.503, less than 10% values of S5 and S7. It shows that there are only readouts of S5 and S7 when My is applied. The

R^2 of the gauges values are the 0.9082 to 0.9988, which means that the lines fit the experimental data well.

5.2.6 Applying Mz on the sensor

The measured strains when M_z is applied on the sensor frame are shown in Figure 5.7. The coefficient R^2 is calculated in Table 9.

Table 9 The coefficient when applying Mz

	R^2	α	β
S1	0.9895	1.0e-007 *0.0375	1.0e-007 *(-0.1751)
S2	0.9794	1.0e-007 *0.0349	1.0e-007 *0.1322
S3	0.9837	1.0e-008 *0.2748	1.0e-008 *(-0.7264)
S4	0.9872	1.0e-008 *0.2717	1.0e-008 *(-0.6082)
S5	0.9765	1.0e-008 *0.3079	1.0e-008 *(-0.8036)
S6	0.9967	1.0e-008 *0.2988	1.0e-008 *(-0.0282)
S7	0.9786	1.0e-008 *0.2507	1.0e-008 *(-0.6227)
S8	0.9885	1.0e-008 *0.2978	1.0e-008 *0.2591
S9	0.9988	1.0e-007 *0.4235	1.0e-007 *(-0.5873)
S10	0.9988	1.0e-007 *((-0.4235)	1.0e-007 *0.5873

Least Square Line Fit to Measurement Data

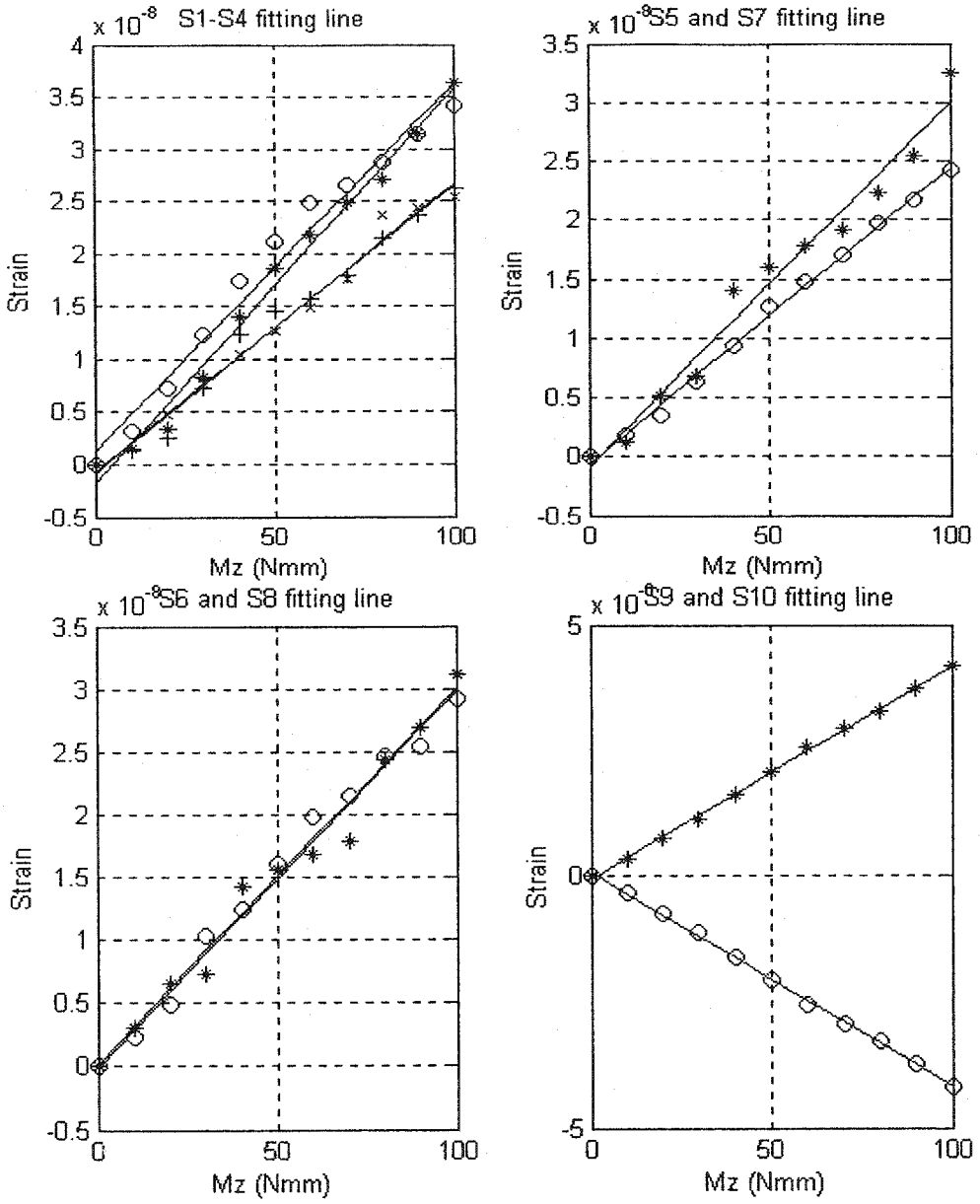

Figure 5.7 Strain Gauge Line Fit when Applying Mz

From following data analysis, it can be seen that when Mz is applied on the sensor, the α of S9 and S10 are 1.0e-007*0.4235. The α of other gauges' (S1, S2, S3 S4, S5, S6, S7 and S8) are 1.0e-008*0.2507 to 1.0e-008*0.3750, less than 10% values of S9 and S10. It shows that there are only readouts of S9 and S10 when Mz is applied. The R^2

of the gauges values are the 0.9765 to 0.9988, which means that the lines fit the experimental data well.

5.3 Calibration Matrix

With the analysis data, the C matrix can be obtained as

$$C = \begin{bmatrix} 32.5 & 2.3 & 0.3 & 7.2 & 4.3 & 3.6 \\ 2.5 & 34.6 & 0.5 & 6.5 & 4.8 & 3.4 \\ -35.0 & 2.3 & 0.4 & 6.4 & 4.1 & 2.6 \\ 2.9 & -32.4 & 0.3 & 5.3 & 3.7 & 2.5 \\ 2.5 & 2.8 & 21.4 & 5.1 & 96.0 & 3.2 \\ 2.7 & 2.4 & 23.9 & 97.2 & 4.7 & 3.1 \\ 2.2 & 2.5 & 21.8 & 4.6 & -103.0 & 2.4 \\ 2.2 & 2.4 & 24.0 & 87.0 & 4.0 & 2.9 \\ 0.5 & 0.6 & 0.3 & 4.7 & 5.3 & 41.8 \\ -0.5 & -0.6 & -0.3 & -4.7 & -5.3 & -41.8 \end{bmatrix} \times 10^{-8} \quad (5.22)$$

The pseudo-inverse matrix is given by

$$C^{+} = \begin{bmatrix} 1.412 & 0.115 & -1.527 & 0.115 & 0.012 & -0.002 & 0.017 & -0.021 & -0.002 & 0.002 \\ 0.110 & 1.53 & 0.089 & -1.44 & 0.003 & -0.002 & 0.028 & -0.02 & -0.003 & 0.003 \\ -0.326 & 0.317 & 0.017 & 0.019 & 2.53 & -0.264 & 2.32 & 0.078 & -0.013 & 0.013 \\ 0.082 & 0.069 & 0.084 & 0.067 & -0.678 & 0.637 & -0.572 & 0.486 & -0.001 & 0.001 \\ 0.013 & 0.013 & 0.021 & 0.022 & 0.51 & -0.0056 & 0.493 & -0.002 & -0.001 & 0.001 \\ -0.002 & -0.0023 & 0.0015 & 0.0017 & -0.001 & -0.001 & 0.011 & -0.0056 & 1.194 & -1.194 \end{bmatrix} \times 10^{-6} \quad (5.23)$$

5.4 The Comparison of Results

Now, the experimental results are compared with the FEM and beam theory analysis results in order to see the advantage and disadvantage of the different analysis methods.

5.4.1 Applying Fx

Figure 5.8 shows the comparison of results when F_x is applied on the sensor frame.

From follow figure, it shows the gauge S1 and S3 value of the experimental data, FEM and beam theory model analysis result of strain when Fx is applied on the sensor.

The figure is the relationship between S1, S3 and force that applied on the x direction. The ♦ line is beam theory calculation result, the ■ one is Finite element method analysis result and the ▲ one is experiment data. In the first figure, the slope of beam theory model is $4.23*10^{-7}$, the slope of FEM is $3.375*10^{-7}$ and the slope of experimental data is $3.361*10^{-7}$. In the second figure, the slope of beam theory model is $-4.23*10^{-7}$, the slope of FEM is $-3.565*10^{-7}$ and the slope of experimental data is $-3.333*10^{-7}$.

By referring to Figure 5.8, it can be concluded that the maximum difference between the results of FEM model and those obtained from the experimental work is approximately 5%. Furthermore, it is observed that the maximum difference between the results calculated by the beam theory and the corresponding experimental data is about 26.4%.

It is seen that the experimental data are in close agreement with the FEM results. However, the calculated beam theory results are somewhat different from the experimental data. It indicates the Finite Element Method is more accurate than Beam

theory. The sensor has complicated structure and has larger error using the simplified beam theory model.

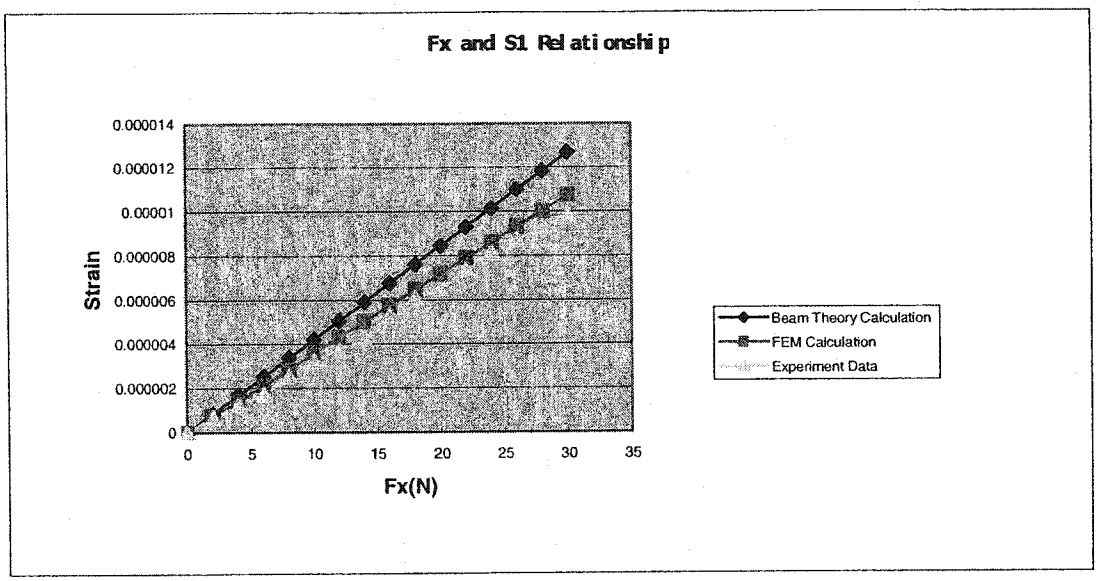

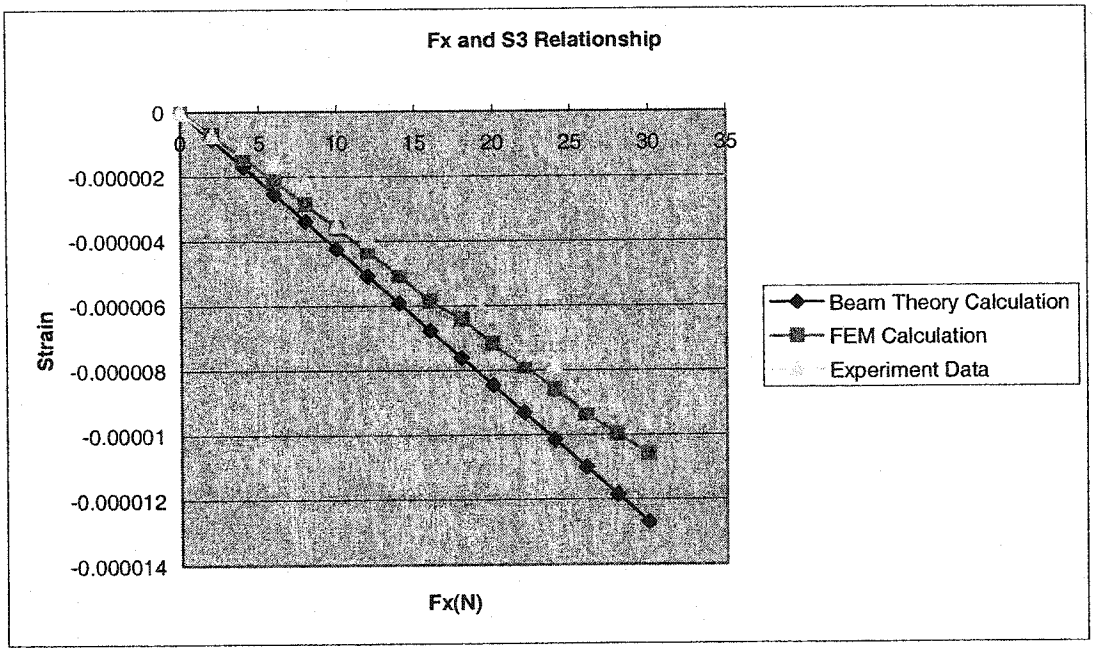

Figure 5.8 Data Comparison when applying Fx (0 to 30 N)

5.4.2 Applying Fy

Figure 5.9 shows the comparison of results when F_y is applied on the sensor frame.

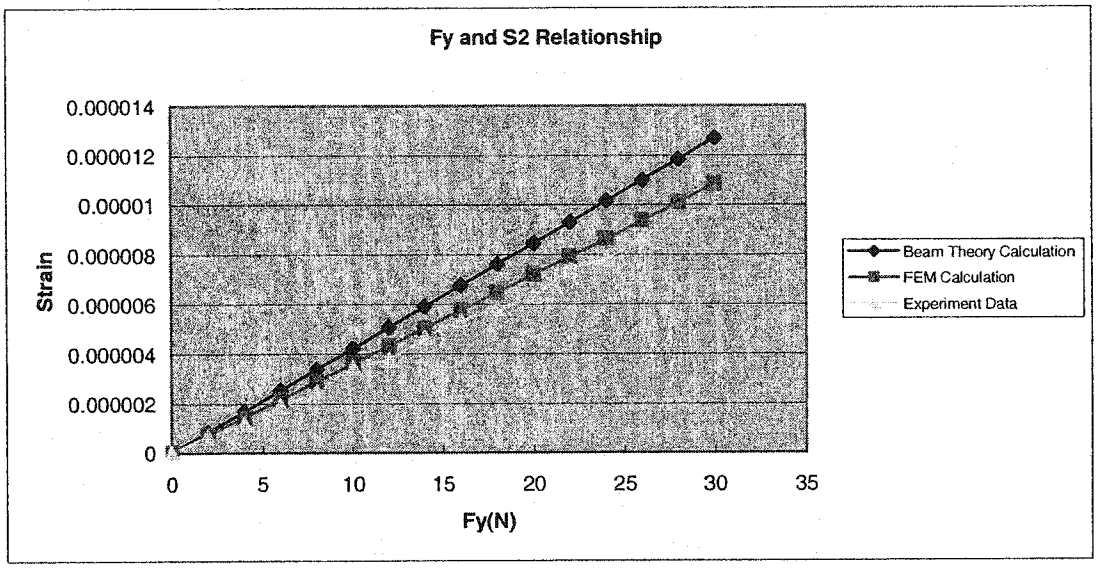

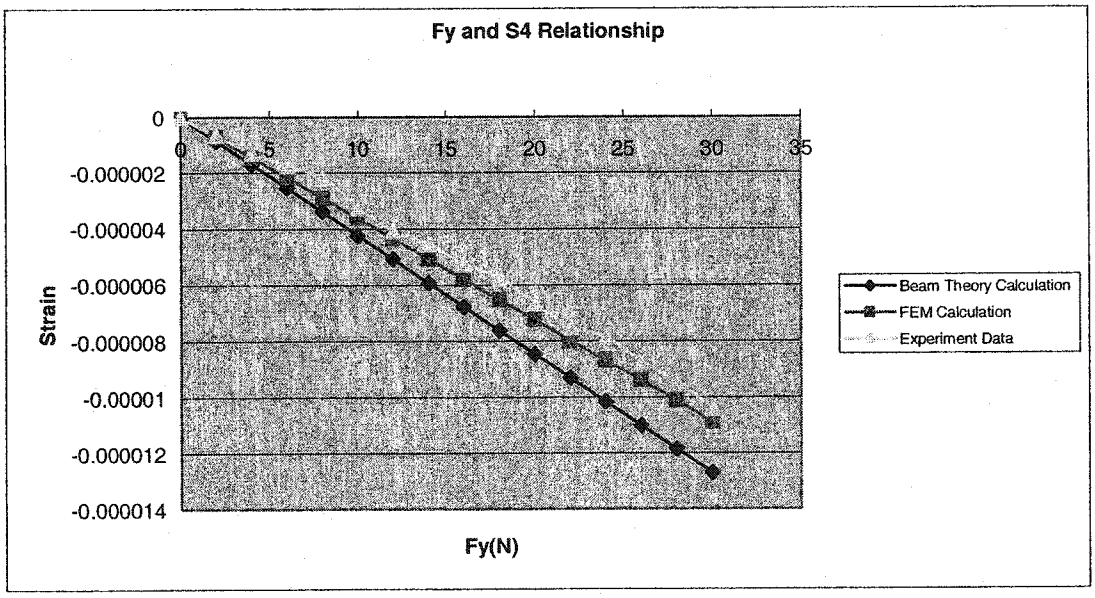

Figure 5.9 Data Comparison when applying Fy (0 to 30 N)

Figure 5.9 shows the gauge S2 and S4 value of the experimental data, FEM and beam theory model analysis result of strain when Fy is applied on the sensor.

The figure is the relationship between S2, S4 and force that is applied in the y direction. The ♦ line is beam theory calculation result, the ■ one is Finite element method analysis result and the ▲ one is experiment data. From the figure, the slope of beam theory model is $4.23*10^{-7}$ and $-4.23*10^{-7}$, the slope of FEM model is $3.6145*10^{-7}$ and $-3.615*10^{-7}$, the slope of experimental data is $3.326*10^{-7}$ and $-3.436*10^{-7}$.

By referring to Figure 5.9, it can be concluded that the maximum difference between the results of FEM model and those obtained from experimental work is about 6.95%. Furthermore, it is observed that the maximum difference between the results calculated by the beam theory and the corresponding experimental data is approximately 37.03%. Hence it is seen that the experimental data are in lose agreement with the FEM results. However, the calculated beam theory results are somewhat different from the experimental data. FEM is more accurate than Beam theory. Considering the structure is beam model brings more calculation error because the sensor frame has complicated structure and is not a simplified beam model.

5.4.3 Applying Fz

Figure 5.10 shows the comparison results when F_z is applied on the sensor frame.

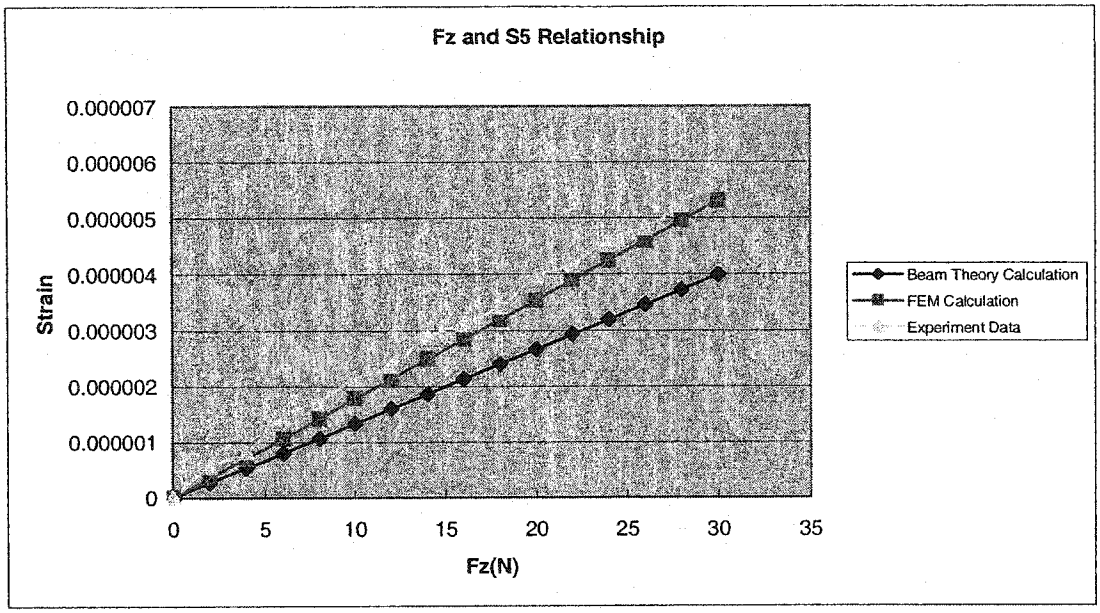

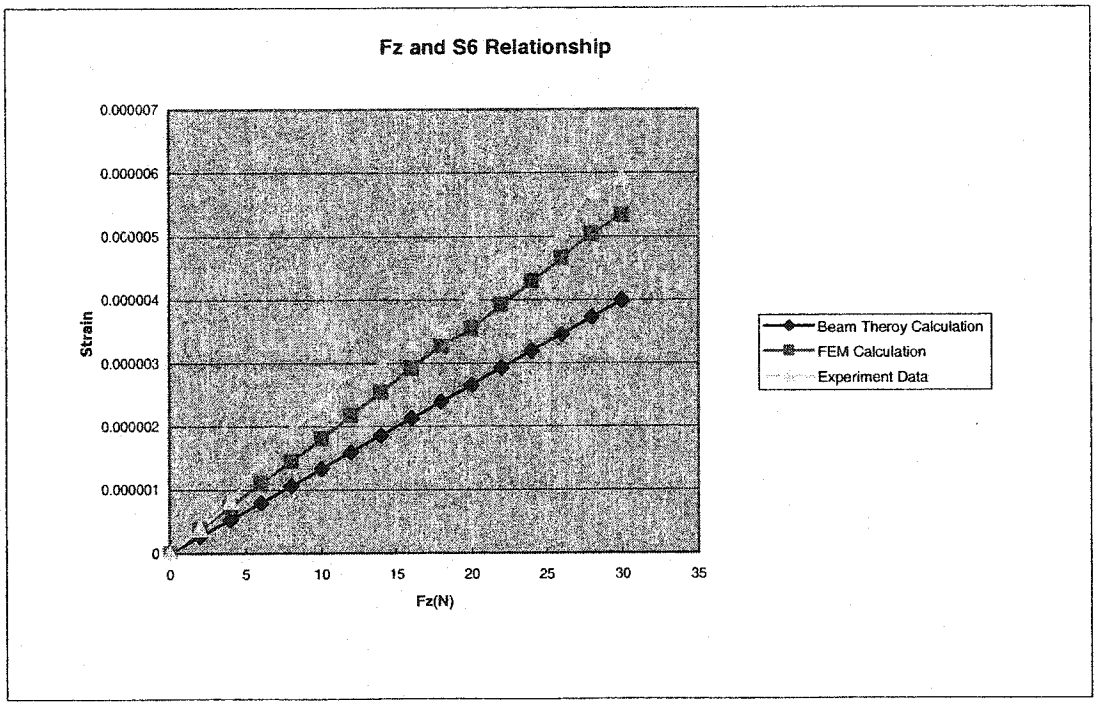

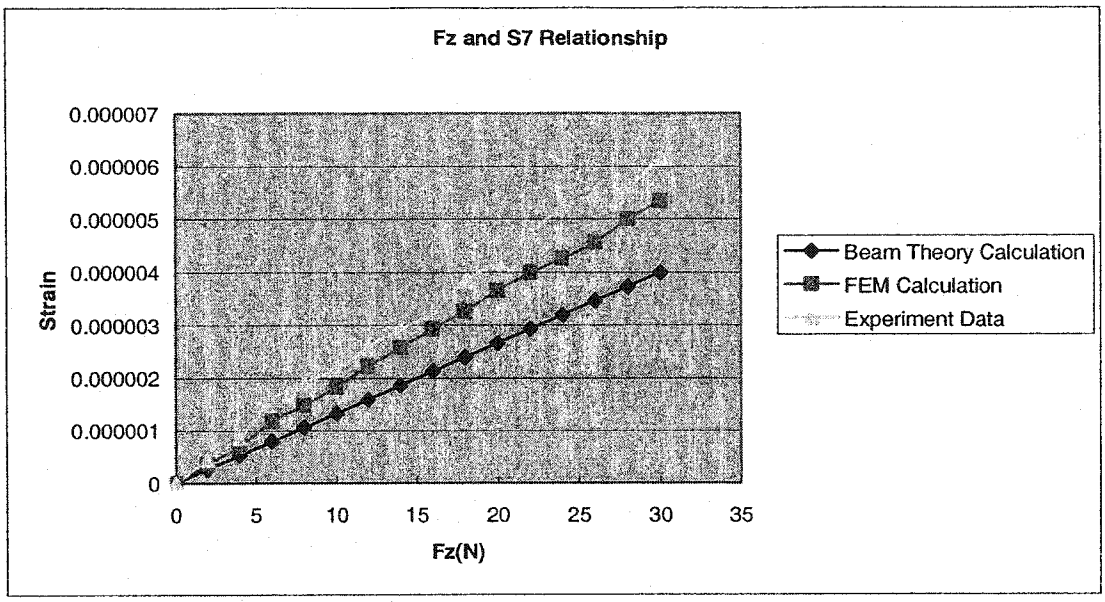

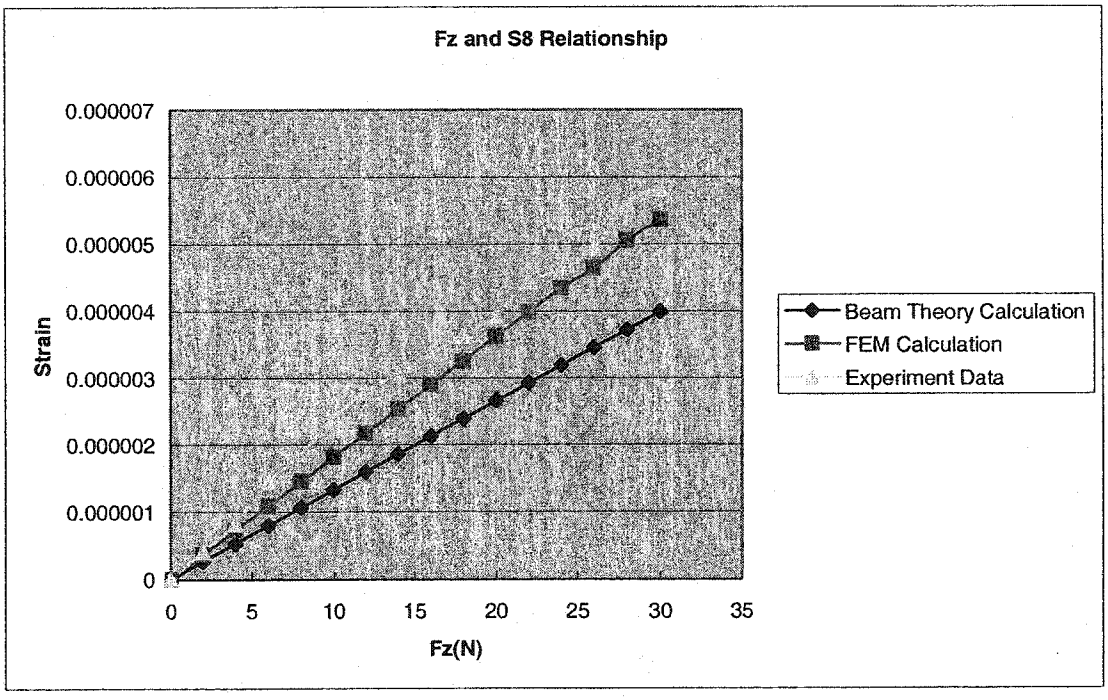

Figure 5.10 Data Comparison when applying Fz (0 to 30 N)

Figure 5.10 shows the values of strain gauge S5, S6, S7 and S8 value of the experimental data, FEM and beam theory model analysis result of strain when Fz is applied on the sensor.

The ♦ line is beam theory calculation result, the ■ one is Finite element method analysis result and the ▲ one is experiment data. From the figure, the slope of experimental data are $1.843*10^{-7}$, $1.938*10^{-7}$, $2.301*10^{-7}$, $1.89*10^{-7}$ respectively, the slope of FEM are $1.725*10^{-7}$, $1.84*10^{-7}$, $1.805*10^{-7}$, $1.81*10^{-7}$ respectively, and the slope of beam theory is $1.33*10^{-7}$.

Similarly comparing with experiment data, it can be found that the maximum difference between the results of FEM model and those obtained from the experimental work is about 10%. Furthermore, it is observed that maximum difference between the results calculated by the beam theory and the corresponding experimental data is approximately 33%. Hence the same result as Figure 5.8 is obtained that the experimental data are in close agreement with the FEM results. However, the calculated beam theory results are somewhat different from the experimental data. It can be concluded that FEM is more accurate than Beam theory.

5.4.4. Applying Mx

Figure 5.11 shows the comparison results when apply M_x is applied on the sensor.

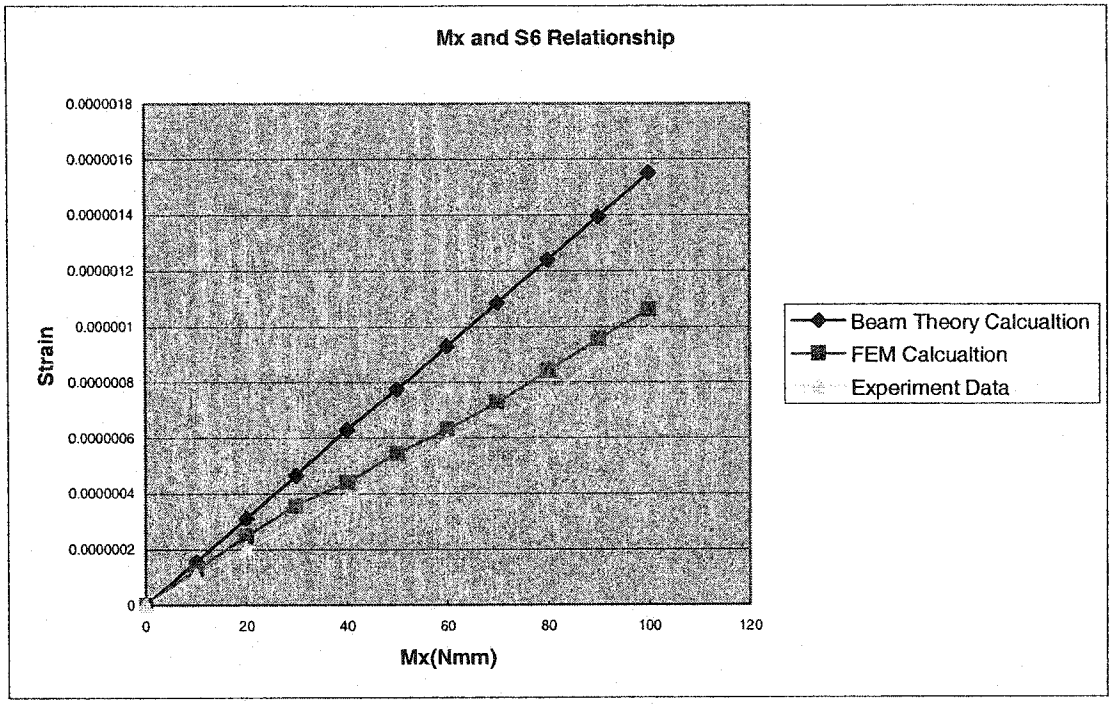

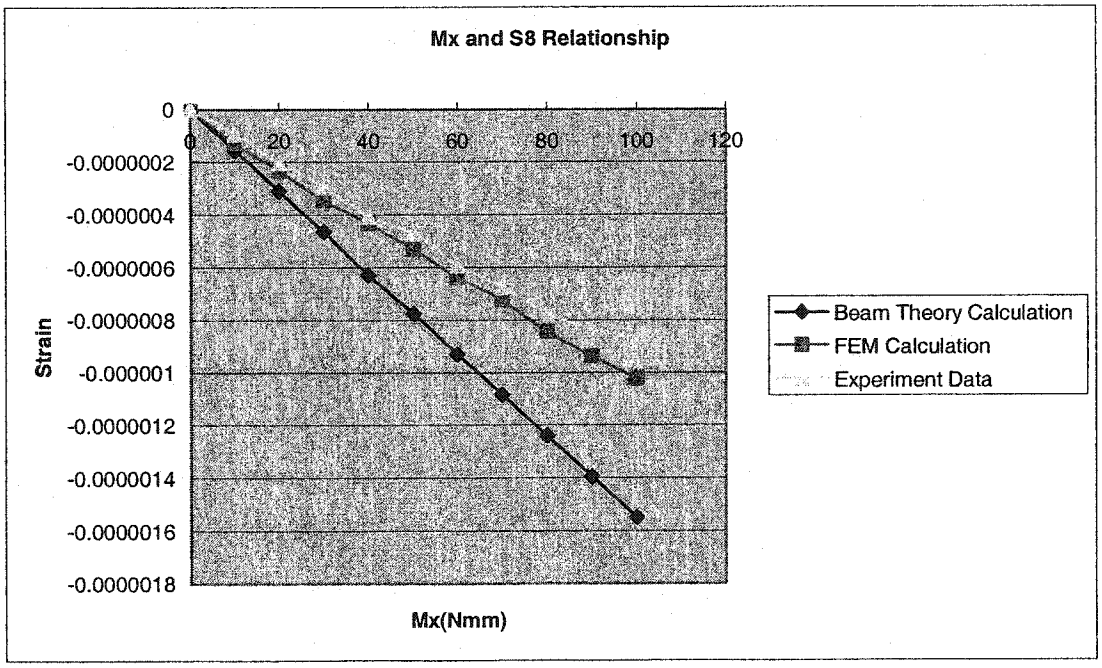

Figure 5.11 Data Comparison when applying Mx (0 to 100 Nmm)

Figure 5.11 shows the values of strain gauge S6 and S8 value of the experimental data, FEM and beam theory analysis result of strain with the moment that is applied in the x direction.

The ♦ line is beam theory calculation result, the ■ one is Finite element method analysis result and the ▲ one is experiment data. From the figure, the slope of beam theory model are $1.55*10^{-8}$ and $-1.55*10^{-8}$, the slope of FEM is $1.2801*10^{-8}$ and $-1.29*10^{-8}$, the slope of experimental data is $9.635*10^{-9}$ and $-9.09*10^{-9}$.

By referring to Figure 5.11, it can be concluded that the maximum difference between the results of FEM model and those obtained from the experimental work is approximately 16.6%. Furthermore, it is observed that the maximum difference between the results calculated by the beam theory and the corresponding experimental data is about 35.4%. It is seen that the experimental data are in close agreement with the FEM results. However, the calculated beam theory results are somewhat different from the experimental data. It indicates the Finite Element Method model is more accurate than Beam theory model.

5.4.5 Applying My

Figure 5.12 shows the comparison of results when M_y is applied on sensor.

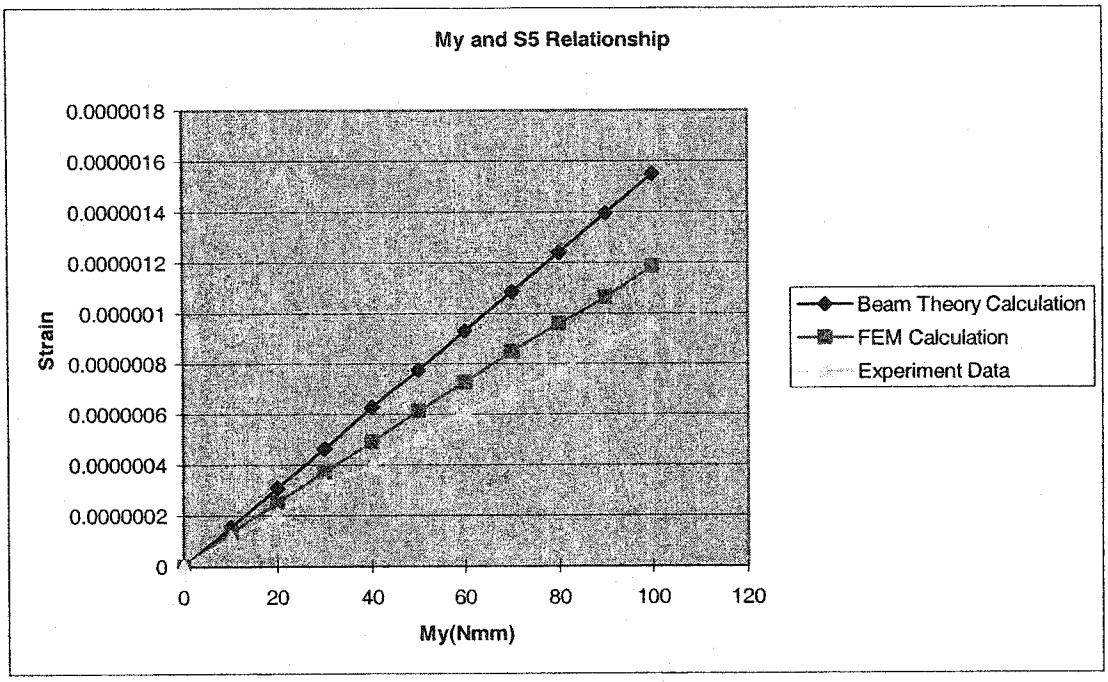

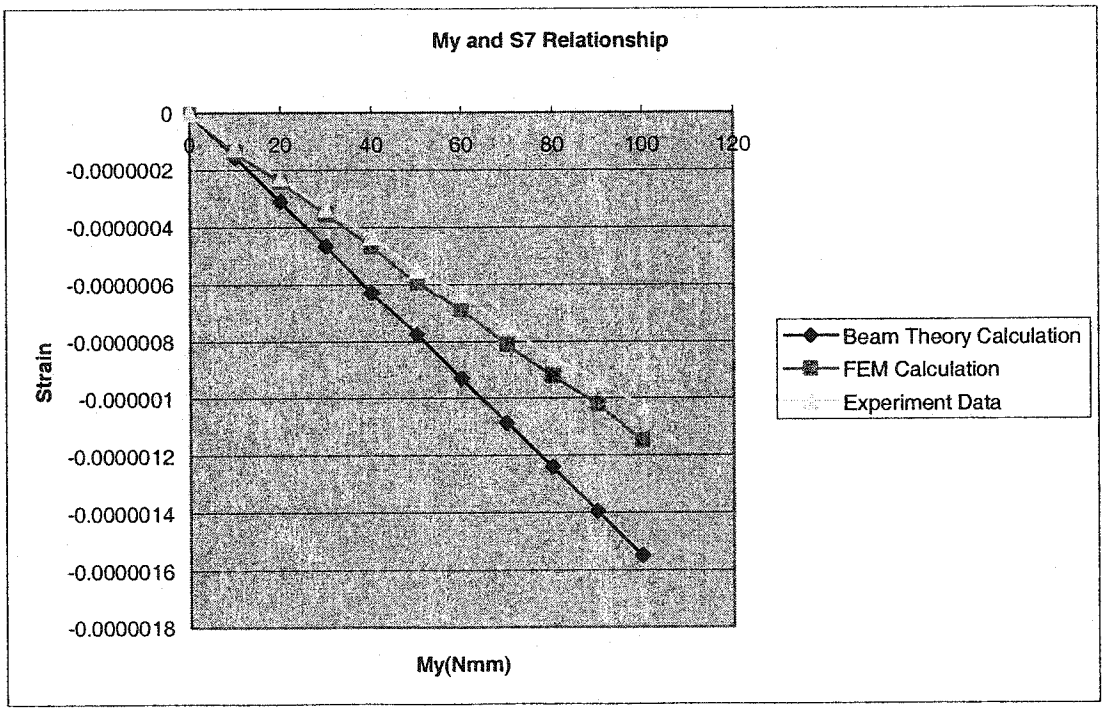

Figure 5.12 Data Comparison when applying My (0 to 100 Nmm)

Figure 5.12 shows the readouts of strain gauge S5 and S7 with the moment that is applied in the y direction.

The ♦ line is beam theory calculation result, the ■ one is Finite element method analysis result and the ▲ one is experimental data. From the figure, the slopes of beam theory model are $1.55*10^{-8}$ and $-1.55*10^{-8}$, the slope of FEM is $1.32*10^{-8}$ and $-1.38*10^{-8}$ and the slope of experimental data is $9.55*10^{-9}$ and $-1.029*10^{-8}$.

By referring to Figure 5.12, it can be concluded that the maximum difference between the results of FEM model and those obtained from the experimental work is approximately 16.1%. Furthermore, it is observed that the maximum difference between the results calculated by the beam theory and the corresponding experimental data is about 36.25%. It is seen that the experimental data are in close agreement with the FEM results. However, the calculated beam theory results are somewhat different from the experimental data. It indicates the Finite Element Method model is more accurate than Beam theory model.

5.4.6 Applying Mz

Figure 5.13 shows the comparison of results when M_z is applied on sensor.

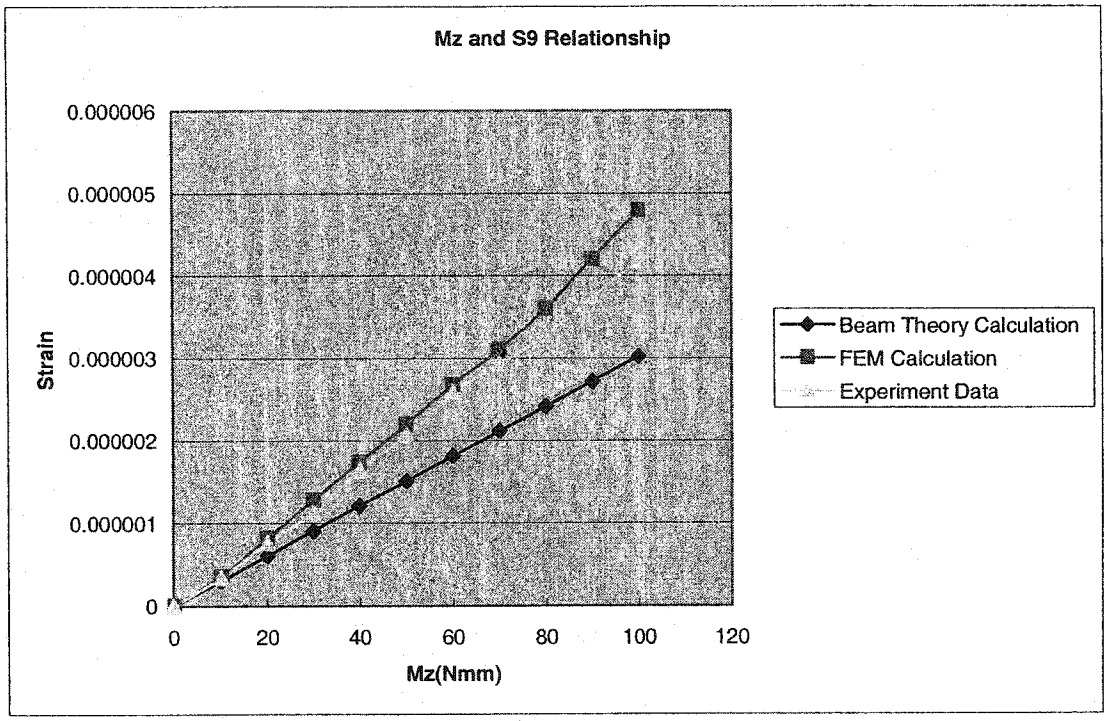

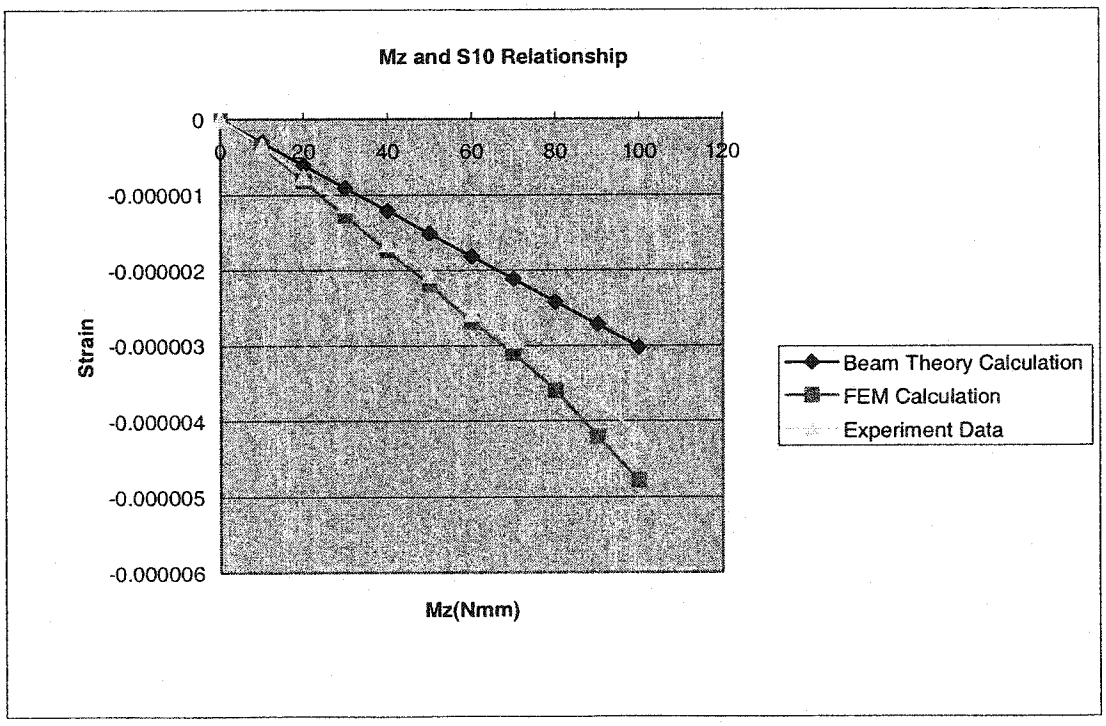

Figure 5.13 Data Comparison when applying Mz (0 to 100 Nmm)

Figure 5.13 shows the readout of strain gauge S9 and S10 when Mz is applied on the sensor.

The figure is the relationship between S9, S10 and the moment that is applied in the z direction. The ♦ line is beam theory calculation result, the ■ one is Finite element method analysis result and the ▲ one is experimental data. From the figure, the slopes of beam theory model are $3.02*10^{-8}$ and $-3.02*10^{-8}$, the slopes of experimental data are $4.235*10^{-9}$ and $-4.235*10^{-9}$, the slopes of FEM model are $4.79*10^{-9}$ and $-4.79*10^{-9}$.

By referring to Figure 5.13, it can be concluded that the maximum difference between the results of FEM model and those obtained from the experimental work is approximately 11.59%. Furthermore, it is observed that the maximum difference between the results calculated by the beam theory and the corresponding experimental data is about 36.95%. It is seen that the experimental data are in close agreement with the FEM results. However, the calculated beam theory results are somewhat different from the experimental data. It indicates the Finite Element Method model is more accurate than Beam theory model. Hence the conclusion is obtained that making simply beam model to solve the complicated structure will definitely bring some calculation error.

From the above analysis, it can be seen that:

1. The sensor can successfully satisfy the expected function of measuring force/torque.
2. The sensor exhibits good linearity.
3. There is a reasonable correspondence between the experimental results and the results obtained by FEM.
4. Beam model can provide some useful insight in the preliminary design of the sensor.
5. The results of FEM closely match those of experimental data. FEM predicts the experimental data more closely than the beam theory aproach.

In next chapter, the total conclusion of this thesis will be obtained. Then the suggestions for future work will be discussed.

Chapter 6

Conclusions and Suggestions for Future Work

In the preceding chapter, the six-degree freedom force/torque sensor was fabricated and experiments were carried out. The calibration matrix was calculated and the experimental results were compared with FEM model and beam theory model. In this chapter, the summary of the thesis will be presented, conclusions based on the present study will be drawn and suggestions for future work will be provided.

6.1 Summary

Motivated by the need of MIS force/ torque sensing in surgery tools and simulation training, a new 6-DOF-force/torque sensor has been designed based on the Weiyi's result. Its key features are linearity, very low cross sensitivity along different axes, light weight, and simplicity of the structure. In addition, sensor structure was designed such that it could be integrated with the cylindrical tube of an endoscopic tool. The sensor geometry was analyzed by the beam theory model and FEM model. By combining the micro strain gauge, the way of arranging and locating appropriately the strain gauge was considered. Then the sensor was tested extensively to validate the design and analysis and to ensure their suitability as a force/torque sensor. The calibration for six components of force versus output voltages was carried out. This sensor exhibits outstanding linear and decoupling characteristics. The sensitivities and linearity, close to the design values, and high enough to measure the forces and moments expected to act on

the endoscopes.

6.2 Conclusions

Based on the results of analysis and experimental investigations, the following conclusions are drawn:

1. Thorough analysis was performed on the assumptions made on the linearity and low cross sensitivity of the sensor along different axes. Both experimental and theoretical approaches were used and consequently, both of the assumptions were validated.
2. The experimental results were in close correspondence with the results obtained by finite element modeling. It was concluded that there was a difference of approximately 10% between the finite element modeling results and that experimental data. This means that FEM is quite adequate in predicting the experimental results for the designed sensor assembly.
3. The conventional simple beam theory can be adequately utilized in the design of the sensor. The calculations show that there is an average discrepancy of about 35% between the two sets of data, i.e., the experiment data and those predicated by the simple beam theory approach, both methods give rise to similar general trends, and are considered to be acceptable.
4. It is of great importance to be able to integrate a force/torque sensor with an endoscopic tool to compensate for the loss of tactile sensing. Considering the cylindrical structure of the designed sensor. Together with high sensitivity and good linearity of the system, the designed sensor is suitable to be integrated with the cylindrical tube of an endoscopic tool.

6.3 Suggestions for Future Work

In the thesis, a prototype sensor is designed for mounting on endoscopic handle. The dimensions of the sensor frame were chosen from the prior of views of ease fabrication. The dynamitic characteristics of the sensor are not considered. The following suggestions for future work are given:

- Optimize the sensor structure to get better mechanical features, including the linearity, cross sensitivity, weight, and stiffness characteristics, etc.
- Fabricate the sensor in proper dimension to install on endoscopic tools or other applications where the force and torque is required to be measured.
- The dynamic characteristics of the sensor should be considered in the design, the structure of sensor should have good dynamic feature, and the dynamic experiments also should be set up to test the sensor.
- Develop the interface between the sensor and computer, so the output of strain gauges can be sent to the computer and displayed directly.
- For improving the measurement precision, the number of gauges should be increased. Then the temperature compensation and ratio of signal to noise problem can be advanced satisfactorily.
- MEMS technique will be applied in the sensor fabrication.

REFERENCES

[1] John G.Webster: "Mechanical Variables Measurement", *Boca Raton, Fla : CRC Press*, c2000.

[2] Stephan Fahlbusch, Sergej Fatikow: "Force Sensing in Microrobotic Systems-An Overview", *Electronics, Circuits and Systems, 1998, IEEE International Conference on* , Vol 3, pp 259 -262 .

[3] Keith A.Morris, "Has Force/Torque Sensing Gained Factory Acceptance?" Proceedings of the 1992 IEEE/RSJ international conference on Intelligent Robots and System, Raleigh, N C, July 7-10, 1992.

[4] Jacob Rosen, Mark Macfarlane, Christina Richard, Blacke Hannaford, Mika Sinnanan, "Surgeon-Tool force/Torque Signatures Evaluation of Surgical Skills in Minimally Invasive Surgery". *Proceeding of Medicine Meets virtual reality, MMVR-7, IOS Press. San Francisco, CA.* January 1999.

[5] SAGES, "Framework for post-residency surgical education and training": *A SAGES Guideline.* 1994.

[6] Chen E., Marcus B., "Force Feedback for Surgical Simulation", *Procedings, of The IEEE, Mar.1998,* Vol.86, *no.3.* pp 524-530.

[7] Dargahi. J, "Micro-strain gauge endoscopic tactile sensor using two sensing elements for tissue manipulation", *Proceedings - IEEE International Conference on Robotics and Automation*, Vol 1, 1999, pp 299-304

[8] Dargahi. J, "Micromachined piezoelectric teeth-like laparoscopic tactile sensor: theory, fabrication and experiments", *Journal of Mechanical Design, Transactions of the ASME*, Vol.124, n 3, September 2002, pp 576-582.

[9] Declercq, S.M, "A smart 6-DOF load cell development", *Proceedings of SPIE – The International Society for Optical Engineering*, Vol.4753 I, 2002, pp 844-853.

[10] Farhad. Aghil, Martin. Buehler, John. M. Hollerbach, "Design of a hollow hexaform forque sensor for robot joints", *International Journal of Robotics Research*, Dec 2001.

[11] Klafter,R.D, Chmielewski, T.A, and Negin, M.: "An Integrated Approach".*Robotics Engineering* Englewood Cliffs, NJ:Prentice Hall. 1989.

[12] Akihiko Yabuki, "Six-Axis Force/Torque Sensor for Assembly Robots" *Source: Fujitsu Scientific and Technical Journal, v 26, n 1, Spring, 1990*, pp 41-47.

[13] Uchiyama. M, Bayo. E., Palma-Villalon. E: "A Systematic Design Procedure to Minimize a Performance Index for Robot Force Sensors", *Journal of Dynamic Systems, Measurement, and Control*, September 1991, Vol.1. pp 113/389.

[14] Lu-Ping Chao, Kuen-Tzong Chen: "Shape Optimal Design and Force Sensitivity Evaluation of Six-Axis Force Sensors", *Sensor and Actuators* A 63(1997) pp105-112.

[15] Tsuneo Yoshikawa and Taizou Miyazaki: "A Six-Axis Force Sensor with Three-Dimensional Cross-Shape Structure", *Robotics and Automation, 1989. Proceedings., 1989 IEEE International Conference on* , vol.1, 14-19 May 1989, pp 249 –255.

[16] Chul-Goo kang, "Maximum Structure Error Propagation of Multi-axis Force Sensor", *JSME International Journal*, Series C, Vol .44, No.3, 2001.

[17] Svinin M. M., Uchiyama M., "Optimal Geometric Structures of Force/Torque Sensors", *The International Journal of Robotics Research*, Vol. 14, No.6, December 1995, pp 560-573.

[18] Kim.Gab-Soon: "The design of a six-component force/moment sensor and evaluation of its uncertainty", *Measurement Science & Technology* [H.W. Wilson – AST], Sep 2001.

[19] Anotonia Bicchi: "A Criterion for Optimal Design of Aulti-Axis Force Sensors". *Robotics and Autonomous Systems*, Vol.10, 1992, pp 269-286.

[20] Anotonia Bicchi, J. Kenneth Salishbury and David L. Brock: "Contact Sensing from Force Measurements", *International Journal of Robotics Research*, Vol. 12, Number 3, 1993.

[21] D. Stewart: "A platform with six degree of freedom", *Proc. Inst. Mech. Eng.* 180 (1965) pp 371-386.

[22] Chul-Goo Kang: " Closed-form Force Sensing of a 6-Axis Force Transducer based on the Stewart Platform", *Sensors and Actuators* A 90(2001) pp 31-37.

[23] Sorli M. and Pastorelli S.: "Six-Axis Reticulated Structure Force/Torque Sensor with Adaptable Performances", *Mechatronics* Vol.5. No.6, 1995, pp 585-601.

[24] Makoto Kaneko: "Twin-Head Six-Axis Force Sensors", *IEEE Transactions On Robotics and Automation*, Vol. 12, No.1, February 1996.

[25] Makoto Kaneko: "A New Design of Six-Axis Force Sensors", *in Proceeding IEEE Int. Conf. Robotics and Automation*, 1993, pp 961-967.

[26] Koichi Nishiwaki, Yohsifumi Murakami, Satoshi Kagami, Yasuo Kuniyoshi, Masayuki Inaba and Hirochika Inoune: "A Six-axis Force Sensor with Parallel Support Mechanism to Measure the Ground Reaction Force of Humanoid Robot", *Proceedings of the 2002 IEEE, International Conference on Robotics & Automation Washington, DC.* May 2002.

[27] Dirk Didden, Dominiek Reynaerts, Hendrik Van Brussel, "Design of a ring-shaped three-axis micro force/torque sensor", *Sensors and Actuators* Wol. 46-47(1995) pp 225-232.

[28] E. Bayo, J.R.Stubbe, "Six-axis force sensor evaluation and a new type of optimal frame truss design for robotic application", *J Robotic system* Vol.6(2), (April 1989), pp191-208

[29] Dzung Viet Dao, Toshiyuki Toriyama, John Wells and Susmum Sugiyama: "Six Degree of Freedom Micro Force-Moment Sensor for Application in Geophysics", *Micro Electro Mechanical Systems, 2002. The Fifteenth IEEE International Conference on, 2002* pp: 312 –315.

[30] Y.H.Chang, John E.A.Bertram and Andy Ruina: "A Dynamic Force And Moment Analysis System For Brachiation", *The Journal of Experimental Biology 200,* 1997,pp 3013-3032.

[31] St. Fahlbusch and S. Fatikow: "Micro Force Sensing in a Micro Robotic System", *Proceedings of the 2001 IEEE International Conference on Robotics & Automation Seoul, Korea.* May21-26, 2001.

[32] Antonio Bicchi, Gaetano Canepa, Danilo De Rossi, Peitro Iacconi and Enzo P.Scilingo: "A Sensorized Minimally Invasive Surgery Tool for Detecting Tissutal Elastic Properties" *Proceedings of the 1996 IEEE International Conference on Robotics and Automation Minneapolis, Minnesota*-April 1996.

[33] Evangelos Papadopulos, Kostas Vlachos and Dionyssios Mitroppulos: "Design of 5-dof Haptic Simulation for Urological Operations", *Proceedings 2002 IEEE International Conference on Robotics and Automation. ICRA 02, Washington DC,* May 11-15 2002.

[34] Dong-Soo Kwon, Ki Young Woo, Se Kyong song, Wan Soo Kim,

Hyung Suck Cho, "Microsurgical Telerobot System", Proceedings of the IEEE/RSJ International Conference on Intelligent Robots and Systems", 1998, pp 945-950,

[35] Anotonia Bicchi, Caiti. A. and Prattischizzo .D.: "Optimal design of dynamic multi-axis force/torque sensor", *Proceedings of the 38th Conference on Decision & Control* Phoenix, Arizona USA. December 1999.

[36] Di Xiao, Bijoy K. Ghosh, Ning Xi and T.J.Tarn: "Sensor-Based Hybrid Position/Force Control of a Robot Manipulator in an Un-calibrated Environment". *IEEE Transactions On Control System Technology,* Vol, 8, *No4,* July, 2000.

[37] Tsujimura, T. and T. Yabuta: "Object detection by tactile sensing method employing force/moment information", *IEEE Tans on Robotics and Automation*, Vol .5, no.4, 1988.

[38] Ferraresi .C., Pastorelli .S., Sorli .M., Zhmud .N., "Static and dynamic behavior of a high stiffness Stewart Platform-base", *J Robotic System*, Vol.12(12), Dec, 1995 pp 883-893.

[39] Mills. J. K "Dynamic Modeling of Robotic Manipulators with a force-torque sensor during compliant motion", *Proc. IEEE Int. Conf. Robotics and Automation*, 1989, pp1672-1677.

[40] Hirzinger. G. and Dietrich. J, "Multisensory Robots and Sensor based Path Generation", *Proc IEEE International Conference on Robotics and Automation*, (1986), pp 1992-2001.

[41] Kvasnica. M, "Six-Component Force-Torque Sensing by Means of One Square CCD or PSD Element", *Proc. International Symposium on Measurement and Control in Robotics Japan (1992).*

[42] Nabil Maalej, John G.Webster, "A Miniature Electrooptical Force Transducer", *IEEE Trans On Biomedical Engineering*, Vol.33 No.2 Feb 1988.

[43] Window .A.L., Holister. G. S.: "Strain Gauge Technology", London:*Applied Science Publishers*. C 1982.

[44] Albert, "Regression and the Moore-penrose Pseudoinverse", New York: *ACADEMIC PRESS*, INC 1972.

[45] Herstein .I. N., David J. Winter: " Matrix Theory and Linear Algebra" *New York; Macmillan; London: Collier Macmillan, c1988.*

[46] Weiyi Huang, Hongming Jiang, Hanqing Zhou: "Mechanical Analysis of a Novel Six-Degree-Freedom Wrist Force Sensor". *Sensor and Actuators* A.35(1993), pp 203-208.

[47] Alexander Blake: "Practical Stress Analysis in Engineering Design" *Lawrence Livermore National Laboratory*, Livermore, California, New York: Marcel Dekker, Inc.New Your and Basel.c1990.

[48] Cook .R. D., Malkus .D. S. and Plesha .M. E.: " Concept and Application of Finite Element Analysis" *New York : Wiley*, c1989.

[49] Bathe .K. J.: "Finite Element Procedures", *Englewood Cliffs, N.J. :*

Prentice Hall, c1996.

[50] Rockey, R.C., Kenneth, Charles: "The Finite Element Method; A Basic Introduction for Engineers" *London ; Toronto : Granada Pub.*, 1979, c1975.

[51] Reddy .J. N.: "An Introduction to the Finite Element Method", *New York : McGraw-Hill*, c1993 .

[52] SWANSON ANALYSIS SYSTEM, INC, "ANSYS: User's Manual (Revision 5.0) Volume III Element".

[53] Entran Company Website: http:// www.entran.com.

[54] Enders A. Robinson. "Least Squares Regression Analysis Terms of Linear Algebra" *Houston. Tex, Goose Pond Press*, c1981.

[55] Norma Gilbert : "Statistics" (2nd Edition) *Philadelphia; Saunders College Pub.* C1981.

APPENDIX A

Matlab Code

```
%-----------------------------Author: Shengmei Wang----------------------------------------

%-------------------------------Date:        2003/05/12 -----------------------------------------

%-------------------------------Title:   The Check Calibration --------------------------------

clear;


%%%%%%%%%%%%%%%%%%%%%%%%%%%%%%%%%%%%%%%%%%%%%%

h=1;             % The thickness of vertical and horizontal is 1 mm

H=17.5;          % Acccording to the three basic assumptions h/H<1/10, H= 20 mm

S=35;            % The length of the beam is 35 mm

L1=10;           % Acccording to the assumptions h/L1<1/10, L1= 10 mm

L2=11;           % Acccording to the assumptions h/L2<1/10, L2 H= 11 mm

R=L1+L2;         % Inside radius R=L1+L2

b=6;             % The perimeter l= 2*3.14*R,b< l/4

E=2.067*10^7;% The Young's modulus of standard steel

Fx=1;            % The Maximum Force of X direction

Fy=1;            % The Maximum Force of Y direction

Fz=1;            % The Maximum Force of Z direction

Mx=100;           % The Maximum Moment of X direction

My=100;           % The Maximum Moment of Y direction
```

```
Mz=100;          % The Maximum Moment of Z direction

I=b*h*h*h/12;    % The moment of inertia of the section of the beam

M1=Fx*H/2;       % Only Fx is applied , beam OA,OC occure bending moment

M2=Fy*H/2;       % Only Fy is applied , beam OB,OD occure bending moment

M3=Fz*L2/4;      % Only Fz is applied, beam OA,OB,OC,OD occure bending moment

M4=Mx*L1/(2*R);  % Only Mx is applied, beam OB,OD occure bending moment

M5=My*L1/(2*R);  % Only My is applied, beam OA, OC occure bending moment

M6=Mz*R/(4*R);   % Only Mz is applied, AE,BF,CG,DH occure bending moment

Stress1=M1*(h/2)/I;   %The stress of the beam AE and CG under Fx is applied only

Stress2=M2*(h/2)/I;   %The stress of the beam BF and DH under Fy is applied only

Stress3=M3*(h/2)/I;   %The stress of the beam OA,OB,OC and OD under Fz is applied

Stress4=M4*(h/2)/I;   %The stress of the beam OB and OD under Mx is applied only

Stress5=M5*(h/2)/I;   %The stress of the beam OA and OC under My is applied only

Stress6=3*M6/(2*b*h); %The shear stress of the beam AE.BF,CG.DH under Mz applied

S1=Stress1/E;         %The readout of the first and third strain gague under Fx

S2=Stress2/E;         %The readout of the second and the forth strain gague under Fy

S3=Stress3/E;         %The readout of the fifth, sixth, seventh, eigth strain gague

S4=Stress4/E;         %The readout of the sixth and eigth strain gague under Mx

S5=Stress5/E;         %The readout of the fifth and seventh strain gague under My
```

```
S6=Stress6/E;          %The readout of the first, second, third and the forth gague Mz

K1=Fx/(2*S1);          %The coefficient of K1

K2=Fy/(2*S2);          %The coefficient of K2

K3=Fz/(4*S3);          %The coefficient of K3

K4=Mx/(2*S4);          %The coefficient of K4

K5=My/(2*S5);          %The coefficient of K5

K6=Mz/(4*S6);          %The coefficient of K6

%%%%%%%%%%%%%%%%%%%%%%%%%%%%%%%%%%%%%%%%%%%%%%%%%%%%%%%%%%%%%%%%%%%%%%%%%%%%

m=0;

Fx=0;

Fy=0;

Fz=0;

Mx=0;

My=0;

Mz=0;

for n=0:1:10;

m=m+1;
```

```
I=b*h*h*h/12;

M1=Fx*H/2;

M2=Fy*H/2;

M3=Fz*L2/4;

M4=Mx*L1/(2*R);

M5=My*L1/(2*R);

M6=Mz*R/(4*R);


Stress1=M1*(h/2)/I;

Stress2=M2*(h/2)/I;

Stress3=M3*(h/2)/I;

Stress4=M4*(h/2)/I;

Stress5=M5*(h/2)/I;

Stress6=3*M6/(2*b*h);


S1(m)=Stress1/E;

S2(m)=Stress2/E;

S3(m)=Stress3/E;

S4(m)=Stress4/E;

S5(m)=Stress5/E;

S6(m)=Stress6/E;
```

```
Fx=Fx+1;

Fy=Fy+1;

Fz=Fz+1;

Mx=Mx+10;

My=My+10;

Mz=Mz+10;


end;


Fx=0:1:10;

Fy=0:1:10;

Fz=0:1:10;

Mx=0:10:100;

My=0:10:100;

Mz=0:10:100;
```

To be continued

%----------Calibration Matrix ----------

%----------2003/04/18----------

%----------Author: Shengmei----------

clear;

%--------- The Beam Model Calibration Mztrix----------

```
C=[48.3793E-08 0    0    0    0    0
   0    48.3793E-080    0    0    0
   -48.3793E-08     0    0    0    0    0
   0    -48.3793E-08   0      0    0    0
   0    0    13.3042E-080    115.189E-080
   0    0    13.3042E-08115.189E-080    0
   0    0    13.3042E-080    -115.189E-08    0
   0    0    13.3042E-08-115.189E-08    0    0
   0     0    0     0    0   30.237E-08
   0     0    0     0    0   -31.237E-08];
```

Cplus=inv(C'*C)*C'

%--------- The FEM Model Calibration Matrix----------

C1=[3.62E-07 5.83E-08 -3.59E-07 -2.62E-08 6.02E-09 -2.05E-08

```
    -1.03E-08    1.06E-08    3.5338E-09  -3.5340E-09
   2.95E-083.63E-07    -1.25E-08    -3.62E-07    -1.06E-08    6.08E-08    1.33E-08
    6.02E-08    6.03E-09    -6.04E-09
    -2.18E-08    3.09E-08    2.04E-08    2.99E-08    1.78E-07    1.80E-07
    1.83E-07    1.82E-07    7.7394E-09  -7.7414E-09
   1.90E-083.62E-08    -1.89E-08    3.66E-08    -9.99E-08    1.06E-06    7.71E-08
    -1.02E-06    1.56E-08    -1.55E-08
    -3.70E-08    -1.92E-08    -3.69E-08    -1.92E-08    1.18E-06    2.33E-08
    -1.15E-06    -2.32E-08    1.50E-08    -1.49E-08
  2.78E-08  2.66E-08    -2.82E-08    2.68E-08    -1.12E-07    4.57E-08    1.23E-07
    -4.12E-08    4.79E-06    -4.81E-06];
C1=C1'
C1plus=inv(C1'*C1)*C1'

%--------- The Experimental Calibration Matrix----------------------------------

C2=[3.25E-07    2.50E-08    -3.50E-07    2.95E-08    2.50E-08    2.75E-08
    2.15E-08    2.25E-08    5.25E-09 -5.26E-09
    2.35E-083.46E-07    2.35E-08    -3.24E-07    2.80E-08    2.45E-08    2.50E-08
    2.45E-08    5.85E-09 -5.86E-09
    3.42E-094.82E-09    4.42E-09    3.42E-09    2.14E-07    2.39E-07    2.18E-07
```

2.40E-07 3.20E-09 -3.21E-09

7.24E-086.47E-08 6.37E-08 5.27E-08 5.07E-08 9.72E-07 4.57E-08

8.70E-07 4.75E-08 -4.75E-08

4.28E-084.80E-08 4.10E-08 3.72E-08 9.60E-07 4.72E-08 -1.03E-06

4.02E-08 5.31E-08 -5.31E-08

3.64E-083.42E-08 2.62E-08 2.54E-08 3.25E-08 3.12E-08 2.42E-08

2.92E-08 4.18E-06 -4.19E-06];

C2=C2'

C2plus=inv(C2'*C2)*C2'

To be continued

```
%----------Author: Shengmei----------

%----------2003/05/18----------

%----------Data Process----------

clear;

N=16;

force=0:2:30;

%N=10;

%force=0:10:100;


%----------Fx is aplied on the sturcute----------


s1=[0 6.75E-07 1.25E-06 1.75E-06 2.55E-06 3.25E-06 3.75E-06
    4.25E-06 5.32E-06 6.09E-06 6.52E-06 7.39E-06 8.15E-06
    8.72E-06 9.23E-06 9.85E-06];
s2=[0 4.30E-08 8.27E-08 1.50E-07 1.79E-07 2.50E-07 3.20E-07
    4.32E-07 4.87E-07 5.57E-07 6.62E-07 7.15E-07 7.56E-07
    8.02E-07 8.90E-07 9.22E-07];
s3=[0 -7.12E-07 -1.05E-06 -1.60E-06 -2.15E-06 -3.50E-06
    -3.94E-06 -4.62E-06 5.12E-06 -5.72E-06 -6.25E-06
    -7.50E-06 -7.82E-06 -8.92E-06 -9.16E-06 -9.59E-06];
```

s4=[0 5.70E-08 1.20E-07 1.70E-07 1.90E-07 2.95E-07
3.60E-07 3.97E-07 5.21E-07 5.91E-07 6.20E-07
7.12E-07 7.60E-07 7.90E-07 8.60E-07 8.55E-07];

s5=[0 4.20E-08 9.30E-08 1.20E-07 2.10E-07 2.50E-07
3.30E-07 3.80E-07 4.90E-07 5.60E-07 5.90E-07
6.50E-07 7.20E-07 7.80E-07 8.20E-07 9.20E-07];

s6=[0 4.12E-08 7.53E-08 9.90E-08 2.41E-07 2.75E-07
3.13E-07 3.48E-07 4.27E-07 5.36E-07 5.49E-07
6.15E-07 7.32E-07 7.68E-07 7.90E-07 8.90E-07];

s7=[0 2.32E-08 5.23E-08 7.20E-08 1.39E-07 2.15E-07
3.53E-07 4.20E-07 4.79E-07 5.26E-07 5.48E-07
6.15E-07 7.80E-07 7.82E-07 8.20E-07 8.52E-07];

s8=[0 5.20E-08 5.73E-08 1.02E-07 1.21E-07 2.25E-07
2.43E-07 2.90E-07 3.90E-07 4.70E-07 4.90E-07
5.60E-07 6.75E-07 6.80E-07 7.20E-07 7.70E-07];

s9=[0 3.50E-08 4.20E-08 4.70E-08 4.90E-08 5.25E-08
6.20E-08 6.70E-08 7.20E-08 7.80E-08 8.70E-08
9.72E-08 1.06E-07 1.29E-07 1.60E-07 1.83E-07];

s10=[0 -3.50E-08 -4.20E-08 -4.70E-08 -4.90E-08
-5.25E-08 -6.20E-08 -6.70E-08 -7.20E-08
-7.80E-08 -8.70E-08 -9.72E-08 -1.06E-07

-1.29E-07 -1.60E-07 -1.83E-07];

%----------Fy is applied on the strucutre----------

s1=[0 3.90E-08 8.47E-08 1.35E-07 1.70E-07 2.35E-07 2.90E-07
3.60E-07 4.27E-07 4.70E-07 5.30E-07 6.50E-07 7.26E-07
7.92E-07 8.50E-07 9.12E-07];

s2=[0 6.63E-07 1.18E-06 1.89E-06 2.48E-06 3.46E-06 3.79E-06
4.68E-06 5.32E-06 5.82E-06 6.32E-06 7.39E-06 7.83E-06
8.71E-06 9.38E-06 9.82E-06];

s3=[0 4.30E-08 9.27E-08 1.35E-07 1.69E-07 2.35E-07 3.40E-07
4.42E-07 4.87E-07 5.57E-07 6.12E-07 7.23E-07 7.46E-07
8.32E-07 8.70E-07 9.22E-07];

s4=[0 -6.52E-07 -1.28E-06 -1.75E-06 -2.17E-06 -3.24E-06
-4.07E-06 -4.56E-06 -5.25E-06 -5.75E-06 -6.66E-06
-7.52E-06 -7.85E-06 -8.75E-06 -9.42E-06 -1.04E-05];

s5=[0 5.30E-08 8.70E-08 1.25E-07 1.90E-07 2.80E-07 3.70E-07
4.20E-07 5.10E-07 5.40E-07 5.90E-07 6.85E-07 7.20E-07
7.90E-07 8.91E-07 9.42E-07];

s6=[0 4.02E-08 9.23E-08 1.22E-07 1.90E-07 2.45E-07 3.53E-07
3.70E-07 4.79E-07 5.26E-07 5.80E-07 6.55E-07 6.80E-07

7.68E-07 8.62E-07 9.52E-07];

s7=[0 4.20E-08 8.73E-08 1.32E-07 2.10E-07 2.50E-07 3.43E-07

3.90E-07 4.90E-07 5.70E-07 5.90E-07 6.50E-07 7.50E-07

7.80E-07 8.20E-07 8.70E-07];

s8=[0 4.02E-08 9.23E-08 1.22E-07 1.90E-07 2.45E-07 3.53E-07

3.70E-07 4.79E-07 5.26E-07 5.80E-07 6.55E-07 6.80E-07

7.68E-07 8.62E-07 9.52E-07];

s9=[0 3.46E-08 4.20E-08 4.76E-08 5.06E-08 5.85E-08 7.60E-08

9.70E-08 1.21E-07 1.69E-07 1.62E-07 1.72E-07 1.86E-07

1.93E-07 2.57E-07 2.73E-07];

s10=[0 -3.46E-08 -4.20E-08 -4.76E-08 -5.06E-08 -5.85E-08

-7.60E-08 -9.70E-08 -1.21E-07 -1.69E-07 -1.62E-07

-1.72E-07 -1.86E-07 -1.93E-07 -2.57E-07 -2.73E-07];

%----------Fz is applied on the structure----------

s1=[0 1.30E-08 2.07E-08 2.80E-08 3.20E-08 3.42E-08 3.80E-08

4.20E-08 5.30E-08 5.50E-08 6.10E-08 6.70E-08 6.82E-08

7.30E-08 7.82E-08 8.20E-08];

s2=[0 1.34E-08 2.57E-08 3.80E-08 4.32E-08 4.82E-08 4.98E-08

5.20E-08 5.43E-08 5.50E-08 5.91E-08 6.27E-08 6.82E-08

7.13E-08 7.52E-08 7.90E-08];

s3=[0 1.43E-08 2.17E-08 3.38E-08 4.20E-08 4.42E-08 4.80E-08

5.02E-08 5.13E-08 5.35E-08 5.61E-08 6.27E-08 6.72E-08

6.97E-08 7.42E-08 8.02E-08];

s4=[0 1.15E-08 1.90E-08 2.68E-08 3.12E-08 3.42E-08 3.90E-08

4.60E-08 4.90E-08 5.15E-08 5.61E-08 5.87E-08 6.22E-08

6.73E-08 7.20E-08 7.82E-08];

s5=[0 5.63E-07 8.26E-07 1.47E-06 1.74E-06 2.14E-06 2.37E-06

2.88E-06 3.12E-06 3.42E-06 3.96E-06 4.18E-06 4.62E-06

4.83E-06 5.24E-06 5.86E-06];

s6=[0 3.95E-07 8.15E-07 1.48E-06 1.92E-06 2.39E-06 2.84E-06

2.99E-06 3.29E-06 3.52E-06 4.08E-06 4.64E-06 4.68E-06

5.07E-06 5.72E-06 5.93E-06];

s7=[0 4.63E-07 8.74E-07 1.59E-06 1.92E-06 2.18E-06 2.58E-06

2.93E-06 3.25E-06 3.83E-06 4.20E-06 4.73E-06 5.21E-06

5.47E-06 5.62E-06 6.15E-06];

s8=[0 4.15E-07 8.28E-07 1.44E-06 1.86E-06 2.40E-06 2.79E-06
3.08E-06 3.37E-06 3.64E-06 3.93E-06 4.45E-06 4.60E-06
4.93E-06 5.60E-06 5.83E-06];

s9=[0 1.80E-08 2.12E-08 2.56E-08 2.90E-08 3.20E-08 3.60E-08
3.90E-08 4.30E-08 4.90E-08 5.20E-08 5.72E-08 6.10E-08
6.79E-08 8.17E-08 9.23E-08];

s10=[0 -1.80E-08 -2.12E-08 -2.56E-08 -2.90E-08 -3.20E-08
-3.60E-08 -3.90E-08 -4.30E-08 -4.90E-08 -5.20E-08
-5.72E-08 -6.10E-08 -6.79E-08 -8.17E-08 -9.23E-08];

%----------Mx is applied on the structure----------

s1=[0 1.40E-08 2.94E-08 3.40E-08 4.16E-08 4.87E-08
5.20E-08 5.74E-08 6.24E-08 6.85E-08 7.24E-08];
s2=[0 1.05E-08 1.68E-08 2.63E-08 3.16E-08 3.72E-08
4.22E-08 4.94E-08 5.31E-08 5.95E-08 6.47E-08];
s3=[0 1.20E-08 2.40E-08 2.93E-08 3.46E-08 3.70E-08

4.20E-08 4.84E-08 5.31E-08 5.75E-08 6.37E-08];

s4=[0 1.16E-08 1.80E-08 2.30E-08 2.86E-08 3.17E-08

3.62E-08 3.93E-08 4.31E-08 4.85E-08 5.27E-08];

s5=[0 1.21E-08 1.84E-08 2.20E-08 2.62E-08 2.92E-08

3.20E-08 3.74E-08 4.28E-08 4.85E-08 5.07E-08];

s6=[0 1.04E-07 2.02E-07 2.91E-07 3.88E-07 4.66E-07

5.87E-07 6.79E-07 7.51E-07 8.83E-07 9.72E-07];

s7=[0 1.58E-08 1.84E-08 2.13E-08 2.56E-08 2.87E-08

3.02E-08 3.24E-08 3.79E-08 4.04E-08 4.57E-08];

s8=[0 9.20E-08 2.01E-07 2.93E-07 4.06E-07 4.70E-07

5.92E-07 6.74E-07 7.78E-07 8.35E-07 8.70E-07];

s9=[0 1.20E-08 1.74E-08 2.16E-08 2.60E-08 3.07E-08

3.42E-08 3.83E-08 4.10E-08 4.35E-08 4.75E-08];

s10=[0 -1.20E-08 -1.74E-08 -2.16E-08 -2.60E-08 -3.07E-08

-3.42E-08 -3.83E-08 -4.10E-08 -4.35E-08 -4.75E-08];

%----------My is applied on the structure----------

s1=[0 8.20E-09 1.47E-08 2.31E-08 2.64E-08 2.93E-08

3.18E-08 3.32E-08 3.61E-08 3.92E-08 4.28E-08];

s2=[0 1.01E-08 1.81E-08 2.84E-08 3.20E-08 3.52E-08

3.92E-08 4.13E-08 4.25E-08 4.53E-08 4.80E-08];

s3=[0 1.15E-08 1.72E-08 2.30E-08 2.50E-08 2.93E-08

3.12E-08 3.31E-08 3.48E-08 3.82E-08 4.10E-08];

s4=[0 1.02E-08 1.64E-08 1.92E-08 2.20E-08 2.50E-08

2.73E-08 2.90E-08 3.20E-08 3.52E-08 3.72E-08];

s5=[0 1.15E-07 2.05E-07 3.25E-07 3.95E-07 5.06E-07

6.12E-07 6.84E-07 7.69E-07 8.84E-07 9.60E-07];

s6=[0 1.00E-08 1.62E-08 2.13E-08 2.50E-08 2.80E-08

3.13E-08 3.45E-08 4.00E-08 4.31E-08 4.72E-08];

s7=[0 -1.24E-07 -2.28E-07 -3.36E-07 -4.34E-07 -5.50E-07

-6.35E-07 -7.48E-07 -8.59E-07 -9.37E-07 -1.03E-06];

s8=[0 1.40E-08 1.80E-08 2.13E-08 2.32E-08 2.70E-08

2.98E-08 3.21E-08 3.45E-08 3.72E-08 4.02E-08];

s9=[0 1.12E-08 1.54E-08 2.26E-08 2.76E-08 3.14E-08

3.62E-08 4.10E-08 4.51E-08 4.95E-08 5.31E-08];

s10=[0 -1.12E-08 -1.54E-08 -2.26E-08 -2.76E-08 -3.14E-08

-3.62E-08 -4.10E-08 -4.51E-08 -4.95E-08 -5.31E-08];

%----------Mz is applied on the structure----------

s1=[0 1.53E-09 3.42E-09 8.30E-09 1.40E-08 1.86E-08

```
      2.18E-08 2.48E-08 2.70E-08 3.14E-08 3.64E-08];
s2=[0 3.13E-09 7.20E-09 1.23E-08 1.74E-08 2.11E-08
      2.48E-08 2.65E-08 2.87E-08 3.14E-08 3.42E-08];
s3=[0 1.30E-09 2.50E-09 7.23E-09 1.24E-08 1.46E-08
      1.58E-08 1.80E-08 2.14E-08 2.37E-08 2.62E-08];
s4=[0 1.52E-09 4.72E-09 7.80E-09 1.04E-08 1.26E-08
      1.48E-08 1.75E-08 2.37E-08 2.43E-08 2.54E-08];
s5=[0 1.30E-09 5.20E-09 6.83E-09 1.40E-08 1.60E-08
      1.78E-08 1.92E-08 2.23E-08 2.54E-08 3.25E-08];
s6=[0 3.13E-09 6.50E-09 7.30E-09 1.43E-08 1.56E-08
      1.68E-08 1.78E-08 2.44E-08 2.70E-08 3.12E-08];
s7=[0 1.83E-09 3.50E-09 6.33E-09 9.40E-09 1.26E-08
      1.48E-08 1.70E-08 1.97E-08 2.17E-08 2.42E-08];
s8=[0 2.30E-09 4.92E-09 1.03E-08 1.24E-08 1.61E-08
      1.98E-08 2.15E-08 2.47E-08 2.54E-08 2.92E-08];
s9=[0 3.43E-07 7.62E-07 1.13E-06 1.64E-06 2.06E-06
      2.58E-06 2.93E-06 3.28E-06 3.74E-06 4.18E-06];
s10=[0 -3.43E-07 -7.62E-07 -1.13E-06 -1.64E-06 -2.06E-06
      -2.58E-06 -2.93E-06 -3.28E-06 -3.74E-06 -4.18E-06];

s1=s1';
```

```
s2=s2';

s3=s3';

s4=s4';

s5=s5';

s6=s6';

s7=s7';

s8=s8';

s9=s9';

s10=s10';


%subplot 1

subplot(2,2,1);

[a,S]=polyfit(force,s1,1);

[simval,delta]=polyval(a,force,S);

average=sum(s1)/N;

R=sum((simval-average).^2)/sum((s1-average).^2);

R2(1)=R;

a

plot(force,s1,'*');

hold on;

plot(force,simval);
```

```
[a,S]=polyfit(force,s3,1);

[simval,delta]=polyval(a,force,S);

average=sum(s3)/16;

R=sum((simval-average).^2)/sum((s3-average).^2);

R2(3)=R;

a

plot(force,s3,'o');

plot(force,simval);

grid on;

title('S1 and S3 fitting line');

xlabel('Fz (N) ');

ylabel('Strain');

hold off;


%subplot 2

subplot(2,2,2);

[a,S]=polyfit(force,s2,1);

[simval,delta]=polyval(a,force,S);

average=sum(s2)/N;

R=sum((simval-average).^2)/sum((s2-average).^2);
```

```
a

R2(2)=R;

plot(force,s2,'*');

hold on;

plot(force,simval);


[a,S]=polyfit(force,s4,1);

[simval,delta]=polyval(a,force,S);

average=sum(s4)/16;

R=sum((simval-average).^2)/sum((s4-average).^2);

a

R2(4)=R;

plot(force,s4,'o');

plot(force,simval);

grid on;

title('S2 and S4 fitting line');

xlabel('Fz(N) ');

ylabel('Strain');

hold off;


%subplot 3
```

```
subplot(2,2,3);

[a,S]=polyfit(force,s5,1);

[simval,delta]=polyval(a,force,S);

average=sum(s5)/N;

R=sum((simval-average).^2)/sum((s5-average).^2);

a

R2(5)=R;

plot(force,s5,'*');

hold on;

plot(force,simval);


[a,S]=polyfit(force,s6,1);

[simval,delta]=polyval(a,force,S);

average=sum(s6)/N;

R=sum((simval-average).^2)/sum((s6-average).^2);

a

R2(6)=R;

plot(force,s6,'o');

plot(force,simval);


[a,S]=polyfit(force,s7,1);
```

```
[simval,delta]=polyval(a,force,S);

average=sum(s7)/N;

R=sum((simval-average).^2)/sum((s7-average).^2);

R2(7)=R;

a

plot(force,s7,'+');

plot(force,simval);


[a,S]=polyfit(force,s8,1);

[simval,delta]=polyval(a,force,S);

average=sum(s8)/N;

R=sum((simval-average).^2)/sum((s8-average).^2);

R2(8)=R;

a

plot(force,s8,'x');

plot(force,simval);

title('S5-S8 fitting line');

xlabel('Fz(N) ');

ylabel('Strain');

grid on;

hold off;
```

```
%subplot 4

subplot(2,2,4);

[a,S]=polyfit(force,s9,1);

[simval,delta]=polyval(a,force,S);

average=sum(s9)/N;

R=sum((simval-average).^2)/sum((s9-average).^2);

R2(9)=R;

a

plot(force,s9,'*');

hold on;

plot(force,simval);


[a,S]=polyfit(force,s10,1);

[simval,delta]=polyval(a,force,S);

average=sum(s10)/N;

R=sum((simval-average).^2)/sum((s10-average).^2);

a

R2(10)=R;

plot(force,s10,'o');

plot(force,simval);
```

```
grid on;

title('S9 and S10 fitting line');

xlabel('Fz(N) ');

ylabel('Strain');

hold off;

R2
```

To be continued

```
%----------------------------------Author: Shengmei Wang--------------------------------------

%---------------------------------Date:        2002/10/01 ----------------------------------------

%---------Title:   The Structure of Six DOF Endoscopic Force/Torque Sensor------------

clear;

%%%%%%%%%%%%%%%%%%%%%%%%%%%%%%%%%%%%%%%%%%%

h=4;                  % The fist time assuming the thickness is 4 mm

H=80;                 % Acccording to the assumptions h/H<1/20, get the H= 80 mm

L1=80;                % Acccording to the assumptions h/L1<1/20, get the L1= 80 mm

L2=82;                % Acccording to the assumptions h/L2<1/20, H= 82 mm

R=L1+L2;              % Inside radius R=L1+L2

b=50;                 % The perimeter l= 2*3.14*R,b< l/4, it can estimate about 50 mm

E=2.067*10^7;         % The Young's modulus of standard steel

Fx=30;                % The Maximum of X direction

Fy=30;                % The Maximum of Y direction

Fz=30;                % The Maximum of Z direction

Mx=100;               % The Maximum of X direction moment

My=100;               % The Maximum of Y direction moment
```

```
Mz=100;          % The Maximum of Z direction

I=b*h*h*h/12;    % The moment of inertia of the section of the beam

M1=Fx*H/2;       % Only Fx is applied, beam OA,OC occure bending moment

M2=Fy*H/2;       % Only Fy is applied, beam OB,OD occure bending moment

M3=Fz*L2/4;      % Only Fz is applied, beam OA,OB,OC,OD occure bending

M4=Mx*L1/(2*R);  % Only Mx is applied, beam OB,OD occure bending moment

M5=My*L1/(2*R);  % Only My is applied, beam OA, OC occure bending moment

M6=Mz*R/(4*R);   % Only Mz is applied, beam AE,BF,CG,DH occure bending

Stress1=M1*(h/2)/I;   %The stress of the beam AE and CG under Fx is applied only

Stress2=M2*(h/2)/I;   %The stress of the beam BF and DH under Fy is applied only

Stress3=M3*(h/2)/I;   %The stress of the beam OA,OB,OC and OD under Fz is applied

Stress4=M4*(h/2)/I;   %The stress of the beam OB and OD under Mx is applied only

Stress5=M5*(h/2)/I;   %The stress of the beam OA and OC under My is applied only

Stress6=M6*(h/2)/I;   %The stress of the beam AE,BF,CG and DH under Mz is applied

S1=Stress1/E;         %The readout of the first and third strain gauge under Fx

S2=Stress2/E;         %The readout of the second and the forth strain gauge under Fy

S3=Stress3/E;         %The readout of the fifth, sixth, seventh, eighth strain gauge Fz

S4=Stress4/E;         %The readout of the sixth and the eighth strain gauge under Mx
```

```
S5=Stress5/E;        %The readout of the fifth and the seventh strain gauge under My

S6=Stress6/E;        %The readout of the first, second, third and forth strain gauge Mz


%%%%%%%%%%%%%%%%%%%%%%%%%%%%%%%%%%%%%%%%%%%%%%%%%%%%%%%%%%%%%%%%


h=3;                 % The sencond time assuming the thickness is 3 mm

H=60;                % Acccording to the assumptions h/H<1/20, H= 60 mm

L1=60;               % Acccording to the assumptions h/L1<1/20, L1= 60 mm

L2=62;               % Acccording to the assumptions h/L2<1/20, H= 62 mm

R=L1+L2;             % Inside radius R=L1+L2

b=50;                % The perimeter l= 2*3.14*R,b< l/4, it can estimate about 50 mm

E=2.067*10^7;        % The Young's modulus of standard steel

Fx=30;               % The Maximum of X direction

Fy=30;               % The Maximum of Y direction

Fz=30;               % The Maximum of Z direction

Mx=100;              % The Maximum of X direction moment

My=100;              % The Maximum of Y direction moment

Mz=100;              % The Maximum of Z direction


I=b*h*h*h/12;        % The moment of inertia of the section of the beam

M1=Fx*H/2;           % Only Fx is applied, beam OA,OC occure bending moment
```

```
M2=Fy*H/2;          % Only Fy is applied, beam OB,OD occure bending moment

M3=Fz*L2/4;         % Only Fz is applied, beam OA,OB,OC,OD occure bending

M4=Mx*L1/(2*R);     % Only Mx is applied, beam OB,OD occure bending moment

M5=My*L1/(2*R);     % Only My is applied, beam OA, OC occure bending moment

M6=Mz*R/(4*R);      % Only Mz is applied, beam AE,BF,CG,DH occure bending


Stress1=M1*(h/2)/I;     %The stress of the beam AE and CG under Fx is applied only

Stress2=M2*(h/2)/I;     %The stress of the beam BF and DH under Fy is applied only

Stress3=M3*(h/2)/I;     %The stress of the beam OA,OB,OC and OD under Fz is applied

Stress4=M4*(h/2)/I;     %The stress of the beam OB and OD under Mx is applied only

Stress5=M5*(h/2)/I;     %The stress of the beam OA and OC under My is applied only

Stress6=M6*(h/2)/I;     %The stress of the beam AE,BF,CG and DH under Mz is applied

S1=Stress1/E;           %The readout of the first and third strain gauge under Fx

S2=Stress2/E;           %The readout of the second and the forth strain gauge under Fy

S3=Stress3/E;           %The readout of the fifth, sixth, seventh, eighth strain gauge Fz

S4=Stress4/E;           %The readout of the sixth and the eighth strain gauge under Mx

S5=Stress5/E;           %The readout of the fifth and the seventh strain gauge under My

S6=Stress6/E;           %The readout of the first, second, third and forth strain gauge Mz


%%%%%%%%%%%%%%%%%%%%%%%%%%%%%%%%%%%%%%%%%%%%%%%%%%%%%%%%%%%%%%%%%%%%%%%%%%%%
```

```
h=2;              % The third time assuming the thickness is 2 mm

H=40;             % Acccording to the assumptions h/H<1/20, get the H= 40 mm

L1=40;            % Acccording to the assumptions h/L1<1/20, get the L1= 40 mm

L2=42;            % Acccording to the assumptions h/L2<1/20, H= 42 mm

R=L1+L2;          % Inside radius R=L1+L2

b=40;             % The perimeter l= 2*3.14*R,b< l/4, it can estimate about 40 mm

E=2.067*10^7;% The Young's modulus of standard steel

Fx=10;            % The Maximum of X direction

Fy=10;            % The Maximum of Y direction

Fz=10;            % The Maximum of Z direction

Mx=70;            % The Maximum of X direction moment

My=70;            % The Maximum of Y direction moment

Mz=70;            % The Maximum of Z direction


I=b*h*h*h/12;       % The moment of inertia of the section of the beam

M1=Fx*H/2;          % Only Fx is applied, beam OA,OC occure bending moment

M2=Fy*H/2;          % Only Fy is applied, beam OB,OD occure bending moment

M3=Fz*L2/4;         % Only Fz is applied, beam OA,OB,OC,OD occure bending

M4=Mx*L1/(2*R);   % Only Mx is applied, beam OB,OD occure bending moment

M5=My*L1/(2*R);   % Only My is applied, beam OA, OC occure bending moment

M6=Mz*R/(4*R);    % Only Mz is applied, beam AE,BF,CG,DH occure bending
```

```
Stress1=M1*(h/2)/I;     %The stress of the beam AE and CG under Fx is applied only
Stress2=M2*(h/2)/I;     %The stress of the beam BF and DH under Fy is applied only
Stress3=M3*(h/2)/I;     %The stress of the beam OA,OB,OC and OD under Fz is applied
Stress4=M4*(h/2)/I;     %The stress of the beam OB and OD under Mx is applied only
Stress5=M5*(h/2)/I;     %The stress of the beam OA and OC under My is applied only
Stress6=M6*(h/2)/I;     %The stress of the beam AE,BF,CG and DH under Mz is applied
only

S1=Stress1/E;           %The readout of the first and third strain gauge under Fx
S2=Stress2/E;           %The readout of the second and the forth strain gauge under Fy
S3=Stress3/E;           %The readout of the fifth, sixth, seventh, eighth strain gauge Fz
S4=Stress4/E;           %The readout of the sixth and eighth strain gauge under Mx
S5=Stress5/E;           %The readout of the fifth and the seventh strain gauge under My
S6=Stress6/E;           %The readout of the first, second, third and the forth gauge Mz

%%%%%%%%%%%%%%%%%%%%%%%%%%%%%%%%%%%%%%%%%%%%%%%%%%%%%%%%%%%%%%%%%%%%%%%%%%%%%%%

h=1.5;          % The forth time assume the thickness is 1.5 mm
H=30;           % Acccording to the assumptions h/H<1/20, get the H= 30 mm
L1=30;          % Acccording to the assumptions h/L1<1/20, get the L1= 30 mm
```

```
L2=32;          % Acccording to the assumptions h/L2<1/20, H= 32 mm

R=L1+L2;        % Inside radius R=L1+L2

b=20;           % The perimeter l= 2*3.14*R,b< l/4, it can estimate about 20 mm

E=2.067*10^7;   % The Young's modulus of standard steel

Fx=30;          % The Maximum of X direction

Fy=30;          % The Maximum of Y direction

Fz=30;          % The Maximum of Z direction

Mx=100;         % The Maximum of X direction moment

My=100;         % The Maximum of Y direction moment

Mz=100;         % The Maximum of Z direction


I=b*h*h*h/12;       % The moment of inertia of the section of the beam

M1=Fx*H/2;          % Only Fx is applied, beam OA,OC occure bending moment

M2=Fy*H/2;          % Only Fy is applied, beam OB,OD occure bending moment

M3=Fz*L2/4;         % Only Fz is applied, beam OA,OB,OC,OD occure bending

M4=Mx*L1/(2*R);     % Only Mx is applied, beam OB,OD occure bending moment

M5=My*L1/(2*R);     % Only My is applied, beam OA, OC occure bending moment

M6=Mz*R/(4*R);      % Only Mz is applied, beam AE,BF,CG,DH occure bending

Stress1=M1*(h/2)/I;     %The stress of the beam AE and CG under Fx

Stress2=M2*(h/2)/I;     %The stress of the beam BF and DH under Fy

Stress3=M3*(h/2)/I;     %The stress of the beam OA,OB,OC and OD under Fz
```

```
Stress4=M4*(h/2)/I;     %The stress of the beam OB and OD under Mx

Stress5=M5*(h/2)/I;     %The stress of the beam OA and OC under My

Stress6=M6*(h/2)/I;     %The stress of the beam AE,BF,CG and DH under Mz

S1=Stress1/E;           %The readout of the first and strain gauge under Fx

S2=Stress2/E;           %The readout of the second and the forth strain gauge under Fy

S3=Stress3/E;           %The readout of the fifth, sixth, seventh, eighth strain gauge Fz

S4=Stress4/E;           %The readout of the sixth and the eighth strain gauge under Mx

S5=Stress5/E;           %The readout of the fifth and the seventh strain gauge under My

S6=Stress6/E;           %The readout of the first, second, third and the forth gauge Mz

%%%%%%%%%%%%%%%%%%%%%%%%%%%%%%%%%%%%%%%%%%%%%%%%%%%%%%%%%%%%%%%%%%%%%%%%%%%%

h=1;              % The fifth time assuming the thickness is 1 mm

H=20;             % Acccording to the assumptions h/H<1/20, get the H= 20 mm

L1=20;            % Acccording to the assumptions h/L1<1/20, get the L1= 20 mm

L2=22;            % Acccording to the assumptions h/L2<1/20, and H= 22 mm

R=L1+L2;          % Inside radius R=L1+L2

b=10;             % The perimeter l= 2*3.14*R,b< l/4, it can estimate about 10 mm

E=2.067*10^7;     % The Young's modulus of standard steel

Fx=30;            % The Maximum of X direction

Fy=30;            % The Maximum of Y direction
```

```
Fz=30;          % The Maximum of Z direction

Mx=100;         % The Maximum of X direction moment

My=100;         % The Maximum of Y direction moment

Mz=100;         % The Maximum of Z direction


I=b*h*h*h/12;     % The moment of inertia of the section of the beam

M1=Fx*H/2;        % Only Fx is applied , beam OA,OC occure bending moment

M2=Fy*H/2;        % Only Fy is applied , beam OB,OD occure bending moment

M3=Fz*L2/4;       % Only Fz is applied, beam OA,OB,OC,OD occure bending

M4=Mx*L1/(2*R);   % Only Mx is applied, beam OB,OD occure bending moment

M5=My*L1/(2*R);   % Only My is applied, beam OA, OC occure bending moment

M6=Mz*R/(4*R);    % Only Mz is applied, beam AE,BF,CG,DH occure bending

Stress1=M1*(h/2)/I;    %The stress of the beam AE and CG under Fx is applied only

Stress2=M2*(h/2)/I;    %The stress of the beam BF and DH under Fy is applied only

Stress3=M3*(h/2)/I;    %The stress of the beam OA,OB,OC and OD under Fz

Stress4=M4*(h/2)/I;    %The stress of the beam OB and OD under Mx

Stress5=M5*(h/2)/I;    %The stress of the beam OA and OC under My

Stress6=M6*(h/2)/I;    %The stress of the beam AE,BF,CG and DH under Mz

S1=Stress1/E;          %The readout of the first and third strain gauge under Fx

S2=Stress2/E;          %The readout of the second and the forth strain gauge under Fy

S3=Stress3/E;          %The readout of the fifth, sixth, the seventh, the eighth gauge Fz
```

```
S4=Stress4/E;          %The readout of the sixth and the eighth strain gauge under Mx

S5=Stress5/E;          %The readout of the fifth and the seventh strain gauge under My

S6=Stress6/E;          %The readout of the first, second, third and the forth gauge Mz


%%%%%%%%%%%%%%%%%%%%%%%%%%%%%%%%%%%%%%%%%%%


h=1;              % The sixth time assuming the thickness is 1 mm

H=20;             % Acccording to the assumptions h/H<1/20, get the H= 20 mm

L1=20;            % Acccording to the assumptions h/L1<1/20, get the L1= 20 mm

L2=22;            % Acccording to the assumptions h/L2<1/20, H= 22 mm

R=L1+L2;          % Inside radius R=L1+L2

b=15;             % The perimeter l= 2*3.14*R,b< l/4, it can estimate about 15 mm

E=2.067*10^7;     % The Young's modulus of standard steel

Fx=30;            % The Maximum of X direction

Fy=30;            % The Maximum of Y direction

Fz=30;            % The Maximum of Z direction

Mx=100;           % The Maximum of X direction moment

My=100;           % The Maximum of Y direction moment

Mz=100;           % The Maximum of Z direction


I=b*h*h*h/12;     % The moment of inertia of the section of the beam
```

```
M1=Fx*H/2;          % Only Fx is applied, beam OA,OC occure bending moment

M2=Fy*H/2;          % Only Fy is applied, beam OB,OD occure bending moment

M3=Fz*L2/4;         % Only Fz is applied ,beam OA,OB,OC,OD occure bending moment

M4=Mx*L1/(2*R);     % Only Mx is applied, beam OB,OD occure bending moment

M5=My*L1/(2*R);     % Only My is applied, beam OA, OC occure bending moment

M6=Mz*R/(4*R);      % Only Mz is applied, beam AE,BF,CG,DH occure bending

Stress1=M1*(h/2)/I;     %The stress of the beam AE and CG under Fx is applied only

Stress2=M2*(h/2)/I;     %The stress of the beam BF and DH under Fy is applied only

Stress3=M3*(h/2)/I;     %The stress of the beam OA,OB,OC and OD under Fz is applied

Stress4=M4*(h/2)/I;     %The stress of the beam OB and OD under Mx is applied only

Stress5=M5*(h/2)/I;     %The stress of the beam OA and OC under My is applied only

Stress6=M6*(h/2)/I;     %The stress of the beam AE,BF,CG and DH under Mz is applied


S1=Stress1/E;           %The readout of the first and third strain gauge under Fx

S2=Stress2/E;           %The readout of the second and the forth strain gauge under Fy

S3=Stress3/E;           %The readout of the fifth, sixth, seventh, eighth strain gauge Fz

S4=Stress4/E;           %The readout of the sixth and the eighth gauge under Mx

S5=Stress5/E;           %The readout of the fifth and the seventh strain gauge under My

S6=Stress6/E;           %The readout of the first, second, third, the forth strain gauge Mz.


%%%%%%%%%%%%%%%%%%%%%%%%%%%%%%%%%%%%%%%%%%%%%%%%%%%%%%%%%%%%%%%%%%%%%%%%%%%%%%%
```

```
h=1;              % The seventh time assuming the thickness is 1 mm

H=20;             % According to the assumptions h/H<1/20, get the H= 20 mm

L1=20;            % According to the assumptions h/L1<1/20, get the L1= 20 mm

L2=22;            % According to the assumptions h/L2<1/20, H= 22 mm

R=L1+L2;          % Inside radius R=L1+L2

b=20;             % The perimeter l= 2*3.14*R,b< l/4, it can estimate about 10 mm

E=2.067*10^7;     % The Young's modulus of standard steel

Fx=30;            % The Maximum of X direction

Fy=30;            % The Maximum of Y direction

Fz=30;            % The Maximum of Z direction

Mx=100;           % The Maximum of X direction moment

My=100;           % The Maximum of Y direction moment

Mz=100;           % The Maximum of Z direction


I=b*h*h*h/12;     % The moment of inertia of the section of the beam

M1=Fx*H/2;        % Only Fx is applied , beam OA,OC occure bending moment

M2=Fy*H/2;        % Only Fy is applied , beam OB,OD occure bending moment

M3=Fz*L2/4;       % Only Fz is applied, beam OA,OB,OC,OD occure bending

M4=Mx*L1/(2*R);   % Only Mx is applied , beam OB,OD occure bending moment

M5=My*L1/(2*R);   % Only My is applied, beam OA, OC occure bending moment
```

```
M6=Mz*R/(4*R);      % Only Mz is applied, beam AE,BF,CG,DH occure bending

Stress1=M1*(h/2)/I;     %The stress of the beam AE and CG under Fx is applied only

Stress2=M2*(h/2)/I;     %The stress of the beam BF and DH under Fy is applied only

Stress3=M3*(h/2)/I;     %The stress of the beam OA,OB,OC and OD under Fz is applied

Stress4=M4*(h/2)/I;     %The stress of the beam OB and OD under Mx is applied only

Stress5=M5*(h/2)/I;     %The stress of the beam OA and OC under My is applied only

Stress6=M6*(h/2)/I;     %The stress of the beam AE,BF,CG and DH under Mz is applied

S1=Stress1/E;           %The readout of the first and third strain gauge under Fx

S2=Stress2/E;           %The readout of the second and the forth strain gauge under Fy

S3=Stress3/E;           %The readout of the fifth, sixth, seventh, eighth gauge under Fz

S4=Stress4/E;           %The readout of the sixth and the eighth strain gauge under Mx

S5=Stress5/E;           %The readout of the fifth and the seventh gauge under My

S6=Stress6/E;           %The readout of the first, second, third and the forth gauge Mz


%%%%%%%%%%%%%%%%%%%%%%%%%%%%%%%%%%%%%%%%%%%%%%%%%%%%%%%%


h=0.75;         % The eighth time assuming the thickness is 0.75 mm

H=15;           % According to the assumptions h/H<1/20, get the H= 15 mm

L1=15;          % According to the assumptions h/L1<1/20, get the L1= 15 mm

L2=16;          % According to the assumptions h/L2<1/20, H= 16 mm

R=L1+L2;        % Inside radius R=L1+L2
```

```
b=10;              % The perimeter l= 2*3.14*R, b< l/4, it can estimate about 6 mm

E=2.067*10^7; % The Young's modulus of standard steel

Fx=30;             % The Maximum of X direction

Fy=30;             % The Maximum of Y direction

Fz=30;             % The Maximum of Z direction

Mx=100;            % The Maximum of X direction moment

My=100;            % The Maximum of Y direction moment

Mz=100;            % The Maximum of Z direction


I=b*h*h*h/12;      % The moment of inertia of the section of the beam

M1=Fx*H/2;         % Only Fx is applied, beam OA,OC occure bending moment

M2=Fy*H/2;         % Only Fy is applied, beam OB,OD occure bending moment

M3=Fz*L2/4;        % Only Fz is applied, beam OA,OB,OC,OD occure bending

M4=Mx*L1/(2*R);    % Only Mx is applied, beam OB,OD occure bending moment

M5=My*L1/(2*R);    % Only My is applied, beam OA, OC occure bending moment

M6=Mz*R/(4*R);     % Only Mz is applied, beam AE,BF,CG,DH occure bending

Stress1=M1*(h/2)/I;     %The stress of the beam AE and CG under Fx is applied only

Stress2=M2*(h/2)/I;     %The stress of the beam BF and DH under Fy is applied only

Stress3=M3*(h/2)/I;     %The stress of the beam OA,OB,OC and OD under Fz is applied

Stress4=M4*(h/2)/I;     %The stress of the beam OB and OD under Mx is applied only

Stress5=M5*(h/2)/I;     %The stress of the beam OA and OC under My is applied only
```

```
Stress6=M6*(h/2)/I;     %The stress of the beam AE,BF,CG and DH under Mz is applied

S1=Stress1/E;           %Thereadout of the first and third strain gauge under Fx

S2=Stress2/E;           %The readout of the second and the forth strain gauge under Fy

S3=Stress3/E;           %The readout of the fifth, sixth, seventh, eighth gauge under Fz

S4=Stress4/E;           %The readout of the sixth and the eighth strain gauge under Mx

S5=Stress5/E;           %The readout of the fifth and the seventh strain gauge under My

S6=Stress6/E;           %The readout of the first, second, third and the forth gauge Mz


%%%%%%%%%%%%%%%%%%%%%%%%%%%%%%%%%%%%%%%%


h=0.75;          % The ninth time assuming the thickness is 0.75 mm

H=15;            % According to the assumptions h/H<1/20, get the H= 15 mm

L1=15;           % According to the assumptions h/L1<1/20, get the L1= 15 mm

L2=16;           % According to the assumptions h/L2<1/20, H= 16 mm

R=L1+L2;         % Inside radius R=L1+L2

b=5;             % The perimeter l= 2*3.14*R,b< l/4, it can estimate about 20 mm

E=2.067*10^7;    % The Young's modulus of standard steel

Fx=30;           % The Maximum of X direction

Fy=30;           % The Maximum of Y direction

Fz=30;           % The Maximum of Z direction

Mx=100;          % The Maximum of X direction moment
```

```
My=100;          % The Maximum of Y direction moment

Mz=100;          % The Maximum of Z direction


I=b*h*h*h/12;    % The moment of inertia of the section of the beam

M1=Fx*H/2;       % Only Fx is applied , beam OA,OC occure bending moment

M2=Fy*H/2;       % Only Fy is applied , beam OB,OD occure bending moment

M3=Fz*L2/4;      % Only Fz is applied, beam OA,OB,OC,OD occure bending moment

M4=Mx*L1/(2*R); % Only Mx is applied , beam OB,OD occure bending moment

M5=My*L1/(2*R);  % Only My is applied , beam OA, OC occure bending moment

M6=Mz*R/(4*R);   % Only Mz is applied, beam AE,BF,CG,DH occure bending moment

Stress1=M1*(h/2)/I;    %The stress of the beam AE and CG under Fx is applied only

Stress2=M2*(h/2)/I;    %The stress of the beam BF and DH under Fy is applied only

Stress3=M3*(h/2)/I;    %The stress of the beam OA,OB,OC and OD under Fz is applied

Stress4=M4*(h/2)/I;    %The stress of the beam OB and OD under Mx is applied only

Stress5=M5*(h/2)/I;    %The stress of the beam OA and OC under My is applied only

Stress6=M6*(h/2)/I;    %The stress of the beam AE,BF,CG and DH under Mz is applied

S1=Stress1/E;          %The readout of the first and third gauge under Fx

S2=Stress2/E;          %The readout of the second and the forth strain gauge under Fy

S3=Stress3/E;          %The readout of the fifth, sixth, seventh, eighth gauge under Fz

S4=Stress4/E;          %The readout of the sixth and the eighth gauge under Mx

S5=Stress5/E;          %The readout of the fifth and the seventh gauge under My
```

```
S6=Stress6/E;              %The readout of the first, second, third and forth gauge Mz

%%%%%%%%%%%%%%%%%%%%%%%%%%%%%%%%%%%%%%%%%%%%%%

h=0.5;             % The tenth time assuming the thickness is 0.5 mm

H=10;              % According to the assumptions h/H<1/20, get the H= 10 mm

L1=10;             % According to the assumptions h/L1<1/20, get the L1= 10 mm

L2=11;             % According to the assumptions h/L2<1/20, H= 11 mm

R=L1+L2;           % Inside radius R=L1+L2

b=10;              % The perimeter l= 2*3.14*R,b< l/4, it can estimate about 15 mm

E=2.067*10^7; % The Young's modulus of standard steel

Fx=30;             % The Maximum of X direction

Fy=30;             % The Maximum of Y direction

Fz=30;             % The Maximum of Z direction

Mx=100;              % The Maximum of X direction moment

My=100;              % The Maximum of Y direction moment

Mz=100;              % The Maximum of Z direction


I=b*h*h*h/12;      % The moment of inertia of the section of the beam

M1=Fx*H/2;         % Only Fx is applied, beam OA,OC occure bending moment

M2=Fy*H/2;         % Only Fy is applied, beam OB,OD occure bending moment
```

```
M3=Fz*L2/4;        % Only Fz is applied, beam OA,OB,OC,OD occure bending moment

M4=Mx*L1/(2*R);    % Only Mx is applied, beam OB,OD occure bending moment

M5=My*L1/(2*R);    % Only My is applied, beam OA, OC occure bending moment

M6=Mz*R/(4*R);     % Only Mz is applied, beam AE,BF,CG,DH occure bending moment

Stress1=M1*(h/2)/I;    %The stress of the beam AE and CG under Fx is applied only

Stress2=M2*(h/2)/I;    %The stress of the beam BF and DH under Fy is applied only

Stress3=M3*(h/2)/I;    %The stress of the beam OA,OB,OC and OD under Fz is applied

Stress4=M4*(h/2)/I;    %The stress of the beam OB and OD under Mx is applied only

Stress5=M5*(h/2)/I;    %The stress of the beam OA and OC under My is applied only

Stress6=M6*(h/2)/I;    %The stress of the beam AE,BF,CG and DH under Mz is applied

S1=Stress1/E;          %Thereadout of the first and third gauge under Fx

S2=Stress2/E;          %The radout of the second and the forth strain gauge under Fy

S3=Stress3/E;          %The readout of the fifth, sixth, seventh, eighth gauge under Fz

S4=Stress4/E;          %The readout of the sixth and the eighth gauge under Mx

S5=Stress5/E;          %The readout of the fifth and the seventh gauge under My

S6=Stress6/E;          %The readout of the first, second, third and forth strain gauge Mz


%%%%%%%%%%%%%%%%%%%%%%%%%%%%%%%%%%%%%%%%%%%%%%%%


h=0.5;         % The eleventh time assuming the thickness is 0.5 mm

H=10;          % According to the assumptions h/H<1/20, get the H= 10 mm
```

```
L1=10;          % According to the assumptions h/L1<1/20, get the L1= 10 mm

L2=11;          % Acccording to the assumptions h/L2<1/20, H= 11 mm

R=L1+L2;        % Inside radius R=L1+L2

b=5;            % The perimeter l= 2*3.14*R, b< l/4, it can estimate about 25 mm

E=2.067*10^7;   % The Young's modulus of standard steel

Fx=30;          % The Maximum of X direction

Fy=30;          % The Maximum of Y direction

Fz=30;          % The Maximum of Z direction

Mx=100;         % The Maximum of X direction moment

My=100;         % The Maximum of Y direction moment

Mz=100;         % The Maximum of Z direction


I=b*h*h*h/12;       % The moment of inertia of the section of the beam

M1=Fx*H/2;          % Only Fx is applied, beam OA,OC occure bending moment

M2=Fy*H/2;          % Only Fy is applied, beam OB,OD occure bending moment

M3=Fz*L2/4;         % Only Fz is applied, beam OA,OB,OC,OD occure bending moment

M4=Mx*L1/(2*R);     % Only Mx is applied, beam OB,OD occure bending moment

M5=My*L1/(2*R);     % Only My is applied, beam OA, OC occure bending moment

M6=Mz*R/(4*R);      % Only Mz is applied, beam AE,BF,CG,DH occure bending moment

Stress1=M1*(h/2)/I;     %The stress of the beam AE and CG under Fx is applied only

Stress2=M2*(h/2)/I;     %The stress of the beam BF and DH under Fy is applied only
```

```
Stress3=M3*(h/2)/I;     %The stress of the beam OA,OB,OC and OD under Fz is applied

Stress4=M4*(h/2)/I;     %The stress of the beam OB and OD under Mx is applied only

Stress5=M5*(h/2)/I;     %The stress of the beam OA and OC under My is applied only

Stress6=M6*(h/2)/I;     %The stress of the beam AE,BF,CG and DH under Mz is applied

S1=Stress1/E;           %Thereadout of the first and third gauge under Fx

S2=Stress2/E;           %The readout of the second and the forth gauge under Fy

S3=Stress3/E;           %The readout of the fifth, sixth, seventh, the eighth gauge Fz

S4=Stress4/E;           %The readout of the sixth and the eighth gauge under Mx

S5=Stress5/E;           %The readout of the fifth and the seventh gauge under My

S6=Stress6/E;           %The readout of the first, second, third and forth gauge Mz

%%%%%%%%%%%%%%%%%%%%%%%%%%%%%%%%%%%%%%%%%%%%%%%%%%%%%%%%%%%%%%%%%%%%%%%%%%%%

h=0.5;          % The eleventh time assuming the thickness is 0.5 mm

H=20;           % According to the assumptions h/H<1/20, get the H= 10 mm

L1=10;          % According to the c assumptions h/L1<1/20, get the L1= 10 mm

L2=11;          % According to the assumptions h/L2<1/20, H= 11 mm

R=L1+L2;        % Inside radius R=L1+L2

b=5;            % The perimeter l= 2*3.14*R, b< l/4, it can estimate about 25 mm

E=2.067*10^7;   % The Young's modulus of standard steel

Fx=10;          % The Maximum of X direction
```

```
Fy=10;          % The Maximum of Y direction

Fz=10;          % The Maximum of Z direction

Mx=70;          % The Maximum of X direction moment

My=70;          % The Maximum of Y direction moment

Mz=70;          % The Maximum of Z direction


I=b*h*h*h/12;          % The moment of inertia of the section of the beam

M1=Fx*H/2;             % Only Fx is applied , beam OA,OC occure bending moment

M2=Fy*H/2;             % Only Fy is applied , beam OB,OD occure bending moment

M3=Fz*L2/4;            % Only Fz is applied, beam OA,OB,OC,OD occure bending

M4=Mx*L1/(2*R);    % Only Mx is applied , beam OB,OD occure bending moment

M5=My*L1/(2*R);    % Only My is applied , beam OA, OC occure bending moment

M6=Mz*R/(4*R);    % Only Mz is applied, beam AE,BF,CG,DH occure bending moment

Stress1=M1*(h/2)/I;     %The stress of the beam AE and CG under Fx is applied only

Stress2=M2*(h/2)/I;     %The stress of the beam BF and DH under Fy is applied only

Stress3=M3*(h/2)/I;     %The stress of the beam OA,OB,OC and OD under Fz is applied

Stress4=M4*(h/2)/I;     %The stress of the beam OB and OD under Mx is applied only

Stress5=M5*(h/2)/I;     %The stress of the beam OA and OC under My is applied only

Stress6=M6*(h/2)/I;     %The stress of the beam AE,BF,CG and DH under Mz is applied

S1=Stress1/E;           %The readout of the first and third gauge under Fx

S2=Stress2/E;           %The readout of the second and the forth strain gauge under Fy
```

```
S3=Stress3/E;          %The readout of the fifth, sixth, seventh, eighth strain gauge Fz

S4=Stress4/E;          %The readout of the sixth and the eighth gauge under Mx

S5=Stress5/E;          %The readout of the fifth and the seventh gauge under My

S6=Stress6/E;          %The readout of the first, second, third and the forth gauge Mz
```

APPENDIX B

The Calculation and Experimental Results

Beam Theory Model

Table A1 Strains Due to Force in X Direction (Beam Model)

Fx(N)	S1	S2	S3	S4	S5	S6	S7	S8	S9	S10
0	0	0	0	0	0	0	0	0	0	0
2	0.000000846	0	-8.46E-07	0	0	0	0	0	0	0
4	0.000001692	0	-1.69E-06	0	0	0	0	0	0	0
6	0.000002538	0	-2.54E-06	0	0	0	0	0	0	0
8	0.000003384	0	-3.38E-06	0	0	0	0	0	0	0
10	0.00000423	0	-4.23E-06	0	0	0	0	0	0	0
12	0.000005076	0	-5.08E-06	0	0	0	0	0	0	0
14	0.000005922	0	-5.92E-06	0	0	0	0	0	0	0
16	0.000006768	0	-6.77E-06	0	0	0	0	0	0	0
18	0.000007614	0	-7.61E-06	0	0	0	0	0	0	0
20	0.00000846	0	-8.46E-06	0	0	0	0	0	0	0
22	0.000009306	0	-9.31E-06	0	0	0	0	0	0	0
24	0.000010152	0	-1.02E-05	0	0	0	0	0	0	0
26	0.000010998	0	-1.1E-05	0	0	0	0	0	0	0
28	0.000011844	0	-1.18E-05	0	0	0	0	0	0	0
30	0.00001269	0	-1.27E-05	0	0	0	0	0	0	0

Table A2 Strains Due to Force in Y Direction (Beam Model)

Fy(N)	S1	S2	S3	S4	S5	S6	S7	S8	S9	S10
0	0	0	0	0	0	0	0	0	0	0
2	0	0.000000846	0	-8.46E-07	0	0	0	0	0	0
4	0	0.000001692	0	-1.69E-06	0	0	0	0	0	0
6	0	0.000002538	0	-2.54E-06	0	0	0	0	0	0
8	0	0.000003384	0	-3.38E-06	0	0	0	0	0	0
10	0	0.00000423	0	-4.23E-06	0	0	0	0	0	0
12	0	0.000005076	0	-5.08E-06	0	0	0	0	0	0
14	0	0.000005922	0	-5.92E-06	0	0	0	0	0	0
16	0	0.000006768	0	-6.77E-06	0	0	0	0	0	0
18	0	0.000007614	0	-7.61E-06	0	0	0	0	0	0
20	0	0.00000846	0	-8.46E-06	0	0	0	0	0	0
22	0	0.000009306	0	-9.31E-06	0	0	0	0	0	0
24	0	0.000010152	0	-1.02E-05	0	0	0	0	0	0
26	0	0.000010998	0	-1.1E-05	0	0	0	0	0	0
28	0	0.000011844	0	-1.18E-05	0	0	0	0	0	0
30	0	0.00001269	0	-1.27E-05	0	0	0	0	0	0

Table A3 Strains due to Force in Z Direction (Beam Model)

Fz(N)	S1	S2	S3	S4	S5	S6	S7	S8	S9	S10
0	0	0	0	0	0	0	0	0	0	0
2	0	0	0	0	0.000000266	0.000000266	2.66E-07	2.66E-07	0	0
4	0	0	0	0	0.000000532	0.000000532	5.32E-07	5.32E-07	0	0
6	0	0	0	0	0.000000798	0.000000798	7.98E-07	7.98E-07	0	0
8	0	0	0	0	0.000001064	0.000001064	1.064E-06	1.064E-06	0	0
10	0	0	0	0	0.00000133	0.00000133	1.33E-06	1.33E-06	0	0
12	0	0	0	0	0.000001596	0.000001596	1.596E-06	1.596E-06	0	0
14	0	0	0	0	0.000001862	0.000001862	1.862E-06	1.862E-06	0	0
16	0	0	0	0	0.000002128	0.000002128	2.128E-06	2.128E-06	0	0
18	0	0	0	0	0.000002394	0.000002394	2.394E-06	2.394E-06	0	0
20	0	0	0	0	0.00000266	0.00000266	2.66E-06	2.66E-06	0	0
22	0	0	0	0	0.000002926	0.000002926	2.926E-06	2.926E-06	0	0
24	0	0	0	0	0.000003192	0.000003192	3.192E-06	3.192E-06	0	0
26	0	0	0	0	0.000003458	0.000003458	3.458E-06	3.458E-06	0	0
28	0	0	0	0	0.000003724	0.000003724	3.724E-06	3.724E-06	0	0
30	0	0	0	0	0.00000399	0.00000399	3.99E-06	3.99E-06	0	0

Table A4 Strains Due to Torque in X Direction (Beam Model)

Mx (Nmm)	S1	S2	S3	S4	S5	S6	S7	S8	S9	S10
0	0	0	0	0	0	0	0	0	0	0
10	0	0	0	0	0	0.000000155	0	-1.55E-07	0	0
20	0	0	0	0	0	0.00000031	0	-3.1E-07	0	0
30	0	0	0	0	0	0.000000465	0	-4.65E-07	0	0
40	0	0	0	0	0	0.000000629	0	-6.29E-07	0	0
50	0	0	0	0	0	0.000000775	0	-7.75E-07	0	0
60	0	0	0	0	0	0.00000093	0	-9.3E-07	0	0
70	0	0	0	0	0	0.000001085	0	-1.09E-06	0	0
80	0	0	0	0	0	0.00000124	0	-1.24E-06	0	0
90	0	0	0	0	0	0.000001395	0	-1.4E-06	0	0
100	0	0	0	0	0	0.00000155	0	-1.55E-06	0	0

Table A5 Strains Due to Torque in Y Direction (Beam Model)

My (Nmm)	S1	S2	S3	S4	S5	S6	S7	S8	S9	S10
0	0	0	0	0	0	0	0	0	0	0
10	0	0	0	0	0.000000155	0	-1.55E-07	0	0	0
20	0	0	0	0	0.00000031	0	-3.1E-07	0	0	0
30	0	0	0	0	0.000000465	0	-4.65E-07	0	0	0
40	0	0	0	0	0.000000629	0	-6.29E-07	0	0	0
50	0	0	0	0	0.000000775	0	-7.75E-07	0	0	0
60	0	0	0	0	0.00000093	0	-9.3E-07	0	0	0
70	0	0	0	0	0.000001085	0	-1.09E-06	0	0	0
80	0	0	0	0	0.00000124	0	-1.24E-06	0	0	0
90	0	0	0	0	0.000001395	0	-1.4E-06	0	0	0
100	0	0	0	0	0.00000155	0	-1.55E-06	0	0	0

Table A6 Strains Due to Torque in Z Direction (Beam Model)

Mz (Nmm)	S1	S2	S3	S4	S5	S6	S7	S8	S9	S10
0	0	0	0	0	0	0	0	0	0	0
10	0	0	0	0	0	0	0	0	0.000000302	-3.02E-07
20	0	0	0	0	0	0	0	0	0.000000604	-6.04E-07
30	0	0	0	0	0	0	0	0	0.000000906	-9.06E-07
40	0	0	0	0	0	0	0	0	0.000001208	-1.21E-06
50	0	0	0	0	0	0	0	0	0.00000151	-1.51E-06
60	0	0	0	0	0	0	0	0	0.000001812	-1.81E-06
70	0	0	0	0	0	0	0	0	0.000002114	-2.11E-06
80	0	0	0	0	0	0	0	0	0.000002416	-2.42E-06
90	0	0	0	0	0	0	0	0	0.000002718	-2.72E-06
100	0	0	0	0	0	0	0	0	0.00000302	-3.02E-06

Finite Element Model

Table B1 Strains Due to Force in Direction (FEM Model)

Fx(N)	S1	S2	S3	S4	S5	S6	S7	S8	S9	S10
0	0	0	0	0	0	0	0	0	0	0
2	7.123E-07	6.813E-08	-7.132E-07	-5.148E-08	1.244E-08	-4.05E-08	-2.05E-08	2.275E-08	6.95E-09	-6.95E-09
4	1.425E-06	1.263E-07	-1.426E-06	-1.03E-07	2.4875E-08	-8.15E-08	-4.01E-08	4.255E-08	1.407E-08	-1.41E-08
6	2.137E-06	2.044E-07	-2.14E-06	-1.545E-07	3.7315E-08	-1.219E-07	-6.014E-08	6.336E-08	2.11E-08	-2.11E-08
8	2.849E-06	2.725E-07	-2.853E-06	-2.059E-07	4.976E-08	-1.625E-07	-8.019E-08	8.412E-08	2.815E-08	-2.82E-08
10	3.617E-06	5.832E-07	-3.591E-06	-2.617E-07	6.02E-08	-2.05E-07	-1.026E-07	1.057E-07	3.5338E-08	-3.53E-08
12	4.33E-06	6.313E-07	-4.33E-06	-3.154E-07	7.315E-08	-2.486E-07	-1.214E-07	1.2383E-07	4.211E-08	-4.21E-08
14	5.042E-06	6.945E-07	-5.06E-06	-3.502E-07	8.4215E-08	-2.842E-07	-1.406E-07	1.46E-07	4.854E-08	-4.85E-08
16	5.754E-06	7.36E-07	-5.853E-06	-4.059E-07	9.76E-08	-3.225E-07	-1.602E-07	1.6901E-07	5.615E-08	-5.62E-08
18	6.467E-06	7.807E-07	-6.421E-06	-4.68E-07	1.056E-07	-3.683E-07	-1.89E-07	1.82E-07	6.308E-08	-6.31E-08
20	7.179E-06	8.02E-07	-7.187E-06	-5.662E-07	1.242E-07	-4.025E-07	-2.003E-07	2.0334E-07	7.0338E-08	-7.03E-08
22	7.891E-06	8.5E-07	-7.877E-06	-6.162E-07	1.336E-07	-4.456E-07	-2.234E-07	2.2461E-07	7.7129E-08	-7.71E-08
24	8.604E-06	9.13E-07	-8.587E-06	-6.541E-07	1.4423E-07	-4.79E-07	-2.476E-07	2.453E-07	8.4629E-08	-8.46E-08

26	9.316E-06	9.78E-07	-9.34E-06	-7.14E-07	1.553E-07	-5.213E-07	-2.612E-07	2.65E-07	9.14E-08	-9.14E-08
28	1.003E-05	1.033E-06	-9.987E-06	-7.56E-07	1.71E-07	-5.679E-07	-2.874E-07	2.821E-07	9.9834E-08	-9.98E-08
30	1.074E-05	1.08E-06	-1.059E-05	-7.996E-07	1.87E-07	-6.001E-06	-3.068E-07	3.003E-07	1.068E-07	-1.07E-07

Table B2 Strains Due to Force in Y Direction (FEM Model)

Fy(N)	S1	S2	S3	S4	S5	S6	S7	S8	S9	S10
0	0	0	0	0	0	0	0	0	0	0
2	5.968E-08	7.229E-07	-2.546E-08	-7.232E-07	-2.068E-08	1.2015E-07	2.6107E-08	1.27E-07	1.27E-08	-1.27E-08
4	1.194E-08	1.445E-06	-5.105E-08	-1.446E-06	-4.136E-08	2.403E-07	5.2215E-08	2.541E-07	2.54E-08	-2.54E-08
6	1.79E-07	2.169E-06	-7.658E-08	-2.169E-06	-6.02E-08	3.6045E-07	7.832E-08	3.6811E-07	3.6819E-08	-3.68E-08
8	2.387E-07	2.885E-06	-1.02E-07	-2.893E-06	-8.121E-08	4.806E-07	1.0443E-07	4.815E-07	4.79E-08	-4.79E-08
10	2.951E-07	3.627E-06	-1.251E-07	-3.619E-06	-1.055E-07	6.078E-07	1.3269E-07	6.0166E-07	6.03E-08	-6.03E-08
12	3.709E-07	4.324E-06	-1.576E-07	-4.34E-06	-1.215E-07	7.2605E-07	1.5683E-07	7.211E-07	7.3318E-08	-7.33E-08
14	4.208E-07	5.042E-06	-1.749E-07	-5.06E-06	-1.423E-07	8.4205E-07	1.7376E-07	8.4446E-07	8.444E-08	-8.44E-08
16	4.872E-07	5.764E-06	-2.02E-07	-5.785E-06	-1.681E-08	9.6481E-07	2.0443E-07	9.5082E-07	9.509E-08	-9.51E-08
18	5.629E-07	6.468E-06	-2.249E-07	-6.521E-06	-1.93E-08	1.0865E-07	2.4835E-07	1.0717E-07	1.02E-07	-1.02E-07
20	6.512E-07	7.219E-06	-2.58E-07	-7.239E-06	-2.255E-07	1.278E-07	2.7327E-07	1.2655E-07	1.1129E-07	-1.11E-07
22	7.341E-07	7.912E-06	-2.759E-07	-7.977E-06	-2.332E-07	1.348E-07	3.0089E-07	1.3348E-07	1.245E-07	-1.25E-07
24	8.051E-07	8.635E-06	-3.027E-07	-8.687E-06	-2.54E-07	1.4562E-07	3.2567E-07	1.4452E-07	1.362E-07	-1.36E-07
26	8.789E-07	9.358E-06	-3.267E-07	-9.39E-06	-2.877E-07	1.601E-07	3.561E-07	1.58E-07	1.42E-07	-1.42E-07
28	9.636E-07	1.008E-05	-3.568E-07	-1.01E-05	-3.142E-07	1.702E-07	3.762E-07	1.689E-07	1.6126E-07	-1.61E-07
30	1.025E-06	1.084E-05	-3.735E-07	-1.087E-05	-3.567E-07	1.89E-07	4.061E-07	1.88E-07	1.89E-07	-1.89E-07

Table B3 Strains Due to Force in Z Direction (FEM Model)

Fz(N)	S1	S2	S3	S4	S5	S6	S7	S8	S9	S10
0	0	0	0	0	0	0	0	0	0	0
2	-4.27E-08	6.044E-08	4.1609E-08	6.0712E-08	3.5402E-07	3.68E-07	3.6107E-07	3.62E-07	2.45E-08	-2.45E-08
4	-8.41E-08	1.209E-07	8.3219E-08	1.2142E-07	7.034E-07	7.36E-07	7.0318E-07	7.3196E-07	3.94E-08	-3.94E-08
6	-1.27E-07	1.931E-07	1.2483E-07	1.8214E-07	1.055E-06	1.107E-06	1.1768E-06	1.0864E-06	5.12E-08	-5.12E-08
8	-1.68E-07	2.475E-07	1.6644E-07	2.4285E-07	0.00000142	1.447E-06	1.4756E-06	1.4491E-06	6.44E-08	-6.44E-08
10	-2.18E-07	3.09E-07	2.0445E-07	2.9934E-07	1.7835E-06	1.8036E-06	1.8305E-06	1.815E-06	7.7394E-08	-7.74E-08
12	-2.53E-07	3.619E-07	2.4921E-07	3.5921E-07	2.1218E-06	2.1767E-06	2.2177E-06	2.1686E-06	8.956E-08	-8.96E-08
14	-2.94E-07	4.225E-07	2.8125E-07	4.2125E-07	2.478E-06	2.542E-06	2.5706E-06	2.5364E-06	1.02E-07	-1.02E-07
16	-3.31E-07	4.795E-07	3.195E-07	4.795E-07	2.834E-06	2.917E-06	2.9276E-06	2.8961E-06	1.1679E-07	-1.17E-07
18	-3.71E-07	5.412E-07	3.6799E-07	5.3799E-07	3.1861E-06	3.275E-06	3.2671E-06	3.2585E-06	1.2814E-07	-1.28E-07
20	-4.27E-07	6.019E-07	4.2934E-07	6.0293E-07	3.5338E-06	3.5471E-06	3.653E-06	3.6239E-06	1.4178E-07	-1.42E-07
22	-4.67E-07	6.623E-07	4.7616E-07	6.6156E-07	3.8942E-06	3.916E-06	3.9921E-06	3.9829E-06	1.543E-07	-1.54E-07
24	-5.36E-07	7.229E-07	5.481E-07	7.2481E-07	4.2482E-06	4.284E-06	4.257E-06	4.3443E-06	1.6621E-07	-1.66E-07
26	-6E-07	7.824E-07	6.0831E-07	7.831E-07	4.602E-06	4.652E-06	4.557E-06	4.637E-06	1.8002E-07	-1.8E-07
28	-6.56E-07	8.424E-07	6.642E-07	8.442E-07	4.956E-06	5.0341E-06	4.9998E-06	5.0468E-06	1.9945E-07	-1.99E-07
30	-7.12E-07	9.612E-07	7.213E-07	9.513E-07	5.3146E-06	5.3389E-06	5.334E-06	5.3543E-06	2.06E-07	-2.06E-07

Table B5 Strains Due to Torque in X Direction (FEM Model)

Mx Nmm	S1	S2	S3	S4	S5	S6	S7	S8	S9	S10
0	0	0	0	0	0	0	0	0	0	0
10	1.078E-08	2.153E-08	-1.128E-08	2.1439E-08	-7.9E-08	1.2801E-07	4.6571E-08	-1.287E-07	8.839E-09	-8.84E-09
20	1.17E-08	2.29E-08	-1.175E-08	2.29E-08	-8.075E-08	2.467E-07	5.01E-08	-2.33E-07	9.47E-09	-9.47E-09
30	1.26E-08	2.435E-08	-1.22E-08	2.44E-08	-8.25E-08	3.554E-07	5.36E-08	-3.45E-07	1.0116E-08	-1.01E-08
40	1.335E-08	2.58E-08	-1.295E-08	2.59E-08	-8.465E-08	4.41E-07	5.695E-08	-4.34E-07	1.075E-08	-1.08E-08
50	1.41E-08	2.73E-08	-1.37E-08	2.74E-08	-8.628E-08	5.44E-07	6.03E-08	-5.321E-07	1.138E-08	-1.14E-08
60	1.49E-08	2.885E-08	-1.445E-08	2.88E-08	-8.979E-08	6.31E-07	6.365E-08	-6.37E-07	1.2E-08	-1.2E-08
70	1.57E-08	3.04E-08	-1.52E-08	3.04E-08	-9.224E-08	7.28E-07	6.7E-08	-7.24E-07	1.264E-08	-1.26E-08
80	1.682E-08	3.225E-08	-1.649E-08	3.2536E-08	-9.462E-08	8.4026E-07	7.0345E-08	-8.461E-07	1.34E-08	-1.34E-08
90	1.79E-08	3.461E-08	-1.769E-08	3.4342E-08	-9.701E-08	9.5631E-07	7.3421E-08	-9.38E-07	1.4561E-08	-1.46E-08
100	1.902E-08	3.616E-08	-1.889E-08	3.6591E-08	-9.992E-08	0.00000106	7.7123E-08	-1.023E-06	1.5592E-08	-1.56E-08

Table B5 Strains Due to Torque in Y Direction (FEM Model)

My Nmm	S1	S2	S3	S4	S5	S6	S7	S8	S9	S10
0	0	0	0	0	0	0	0	0	0	0
10	-1.9E-08	-1.13E-08	-2.01E-08	1.1314E-08	1.32E-07	1.45E-08	-1.38E-07	-1.44E-08	8.79E-09	-8.79E-09
20	-2.05E-08	-1.23E-08	-2.165E-08	1.22E-08	2.518E-07	1.525E-08	-2.415E-07	-1.56E-08	9.405E-09	-9.41E-09
30	-2.26E-08	-1.32E-08	-2.32E-08	1.31E-08	3.72E-07	1.6E-08	-3.55E-07	-1.681E-08	1.002E-08	-1.01E-08
40	-2.4E-08	-1.4E-08	-2.465E-08	1.39E-08	4.92E-07	1.7E-08	-4.685E-07	-1.74E-08	1.065E-08	-1.07E-08
50	-2.64E-08	-1.48E-08	-2.61E-08	1.47E-08	6.128E-07	1.8E-08	-5.94E-07	-1.8E-08	1.127E-08	-1.13E-08
60	-2.85E-08	-1.57E-08	-2.755E-08	1.55E-08	7.28E-07	1.9E-08	-6.9E-07	-1.885E-08	1.19E-08	-1.19E-08
70	-3.1E-08	-1.65E-08	-2.9E-08	1.63E-08	8.503E-07	0.00000002	-8.114E-07	-1.97E-08	1.252E-08	-1.25E-08
80	-3.31E-08	-1.74E-08	-3.276E-08	1.744E-08	9.5925E-07	2.112E-08	-9.224E-07	-2.12E-08	1.3342E-08	-1.33E-08
90	-3.51E-08	-1.83E-08	-3.469E-08	-1.834E-08	1.0628E-06	2.2319E-08	-1.024E-06	-2.223E-08	1.4238E-08	-1.42E-08
100	-3.7E-08	-1.92E-08	-3.689E-08	-1.924E-08	1.1839E-06	2.3315E-08	-1.149E-06	-2.322E-08	1.5041E-08	-1.5E-08

Table B6 Strains Due to Torque in Z Direction (FEM Model)

Mz Nmm	S1	S2	S3	S4	S5	S6	S7	S8	S9	S10
0	0	0	0	0	0	0	0	0	0	0
10	1.403E-08	1.608E-08	-1.407E-08	1.6092E-08	-6.012E-08	1.1252E-08	8.4549E-08	-1.09E-08	3.59E-07	-3.59E-07
20	1.55E-08	1.725E-08	-1.58E-08	1.726E-08	-6.66E-08	1.495E-08	8.9475E-08	-1.495E-08	8.1754E-07	-8.15E-07
30	1.7E-08	1.84E-08	-1.706E-08	1.8308E-08	-7.31E-08	1.86E-08	9.3411E-08	-1.9E-08	1.2749E-06	-1.28E-06
40	1.85E-08	1.94E-08	-1.84E-08	1.93E-08	-7.73E-08	2.19E-08	9.8114E-08	-2.25E-08	1.7385E-06	-1.74E-06
50	1.98E-08	2.04E-08	-1.982E-08	2.03E-08	-8.15E-08	2.52E-08	1.0234E-07	-2.6E-08	2.1926E-06	-2.19E-06
60	2.12E-08	2.17E-08	-2.19E-08	2.15E-08	-8.69E-08	2.925E-08	1.0735E-07	-2.905E-08	2.679E-06	-2.68E-06
70	2.32E-08	2.3E-08	-2.322E-08	2.1134E-08	-9.23E-08	3.33E-08	1.1031E-07	-3.21E-08	3.1047E-06	-3.11E-06
80	2.47E-08	2.424E-08	-2.464E-08	2.4341E-08	-9.993E-08	3.802E-08	1.1466E-07	-3.541E-08	3.6052E-06	-3.61E-06
90	2.62E-08	2.543E-08	-2.665E-08	2.6003E-08	-1.06E-07	4.2009E-08	1.1956E-07	-3.823E-08	4.2036E-06	-4.2E-06
100	2.78E-08	2.662E-08	-2.822E-08	2.6802E-08	-1.121E-07	4.5682E-08	1.2342E-07	-4.124E-08	4.7892E-06	-4.79E-06

Experimental Results

Table C1 Strains Due to Force in X Direction (Experimental Results)

Fx(N)	S1	S2	S3	S4	S5	S6	S7	S8	S9	S10
0	0	0	0	0	0	0	0	0	0	0
2	6.75E-07	4.30E-08	-7.12E-07	5.70E-08	4.20E-08	4.12E-08	2.32E-08	5.20E-08	3.50E-08	-3.50E-08
4	1.25E-06	8.27E-08	-1.05E-06	1.20E-07	9.30E-08	7.53E-08	5.23E-08	5.73E-08	4.20E-08	-4.20E-08
6	1.75E-06	1.50E-07	-1.60E-06	1.70E-07	1.20E-07	9.90E-08	7.20E-08	1.02E-07	4.70E-08	-4.70E-08
8	2.55E-06	1.79E-07	-2.15E-06	1.90E-07	2.10E-07	2.41E-07	1.39E-07	1.21E-07	4.90E-08	-4.90E-08
10	3.25E-06	2.50E-07	-3.50E-06	2.95E-07	2.50E-07	2.75E-07	2.15E-07	2.25E-07	5.25E-08	-5.25E-08
12	3.75E-06	3.20E-07	-3.94E-06	3.60E-07	3.30E-07	3.13E-07	3.53E-07	2.43E-07	6.20E-08	-6.20E-08
14	4.25E-06	4.32E-07	-4.62E-06	3.97E-07	3.80E-07	3.48E-07	4.20E-07	2.90E-07	6.70E-08	-6.70E-08
16	5.32E-06	4.87E-07	-5.12E-06	5.21E-07	4.90E-07	4.27E-07	4.79E-07	3.90E-07	7.20E-08	-7.20E-08
18	6.09E-06	5.57E-07	-5.72E-06	5.91E-07	5.60E-07	5.36E-07	5.26E-07	4.70E-07	7.80E-08	-7.80E-08
20	6.52E-06	6.62E-07	-6.25E-06	6.20E-07	5.90E-07	5.49E-07	5.48E-07	4.90E-07	8.70E-08	-8.70E-08
22	7.39E-06	7.15E-07	-7.50E-06	7.12E-07	6.50E-07	6.15E-07	6.15E-07	5.60E-07	9.72E-08	-9.72E-08
24	8.15E-06	7.56E-07	-7.82E-06	7.60E-07	7.20E-07	7.32E-07	7.80E-07	6.75E-07	1.06E-07	-1.06E-07
26	8.72E-06	8.02E-07	-8.92E-06	7.90E-07	7.80E-07	7.68E-07	7.82E-07	6.80E-07	1.29E-07	-1.29E-07
28	9.23E-06	8.90E-07	-9.16E-06	8.60E-07	8.20E-07	7.90E-07	8.20E-07	7.20E-07	1.60E-07	-1.60E-07
30	9.85E-06	9.22E-07	-9.59E-06	8.55E-07	9.20E-07	8.90E-07	8.52E-07	7.70E-07	1.83E-07	-1.83E-07

Table C2 Strains Due to Force in Y Direction (Experimental Results)

Fy(N)	S1	S2	S3	S4	S5	S6	S7	S8	S9	S10
0	0	0	0	0	0	0	0	0	0	0
2	3.90E-08	6.63E-07	4.30E-08	-6.52E-07	5.30E-08	4.02E-08	4.20E-08	4.02E-08	3.46E-08	-3.46E-08
4	8.47E-08	1.18E-06	9.27E-08	-1.28E-06	8.70E-08	9.23E-08	8.73E-08	9.23E-08	4.20E-08	-4.20E-08
6	1.35E-07	1.89E-06	1.35E-07	-1.75E-06	1.25E-07	1.22E-07	1.32E-07	1.22E-07	4.76E-08	-4.76E-08
8	1.70E-07	2.48E-06	1.69E-07	-2.17E-06	1.90E-07	1.90E-07	2.10E-07	1.90E-07	5.06E-08	-5.06E-08
10	2.35E-07	3.46E-06	2.35E-07	-3.24E-06	2.80E-07	2.45E-07	2.50E-07	2.45E-07	5.85E-08	-5.85E-08
12	2.90E-07	3.79E-06	3.40E-07	-4.07E-06	3.70E-07	3.53E-07	3.43E-07	3.53E-07	7.60E-08	-7.60E-08
14	3.60E-07	4.68E-06	4.42E-07	-4.56E-06	4.20E-07	3.70E-07	3.90E-07	3.70E-07	9.70E-08	-9.70E-08
16	4.27E-07	5.32E-06	4.87E-07	-5.25E-06	5.10E-07	4.79E-07	4.90E-07	4.79E-07	1.21E-07	-1.21E-07
18	4.70E-07	5.82E-06	5.57E-07	-5.75E-06	5.40E-07	5.26E-07	5.70E-07	5.26E-07	1.69E-07	-1.69E-07
20	5.30E-07	6.32E-06	6.12E-07	-6.66E-06	5.90E-07	5.80E-07	5.90E-07	5.80E-07	1.62E-07	-1.62E-07
22	6.50E-07	7.39E-06	7.23E-07	-7.52E-06	6.85E-07	6.55E-07	6.50E-07	6.55E-07	1.72E-07	-1.72E-07
24	7.26E-07	7.83E-06	7.46E-07	-7.85E-06	7.20E-07	6.80E-07	7.50E-07	6.80E-07	1.86E-07	-1.86E-07
26	7.92E-07	8.71E-06	8.32E-07	-8.75E-06	7.90E-07	7.68E-07	7.80E-07	7.68E-07	1.93E-07	-1.93E-07
28	8.50E-07	9.38E-06	8.70E-07	-9.42E-06	8.91E-07	8.62E-07	8.20E-07	8.62E-07	2.57E-07	-2.57E-07
30	9.12E-07	9.82E-06	9.22E-07	-1.04E-05	9.42E-07	9.52E-07	8.70E-07	9.52E-07	2.73E-07	-2.73E-07

Table C3 Strains Due to Force in Z Direction (Experimental Results)

Fz(N)	S1	S2	S3	S4	S5	S6	S7	S8	S9	S10
0	0	0	0	0	0	0	0	0	0	0
2	1.30E-08	1.34E-08	1.43E-08	1.15E-08	5.63E-07	3.95E-07	4.63E-07	4.15E-07	1.80E-08	-1.80E-08
4	2.07E-08	2.57E-08	2.17E-08	1.90E-08	8.26E-07	8.15E-07	8.74E-07	8.28E-07	2.12E-08	-2.12E-08
6	2.80E-08	3.80E-08	3.38E-08	2.68E-08	1.47E-06	1.48E-06	1.59E-06	1.44E-06	2.56E-08	-2.56E-08
8	3.20E-08	4.32E-08	4.20E-08	3.12E-08	1.74E-06	1.92E-06	1.92E-06	1.86E-06	2.90E-08	-2.90E-08
10	3.42E-08	4.82E-08	4.42E-08	3.42E-08	2.14E-06	2.39E-06	2.18E-06	2.40E-06	3.20E-08	-3.20E-08
12	3.80E-08	4.98E-08	4.80E-08	3.90E-08	2.37E-06	2.84E-06	2.58E-06	2.79E-06	3.60E-08	-3.60E-08
14	4.20E-08	5.20E-08	5.02E-08	4.60E-08	2.88E-06	2.99E-06	2.93E-06	3.08E-06	3.90E-08	-3.90E-08
16	5.30E-08	5.43E-08	5.13E-08	4.90E-08	3.12E-06	3.29E-06	3.25E-06	3.37E-06	4.30E-08	-4.30E-08
18	5.50E-08	5.50E-08	5.35E-08	5.15E-08	3.42E-06	3.52E-06	3.83E-06	3.64E-06	4.90E-08	-4.90E-08
20	6.10E-08	5.91E-08	5.61E-08	5.61E-08	3.96E-06	4.08E-06	4.20E-06	3.93E-06	5.20E-08	-5.20E-08
22	6.70E-08	6.27E-08	6.27E-08	5.87E-08	4.18E-06	4.64E-06	4.73E-06	4.45E-06	5.72E-08	-5.72E-08
24	6.82E-08	6.82E-08	6.72E-08	6.22E-08	4.62E-06	4.68E-06	5.21E-06	4.60E-06	6.10E-08	-6.10E-08
26	7.30E-08	7.13E-08	6.97E-08	6.73E-08	4.83E-06	5.07E-06	5.47E-06	4.93E-06	6.79E-08	-6.79E-08
28	7.82E-08	7.52E-08	7.42E-08	7.20E-08	5.24E-06	5.72E-06	5.62E-06	5.60E-06	8.17E-08	-8.17E-08
30	8.20E-08	7.90E-08	8.02E-08	7.82E-08	5.86E-06	5.93E-06	6.15E-06	5.83E-06	9.23E-08	-9.23E-08

Table C4 Strains Due to Torque in X Direction (Experimental Results)

Mx Nmm	S1	S2	S3	S4	S5	S6	S7	S8	S9	S10
0	0	0	0	0	0	0	0	0	0	0
10	1.40E-08	1.05E-08	1.20E-08	1.16E-08	1.21E-08	1.04E-07	1.58E-08	-9.20E-08	1.20E-08	-1.20E-08
20	2.94E-08	1.68E-08	2.40E-08	1.80E-08	1.84E-08	2.02E-07	1.84E-08	-2.01E-07	1.74E-08	-1.74E-08
30	3.40E-08	2.63E-08	2.93E-08	2.30E-08	2.20E-08	2.91E-07	2.13E-08	-2.93E-07	2.16E-08	-2.16E-08
40	4.16E-08	3.16E-08	3.46E-08	2.86E-08	2.62E-08	3.88E-07	2.56E-08	-4.06E-07	2.60E-08	-2.60E-08
50	4.87E-08	3.72E-08	3.70E-08	3.17E-08	2.92E-08	4.66E-07	2.87E-08	-4.70E-07	3.07E-08	-3.07E-08
60	5.20E-08	4.22E-08	4.20E-08	3.62E-08	3.20E-08	5.87E-07	3.02E-08	-5.92E-07	3.42E-08	-3.42E-08
70	5.74E-08	4.94E-08	4.84E-08	3.93E-08	3.74E-08	6.79E-07	3.24E-08	-6.74E-07	3.83E-08	-3.83E-08
80	6.24E-08	5.31E-08	5.31E-08	4.31E-08	4.28E-08	7.51E-07	3.79E-08	-7.78E-07	4.10E-08	-4.10E-08
90	6.85E-08	5.95E-08	5.75E-08	4.85E-08	4.85E-08	8.83E-07	4.04E-08	-8.35E-07	4.35E-08	-4.35E-08
100	7.24E-08	6.47E-08	6.37E-08	5.27E-08	5.07E-08	9.72E-07	4.57E-08	-8.70E-07	4.75E-08	-4.75E-08

Table C5 Strains Due to Torque in Y Direction (Experimental Results)

My Nmm	S1	S2	S3	S4	S5	S6	S7	S8	S9	S10
0	0	0	0	0	0	0	0	0	0	0
10	8.20E-09	1.01E-08	1.15E-08	1.02E-08	1.15E-07	1.00E-08	-1.24E-07	1.40E-08	1.12E-08	-1.12E-08
20	1.47E-08	1.81E-08	1.72E-08	1.64E-08	2.05E-07	1.62E-08	-2.28E-07	1.80E-08	1.54E-08	-1.54E-08
30	2.31E-08	2.84E-08	2.30E-08	1.92E-08	3.25E-07	2.13E-08	-3.36E-07	2.13E-08	2.26E-08	-2.26E-08
40	2.64E-08	3.20E-08	2.50E-08	2.20E-08	3.95E-07	2.50E-08	-4.34E-07	2.32E-08	2.76E-08	-2.76E-08
50	2.93E-08	3.52E-08	2.93E-08	2.50E-08	5.06E-07	2.80E-08	-5.50E-07	2.70E-08	3.14E-08	-3.14E-08
60	3.18E-08	3.92E-08	3.12E-08	2.73E-08	6.12E-07	3.13E-08	-6.35E-07	2.98E-08	3.62E-08	-3.62E-08
70	3.32E-08	4.13E-08	3.31E-08	2.90E-08	6.84E-07	3.45E-08	-7.48E-07	3.21E-08	4.10E-08	-4.10E-08
80	3.61E-08	4.25E-08	3.48E-08	3.20E-08	7.69E-07	4.00E-08	-8.59E-07	3.45E-08	4.51E-08	-4.51E-08
90	3.92E-08	4.53E-08	3.82E-08	3.52E-08	8.84E-07	4.31E-08	-9.37E-07	3.72E-08	4.95E-08	-4.95E-08
100	4.28E-08	4.80E-08	4.10E-08	3.72E-08	9.60E-07	4.72E-08	-1.03E-06	4.02E-08	5.31E-08	-5.31E-08

Table C6 Strains Due to Torque in Z Direction (Experimental Results)

Mz Nmm	S1	S2	S3	S4	S5	S6	S7	S8	S9	S10
0	0	0	0	0	0	0	0	0	0	0
10	1.53E-09	3.13E-09	1.30E-09	1.52E-09	1.30E-09	3.13E-09	1.83E-09	2.30E-09	3.43E-07	-3.43E-07
20	3.42E-09	7.20E-09	2.50E-09	4.72E-09	5.20E-09	6.50E-09	3.50E-09	4.92E-09	7.62E-07	-7.62E-07
30	8.30E-09	1.23E-08	7.23E-09	7.80E-09	6.83E-09	7.30E-09	6.33E-09	1.03E-08	1.13E-06	-1.13E-06
40	1.40E-08	1.74E-08	1.24E-08	1.04E-08	1.40E-08	1.43E-08	9.40E-09	1.24E-08	1.64E-06	-1.64E-06
50	1.86E-08	2.11E-08	1.46E-08	1.26E-08	1.60E-08	1.56E-08	1.26E-08	1.61E-08	2.06E-06	-2.06E-06
60	2.18E-08	2.48E-08	1.58E-08	1.48E-08	1.78E-08	1.68E-08	1.48E-08	1.98E-08	2.58E-06	-2.58E-06
70	2.48E-08	2.65E-08	1.80E-08	1.75E-08	1.92E-08	1.78E-08	1.70E-08	2.15E-08	2.93E-06	-2.93E-06
80	2.70E-08	2.87E-08	2.14E-08	2.37E-08	2.23E-08	2.44E-08	1.97E-08	2.47E-08	3.28E-06	-3.28E-06
90	3.14E-08	3.14E-08	2.37E-08	2.43E-08	2.54E-08	2.70E-08	2.17E-08	2.54E-08	3.74E-06	-3.74E-06
100	3.64E-08	3.42E-08	2.62E-08	2.54E-08	3.25E-08	3.12E-08	2.42E-08	2.92E-08	4.18E-06	-4.18E-06